



2024

Impact of Drug-Polymer Interactions on Stability in Simvastatin-Based Amorphous Solid Dispersions

Charina Lampa
University of the Pacific

Follow this and additional works at: https://scholarlycommons.pacific.edu/uop_etds

 Part of the [Pharmacy and Pharmaceutical Sciences Commons](#)

Recommended Citation

Lampa, Charina. (2024). *Impact of Drug-Polymer Interactions on Stability in Simvastatin-Based Amorphous Solid Dispersions*. University of the Pacific, Dissertation.
https://scholarlycommons.pacific.edu/uop_etds/4278

This Dissertation is brought to you for free and open access by the University Libraries at Scholarly Commons. It has been accepted for inclusion in University of the Pacific Theses and Dissertations by an authorized administrator of Scholarly Commons. For more information, please contact mgibney@pacific.edu.

Impact of Drug-Polymer Interactions on Stability in Simvastatin-Based
Amorphous Solid Dispersions

By

Charina Lampa

A Dissertation Submitted

In Partial Fulfillment of the

Requirements for the Degree of

DOCTOR OF PHILOSOPHY

Thomas J. Long School of Pharmacy
Pharmaceutical and Chemical Sciences

University of the Pacific
Stockton, California

2024

Impact of Drug-Polymer Interactions on Stability in Simvastatin-Based
Amorphous Solid Dispersions

By

Charina Lampa

APPROVED BY:

Dissertation Advisor: Bhaskara Jasti, Ph.D.

Committee Member: Xiaoling Li, Ph.D.

Committee Member: Xin Guo, Ph.D.

Committee Member: Raj Sevak, Ph.D.

Committee Member: Scott Smith, Ph.D.

Department Chair: William Chan, Ph.D.

Impact of Drug-Polymer Interactions on Stability in Simvastatin-Based
Amorphous Solid Dispersions

Copyright 2024

By

Charina Lampa

Dedication

This dissertation is dedicated to all young minority girls in STEM. May your curiosity be boundless, your determination unyielding, and your dreams limitless. May you find inspiration in the stars, strength in the challenges, and support in the community of trailblazers who came before you. This work is for you and in honor of your potential.

Acknowledgements

I would like to express my deepest gratitude to Dr. Bhaskara Jasti for his invaluable guidance throughout this journey. His unwavering support while I navigated the fine balance of graduate school and industry commitments has endowed me with the resilience and tenacity to confront any challenges that come my way. My sincerest appreciation also goes to the esteemed members of my dissertation committee: Dr. Xiaoling Li, Dr. Xin Guo, Dr. Raj Sevak, and Dr. Scott Smith. Their constructive criticism, insightful suggestions, and scholarly feedback have been instrumental in shaping the direction and quality of this research. I am deeply thankful for their help in refining my critical thinking skills and nurturing my patience as a scientist, and I will always aspire to uphold the standards they have instilled in me. I am also indebted to Dr. David Lechuga-Ballesteros for his guidance and boundless encouragement, which played a pivotal role in my commitment to pursuing graduate studies.

My heartfelt gratitude also extends to my colleagues, both past and present. Kellisa Lachacz, Dr. Susan Hoe, Penny Tan, Behzad Damadzadeh, Dr. Davin Rautiola, Dr. Ed Schreiner, and Thoeun Khuth have provided enlightening discussions and scientific discourse, which have been invaluable to my research. Special appreciation also goes to my labmates Pramila Sharma and Dr. Sridivya Raparla, for their insightful perspectives on research and university life. I am also grateful to Sonya, Lynda, and Kathy for all their administrative support throughout the years.

To my family, whose unconditional love, support, and understanding have been my anchor throughout this challenging journey, I am profoundly grateful. To my parents, Dan and Norma, you are the reason for my being, and I would have never achieved such great heights

without your sacrifices. To my siblings, Daniel, Fatima, Gilbert, and Camille, and siblings-in-law, Eugene, Richard, and Donna – you give me the strength and courage to keep pushing through any obstacles. To my nieces, Olivia and Isla, – you inspire me to be the best I can be. To my in-laws, Paul and Anna, thank you for nurturing a supportive environment and for raising a remarkable son. To my partner in all things, Michael Gou, you are my rock. Your patience, understanding, and belief in my abilities have given me the courage to pursue my dreams. Lastly, to my Creator – I am thankful for all the blessings and hardships that You have placed in my journey, for they have defined the person that I am today.

Impact of Drug-Polymer Interactions on Stability in Simvastatin-Based Amorphous Solid Dispersions

Abstract

By Charina Lampa

University of the Pacific
2024

This study aimed to investigate the drug-polymer interactions between simvastatin (SIM) and three polymers [PVP-VA, HPMC-AS, and Soluplus® (SOL)] in amorphous solid dispersions (ASDs) prepared by hot melt extrusion (HME), and to understand the implications on physical stability. ASDs are of significant interest within the pharmaceutical industry for improving drug bioavailability. However, the amorphous nature of a drug in an ASD presents physical stability challenges. Utilizing novel applications of accessible tools such as ATR-FTIR or DSC aid in understanding the mechanisms of stabilization which are critical to the rational design of ASDs.

ASDs were prepared using HME and were characterized using mDSC, ATR-FTIR, TGA, PXRD, PLM, and UPLC. Mathematical processing of ATR-FTIR spectra and Pearson coefficient analysis was used to quantitatively determine the degree of intermolecular bonds between SIM and each polymer. Results were verified using experimental and theoretical approaches such as mDSC and Flory-Huggins Theory. Formulations were stored at 50°C/96%RH, and physical stability was monitored using PXRD, PLM, and mDSC.

Pearson coefficient analysis of ATR-FTIR data showed that SIM exhibited a higher degree of interactions with PVP-VA and SOL relative to HPMC-AS. Experimental observations and theoretical calculations of SIM miscibility and solubility in the polymers were used as an

indicator of intermolecular interactions, and both were consistent with this ranking of drug-polymer interactions. Stability assessments at 50°C/96%RH demonstrated SIM crystallization in all PVP-VA ASDs and in high SIM load HPMC-AS ASDs, while no crystallization was observed in SOL ASDs. This demonstrated that although the degree of interactions between SIM and PVP-VA were the strongest, the extent of interactions between water and PVP-VA may also play a critical role in the ASD physical stabilization. In addition, although SIM/SOL systems were the lowest overall in glass transition temperature and may perhaps have the highest degree of molecular mobility, the interactions between SOL and SIM were sufficient to inhibit crystallization.

These findings highlight the utility of applying Pearson coefficient analysis to accessible tools such as ATR-FTIR on the understanding of drug-polymer interactions in ASDs. While drug-polymer interactions are a significant factor in maintaining SIM's amorphous nature, other mechanisms of physical stabilization need to be considered in the rational design of ASDs.

Table of Contents

List of Tables..	13
List of Figures.	14
1. Introduction	16
1.1 Introduction	16
1.2 Amorphous Solid Dispersions	18
1.2.1. Amorphous State	18
1.2.2. Solid Dispersion Classification	20
1.2.3. Description	21
1.3 Preparation Methods	22
1.3.1. Solvent-Based Methods	24
1.3.2. Fusion or Melting-Based Methods	26
1.4 Characterization Methods	28
1.4.1. Differential Scanning Calorimetry/Modulated Differential Scanning Calorimetry	28
1.4.2. Powder X-ray Diffraction	29
1.4.3. Polarized Light Microscopy	30
1.4.4. Thermogravimetric Analysis	31
1.4.5. Attenuated Total Reflectance-Fourier Transform Infrared Spectroscopy or Raman Spectroscopy	32
1.4.6. Ultra Performance Liquid Chromatography	33
1.4.7. Solid-State Nuclear Magnetic Resonance	33
1.5 Physical Stability of Amorphous Solid Dispersions	34
1.5.1. Drug-Polymer Interactions	35
1.5.2. Chemical Potential Reduction	37

1.5.3.	Molecular Mobility Reduction.....	38
1.6	Determination of Drug-Polymer Interactions	39
1.6.1.	Evaluation of Drug-Polymer Interactions	39
1.6.2.	Prediction of Drug-Polymer Solubility and Miscibility.....	42
2.	Research Aims.....	50
2.1	Statement of the Problem.....	50
2.2	Purpose.....	50
2.3	Research Aims	51
3.	Preparation and Characterization of Simvastatin-based Amorphous Solid Dispersions Using Hot Melt Extrusion	52
3.1	Introduction.....	52
3.2	Drug Selection	52
3.3	Polymer Selection	53
3.4	Materials	55
3.5	Methods.....	55
3.5.1.	Preparation of Physical Blends	55
3.5.2.	Preparation of Amorphous Solid Dispersions.....	55
3.5.3.	Thermogravimetric Analysis	57
3.5.4.	Modulated Differential Scanning Calorimetry	57
3.5.5.	Powder X-ray Diffraction	57
3.5.6.	Polarized Light Microscopy.....	58
3.5.7.	Ultra Performance Liquid Chromatography	58
3.6	Results and Discussion	58
3.6.1.	Characterization of Starting Materials	58
3.6.2.	Hot Melt Extrusion Observations	65

3.6.3.	Characterization of Amorphous Solid Dispersions Prepared by Hot Melt Extrusion	67
4.	Determination of Intermolecular Interactions	74
4.1	Determination of Intermolecular Interactions.....	74
4.2	Materials	75
4.3	Methods.....	75
4.3.1.	Attenuated Total Reflectance-Fourier Transform Infrared Spectroscopy (ATR-FTIR)	75
4.3.2.	Pearson Moment Correlation Coefficient	76
4.3.3.	Prediction of Intermolecular Interactions using mDSC.....	76
4.3.4.	Kinetic Miscibility using mDSC.....	77
4.3.5.	Prediction of Miscibility using Solubility Parameters	77
4.3.6.	Prediction of Miscibility using Flory-Huggins Interaction Parameter	77
4.3.7.	Miscibility by Gibbs Free Energy of Mixing.....	78
4.3.8.	Solubility using Heat of Fusion ΔH_m	78
4.4	Results and Discussions.....	79
4.4.1.	Prediction of Intermolecular Interactions using mDSC.....	79
4.4.2.	Kinetic Miscibility by mDSC	80
4.4.3.	ATR-FTIR and Pearson Coefficient	81
4.4.4.	Miscibility using Solubility Parameters	85
4.4.5.	Miscibility by Flory Huggins Interaction Parameters	86
4.4.6.	Miscibility by Gibbs Free Energy of Mixing.....	88
4.4.7.	SIM Theoretical Solubility in Polymers	91
5.	Physical Stability of Amorphous Solid Dispersions	93
5.1	Introduction.....	93

5.2	Materials	93
5.3	Methods.....	93
5.3.1.	Stability	93
5.3.2.	Powder X-ray Diffraction	94
5.3.3.	Modulated Differential Scanning Calorimetry	94
5.3.4.	Polarized Light Microscopy.....	94
5.4	Results and Discussions.....	95
6.	Summary and Conclusions.....	100
	References.....	102
	Appendices.....	114
A:	Values used for Melting Point Depression Experiments	115
B:	PXRD Diffractograms	116
C:	PLM Images.....	123

List of Tables

Table

1. Biopharmaceutical Classification System (BCS) and Corresponding Formulation Approaches.....	17
2. Different Types of Intermolecular Interactions in ASDs.....	36
3. Physicochemical Properties of SIM, PVP-VA, HPMC-AS, and SOL	54
4. Composition of ASD Formulations Prepared by Hot Melt Extrusion.....	56
5. Water Content of SIM/Polymer ASDs	71
6. Chemical Purity of SIM/Polymer ASDs.....	72
7. Solubility Parameters for SIM, PVP-VA, HPMC-AS, and SOL.....	85
8. Calculated Interaction Parameters at 25°C and 139°C	88

List of Figures

Figure

1. Thermodynamic Representation of Crystalline and Amorphous States in terms of Enthalpy or Volume as a Function of Temperature	19
2. Classification of Solid Dispersions, Adapted From (Vasconcelos et al., 2007)	21
3. Schematic of Fusion/Melt-Based and Solvent-Based Methods for Preparing ASDs	23
4. Energy Landscape of Crystalline Drug, Amorphous Solid Dispersion (ASD), and Amorphous Drug	38
5. Physical Form of SIM, PVP-VA, HPMC-AS, SOL Starting Materials by PXRD	60
6. PLM Images of SIM, PVP-VA, HPMC-AS, SOL Starting Materials	61
7. TGA (blue curve) and mDSC (green) Thermograms of (A) SIM, (B) PVP-VA, (C) HPMC-AS, (D) SOL Starting Materials	62
8. Chemical Compatibility by Thermogravimetric Analysis for (A) SIM and PVP-VA, (B) SIM and HPMC-AS, (C) SIM and SOL	64
9. Appearance of HME Ribbons and Post Milling Powder Appearance for SIM/PVP-VA, SIM/HPMC-AS, and SIM/SOL ASDs	66
10. PXRD Diffractograms for (A) SIM/PVP-VA ASDs, (B) SIM/HPMC-AS ASDs, (C) SIM/SOL ASDs with Crystalline SIM	68
11. PLM Images for SIM/PVP-VA, SIM/HPMC-AS, SIM/SOL ASDs	69
12. mDSC Thermograms for (A) SIM/PVP-VP ASDs, (B) SIM/HPMC-AS ASDs, (C) SIM/SOL ASDs	70
13. Predicted vs. Measured Tg of SIM/Polymer ASDs	79
14. ATR-FTIR Spectra of (A) SIM/PVP-VA PBs, (B) SIM/PVP-VA ASDs, (C) SIM/HPMC-AS PBs, (D) SIM/HPMC-AS ASDs, (E) SIM/SOL PBs, (F) SIM/SOL ASDs	82

15. Pearson Coefficient as a Measure of Degree of Intermolecular Bonds Between (A) SIM/PVP-VA, (B) SIM/HPMC-AS, (C) SIM/SOL in Physical Blends (blue) and ASDs (orange)	83
16. Melting Point Depression Data for Determination of Interaction Parameters at 139°C.....	877
17. Gibbs Free Energy as a Function of Drug Volume Fraction ϕ_d for (A) SIM/PVP-VA, (B) SIM/HPMC-AS, (C) SIM/SOL	900
18. SIM Theoretical Solubility in PVP-VA, HPMC-AS, and SOL.....	922
19. PXRD Diffractograms of ASDs on Stability at 3 Days, 50°C/96% RH (A) SIM/PVP-VA, (B) SIM/HPMC-AS, (C) SIM/SOL	96
20. PLM Images for SIM/PVP-VA, SIM/HPMC-AS, SIM/SOL ASDs after 3 Days at 50°C/96% RH.....	97
21. DSC Thermograms of ASDs on Stability at 3 Days, 50C/96% RH (A) SIM/PVP-VA, (B) SIM/HPMC-AS, (C) SIM/SOL	98

1. INTRODUCTION

1.1 Introduction

Oral delivery is the most common route of drug administration. As of 2021, around 60% of established small-molecule drug products available commercially are administered via the oral route, and estimates indicate that oral formulations represent about 90% of the global market share of all pharmaceutical formulations intended for human use (Alqahtani et al., 2021). Oral drug delivery affords many advantages, including patient compliance to therapy, the non-invasiveness nature, removal of access barriers due to not needing medical intervention, cost-effectiveness, and ease of manufacturing and development. A key challenge with this route of delivery is the physicochemical barrier that exists in the gastrointestinal tract. A drug must be released from the dosage form and must be able to dissolve in the gastrointestinal tract fluids and subsequently permeate the intestinal membrane. The Biopharmaceutics Classification System (BCS) categorizes a drug into four main categories according to solubility and permeability (Amidon et al., 1995). Solubility is defined as the amount of substance that can be dissolved in a given amount of solvent, and permeability is defined as the quality or state of being permeable (Samineni et al., 2022). A drug is considered highly soluble if the highest single therapeutic dose can be dissolved in 250 milliliter (mL) or less of aqueous media over the pH range of 1.2 – 6.8 at $37 \pm 1^\circ\text{C}$, and is considered highly permeable when the absolute bioavailability is $\geq 85\%$ of the administered dose (Food and Drug Administration, 2021). Class I drugs are drugs with high solubility and high permeability, Class II with low solubility and high permeability, Class III with high solubility and low permeability, and Class IV with low solubility and low permeability. Table 1 shows a summary of the BCS classification system.

Table 1.*Biopharmaceutical Classification System (BCS) and Corresponding Formulation Approaches*

Class	Solubility	Permeability	Formulation Approaches
I	High	High	<ul style="list-style-type: none"> • Immediate release (IR) solid dosage forms
II	Low	High	<ul style="list-style-type: none"> • Crystal modifications <ul style="list-style-type: none"> ○ Metastable polymorphs ○ Salt formation ○ Cocrystal formation • IR solid dosage forms with surfactant • Particle size reduction <ul style="list-style-type: none"> ○ Micronization ○ Nanocrystals • Amorphization • Cyclodextrin complexation • Lipid formulations <ul style="list-style-type: none"> ○ Self-emulsification systems ○ Liquid filled capsule • pH modification
III	High	Low	<ul style="list-style-type: none"> • IR solid dosage forms with absorption enhancer • IR solid dosage form
IV	Low	Low	<ul style="list-style-type: none"> • Combination of approaches for BCS class II and absorption enhancer • Same approaches as BCS class II

Poor aqueous solubility represents a formidable challenge encountered by pharmaceutical scientists, as it determines the dissolution rate, and therefore, the total bioavailability. As of 2016 BCS class II and class IV drugs comprise about 60-70% and 10-20% of new drugs in development, respectively (Nikolakakis & Partheniadis, 2017). The classical Noyes-Whitney Equation demonstrates the factors that are critical to the dissolution rate through the equation below (Noyes, 1897):

$$\frac{dC}{dt} = k_D A (C_s - C_t) \quad (1)$$

where dC/dt is the dissolution rate, k_D is the dissolution rate constant determined by the stirring rate and the diffusion constant, A is the total surface of the drug, C_s is the aqueous saturation solubility of the drug, C_t is the drug concentration dissolved at time t . It is apparent from this equation that the dissolution rate in vivo and in vitro are directly proportional to the total surface area of the drug particles and to the solubility of the drug (Zografi & Newman, 2015). Significant investment of resources towards improving the aqueous solubility of drugs through various formulations strategies. Table 1, as adapted from literature sources, provides an overview (Kawabata et al., 2011). While many of these approaches have seen success, some of the most commercially successful formulations have taken the amorphization approach.

1.2 Amorphous Solid Dispersions

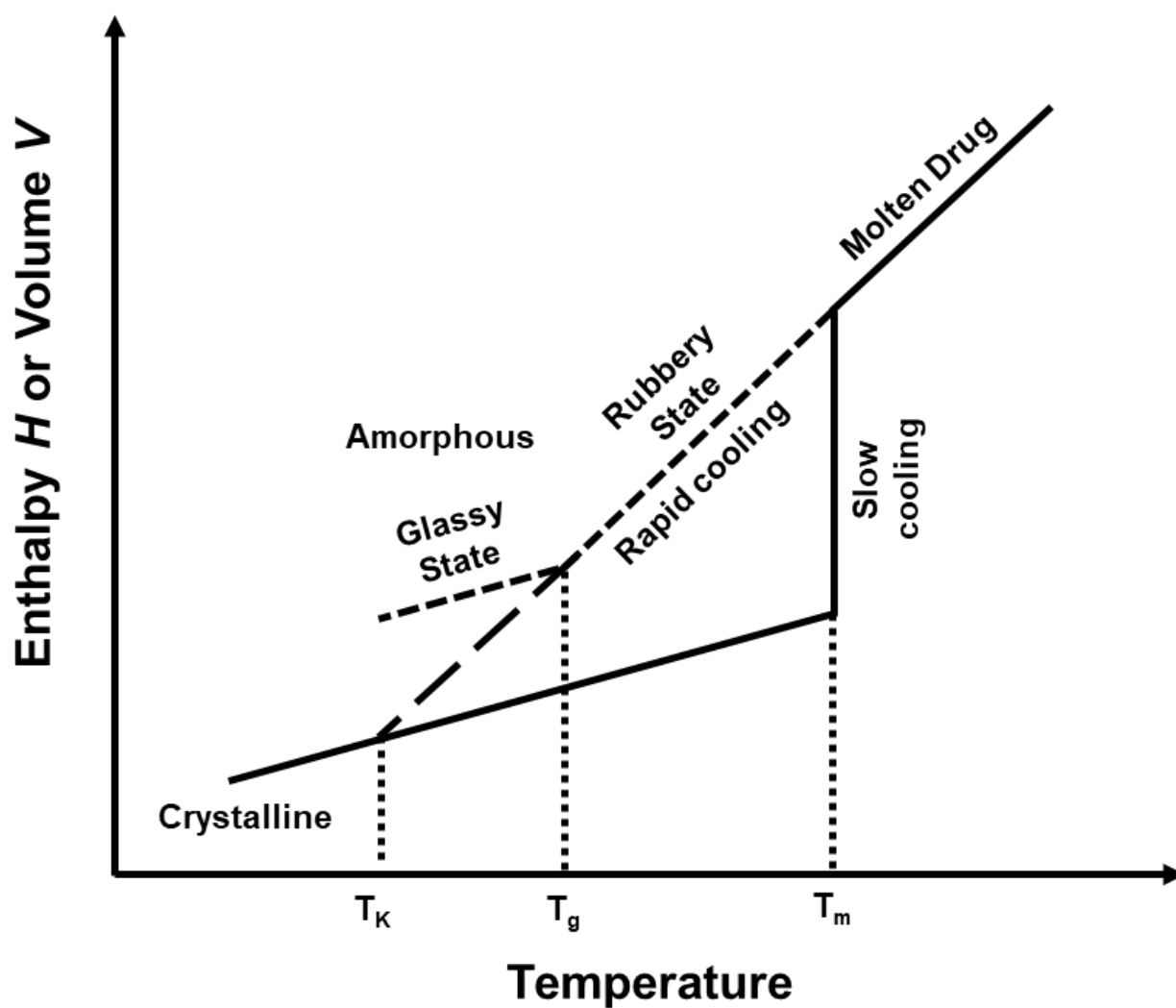
1.2.1. Amorphous State

The key distinction between the crystalline and amorphous form of a drug is rooted in the molecular arrangement and long-range order. This difference dictates the different physicochemical properties between the two forms, including the apparent solubility. The

crystalline state is defined by a lattice of repeating three-dimensional structure and long-range order, whereas the amorphous state lacks long-range order and has a highly disordered arrangement of molecules. This difference can also be explained thermodynamically, by defining the volume V and enthalpy H of a drug as a function of temperature as shown in Figure 1.

Figure 1.

Thermodynamic Representation of Crystalline and Amorphous States in terms of Enthalpy or Volume as a Function of Temperature



Consider a crystalline drug that is heated to the drug melting temperature T_m . At T_m , an equilibrium exists between the solid and liquid phase of a drug, where increasing the heat input into the system does not increase the temperature, but rather results in an increase in V and H (also referred to as the heat of fusion ΔH_m or ΔH_{fus}). Once the last crystal is completely melted, additional heat input results in an increase in V and H of the molten drug in addition to the temperature. If the molten drug were to be cooled slowly through T_m , the molecules would be afforded the opportunity to rearrange itself back into its crystalline lattice, resulting in a first order transition characterized by a stepwise decrease in V and H . However, if the drug were to be rapidly cooled, recrystallization would be prevented and the drug would exist in a supercooled liquid state that is in equilibrium with the molten liquid state. At this point, the drug exists as a rubbery state exhibiting high viscosity. Further cooling beyond the glass transition temperature T_g results in a second order transition characterized by a slope change in V and H , at which point the drug is in a glassy state appearing as a brittle solid with very low viscosity. It is important to note that the glassy state is not at thermodynamic equilibrium and is in a state that was reached through kinetic factors. The supercooled liquid curve may be extrapolated to a point that intersects with the crystal curve at a temperature referred to as the Kauzmann temperature T_K , where the configurational entropy of the system reaches zero. This is the origin of the ‘ $T_g-50^\circ\text{C}$ ’ rule of thumb, as T_K is believed to be a temperature with zero mobility ensuring long-term physical stability of the material (Hancock et al., 1995).

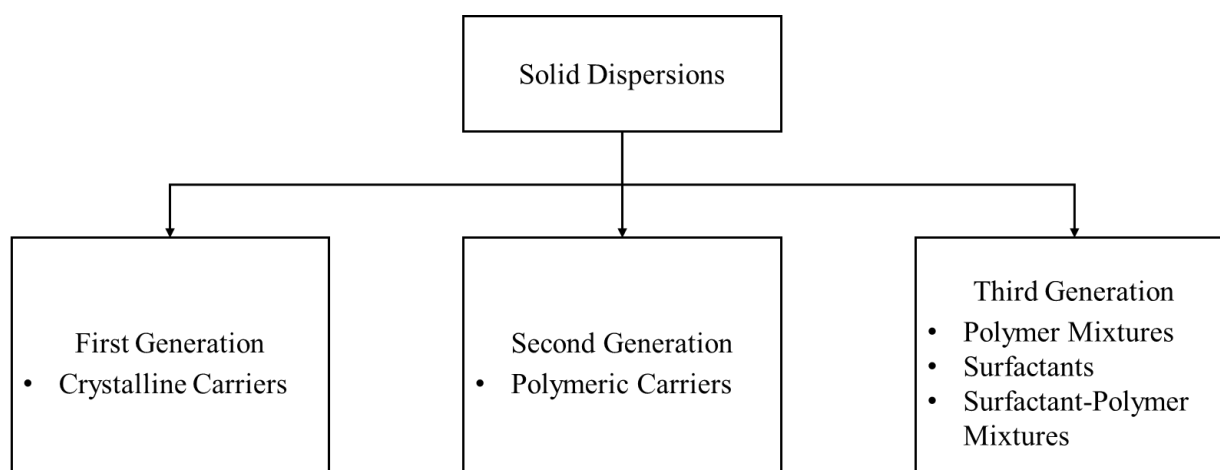
1.2.2. Solid Dispersion Classification

Solid dispersions are dispersions of one or more active ingredients in an inert carrier or matrix at solid state prepared by the melting (fusion), solvent, or melting-solvent method (Chiou & Riegelman, 1971). Dispersions may be categorized into different generations based on the

evolution over time, as shown in Figure 2 (Vasconcelos et al., 2007). The scope of this research is limited to second generation solid dispersions where the amorphous drug is molecularly dispersed in an amorphous polymer.

Figure 2.

Classification of Solid Dispersions, Adapted From (Vasconcelos et al., 2007)



1.2.3. Description

Amorphous solid dispersions (ASDs) have been of significant interest within the pharmaceutical industry for many years as an approach to addressing the issue of poor aqueous solubility. Between 2010 and 2020 alone, at least 24 new drug products were commercially approved for human consumption by the Food and Drug Administration (FDA) and European Medicines Agency (EMA) (Bhujbal, 2021; Vasconcelos, 2016). An ASD system is composed of an amorphous drug stabilized in an excipient matrix, most commonly a polymer. Amorphous forms have higher free energy and therefore have higher aqueous solubility and/or faster dissolution rates compared to crystalline materials (Iyer et al., 2021). The inherent

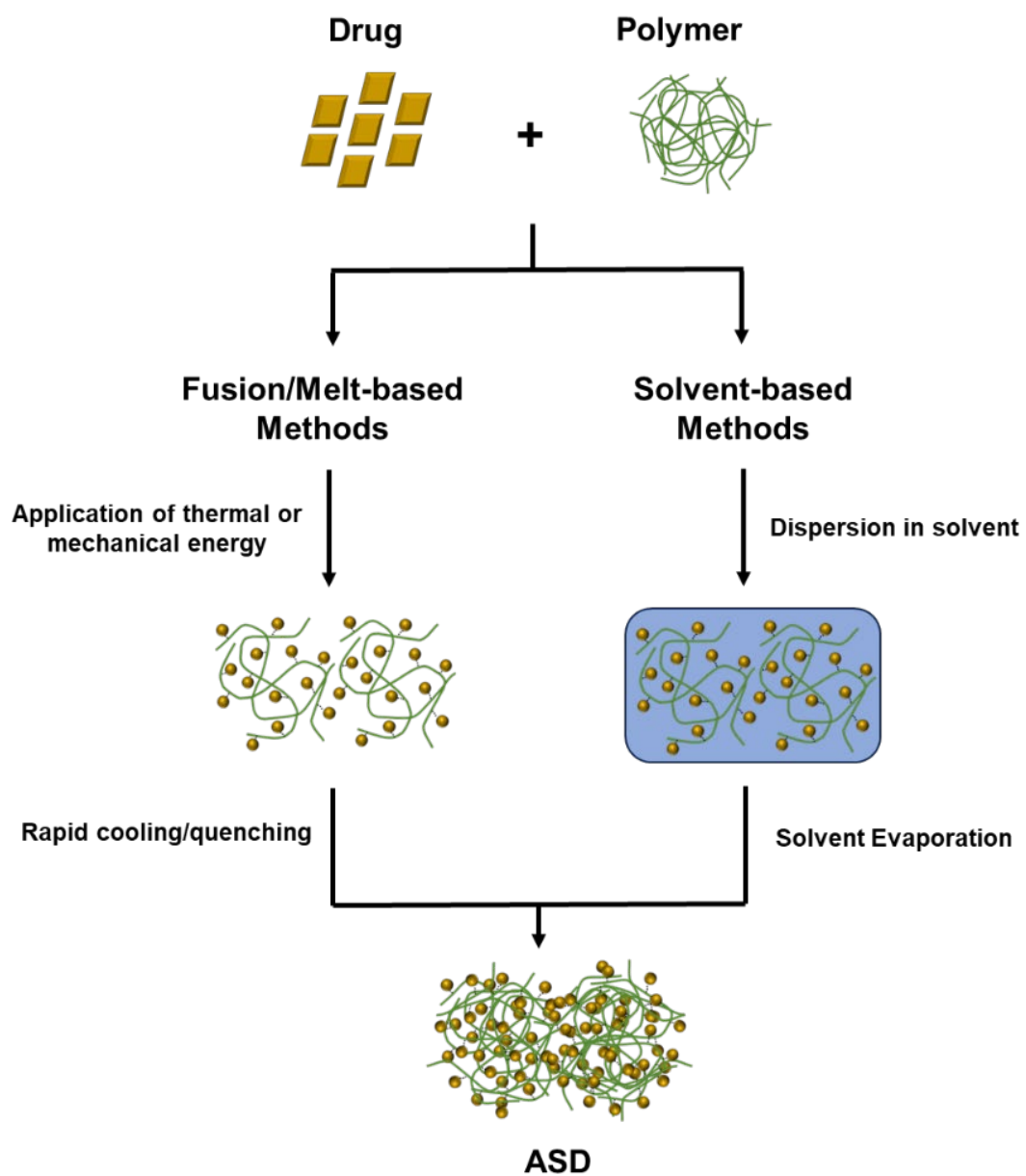
thermodynamic instability means the compound has a propensity to crystallize during processing, storage, or administration (Zografi & Newman, 2015).

1.3 Preparation Methods

There are several well-known methods for preparing ASDs, but they can be categorized into two main categories based on the technology: solvent-based methods and fusion/melt-based methods. Both categories involve initially disrupting the crystal lattice of the drug and converting it to a liquid either by dispersion in a solvent system or by applying thermal and/or mechanical energy. The system is subsequently either dried through solvent evaporation or solidified by rapid cooling/quenching. A schematic of solvent-based and fusion/melt-based methods is shown in Figure 3.

Figure 3.

Schematic of Fusion/Melt-Based and Solvent-Based Methods for Preparing ASDs



1.3.1. Solvent-Based Methods

Solvent-based methods for preparing ASDs require dissolution of the active pharmaceutical ingredient and any necessary excipients in a solvent or combination thereof. The solvent system is subsequently evaporated to leave behind an amorphous solid dispersion. Common examples of solvent-based methods include spray-drying, fluidized bed technology, spray-freeze-drying, and supercritical fluids. These methods are favored due to their nature as a non-thermal process, making it suitable for thermo-labile drugs.

1.3.1.1. *Spray-drying*

Spray-drying is a well-established preparation process that has been around for many years. The first patent application for spray-drying is over 150 years old, and was most extensively utilized in the food and chemical industry (Percy, 1872). The first applications of spray-drying in the pharmaceutical industry involved the processing of neat active pharmaceutical ingredient (API) only and has since evolved to many different applications, including the manufacture of ASDs. At least 13 FDA-approved ASD-based products are prepared through spray-drying (Bhujbal, 2021), establishing that spray-drying is an efficient and commercially scalable process. The first step in preparing ASDs by spray-drying is to combine the API and other necessary excipients in a solvent system to form either a solution or homogenous suspension. The liquid feed solution or suspension is then pumped through an atomizer into a drying chamber fed with a drying gas such as dry air or nitrogen. The atomized droplets containing the drug and excipients travel through the drying chamber, at which point the solvent rapidly evaporates and leaves behind an amorphous solid dispersion. It is important to note the drug is exposed to wet bulb temperatures during drying process and therefore has no exposure to high temperatures during processing. A cyclone is typically installed at the end of

the drying chamber, which allows the separation of the solid dry particles from the gas phase using centrifugal force. The dry particles are directed from the cyclone into a collector for further processing and/or characterization (Singh & Van den Mooter, 2016).

Spray-drying is a continuous and scalable process that is advantageous when processing thermo-labile drugs and drugs with a high melting temperature. On the other hand, challenges such as finding a suitable solvent system that can produce a homogenous feed of drug and excipients, concerns about residual solvents in the ASDs, and use of large amounts of solvents are key considerations for selection of this process.

1.3.1.2. Fluidized Bed Technology

Pharmaceutical processes such as granulation, coating, and drying have utilized fluidized bed technology, and such unit operations have also been applied to preparation of ASDs. Fluidized bed technology is based on the principle of air suspension (Mendonsa et al., 2020). A homogenous mixture of drug and polymer dissolved in a solvent system are sprayed onto inert excipients in a fluid bed granulator/coater, where solvent removal, deposition, and granulation of the solid dispersion occur simultaneously. Additional excipients to tune the drug release profile can also be spray-coated onto the granules during the same step. This eliminates an additional unit operation, making the process more efficient and removes intermediate stability concerns (Newman, 2016). Scalability of the process may be challenging but not impossible, as demonstrated by marketed drug products prepared using this process (Narayan et al., 2015).

1.3.1.3. Supercritical Fluids

Supercritical fluids (SCF) are gases that are present in both liquid and gas states due to the pressure and temperature conditions. The use of supercritical fluid technology capitalizes on the liquid phase present as this solubilizes the drug and polymer, whereas the gas phase aids in

solid diffusion and solvent evaporation (Pasquali et al., 2008). Preparing ASDs using SCFs may be divided into three groups: rapid expansion of supercritical solution (RESS), SCFs as antisolvents, and SCFs as solute. Carbon dioxide is a commonly used fluid in SCF technology because it is non-toxic, cost-effective, environmentally friendly, and easy processing (Srinarong et al., 2011). Advantages of this ASD preparation method is that it is more environmentally friendly and more cost-effective relative to other solvent-based methods. Some limitations with this method include difficulty in removing residual solvents if used and a high initial capital investment (Bhujbal, 2021).

1.3.2. Fusion or Melting-Based Methods

Fusion or melting -based methods that are used in the pharmaceutical industry include hot melt extrusion (HME) and KinetiSol®. In addition, small bench or pilot scale methods such as melt-quench or microwave heating have also been used for preparation of ASDs. Fusion or melting-based methods are popular due to the scalability and solvent-free nature. Challenges such as thermal stability of the drug and identifying drug/polymer combinations where the drug is miscible or soluble in the polymer are some of the key considerations in selection of these methods.

1.3.2.1. Hot Melt Extrusion

Hot melt extrusion (HME) is a recognized manufacturing process, with applications in the food and plastics industry since the 1930s (Shah, 2013). In the last few decades, its prominence has increased in the pharmaceutical industry for the preparation of ASDs, with several key commercial products being prepared using this process. Currently marketed HME products include oral drug products as well as ophthalmic inserts, implants, and devices (Simoes, 2019). HME involves the application of heat and mechanical force to melt and extrude a blend of

drug and polymeric excipients to prepare a homogenous solid product; the heat aspect reduces the viscosity of the blend while the shear from the screw elements improves the homogeneity and dispersion of the components (Repka et al., 2018). The key steps in HME involves feeding of the drug and polymer either individually or as a pre-mixed blend through a hopper into a barrel equipped with screws. The barrel of the HME equipment can be divided into different modules, with the first module of the barrel being responsible for melting and plasticization. The second module is responsible for mixing and kneading. The third module is where discharging and subsequent extrusion through dies of varying shapes and sizes occur. After cooling of the extrudate occurs, the product may be put through a pelletizer that is attached to the HME equipment, or the ribbons may be milled in a separate unit operation. The screws mounted in the barrel are a key piece of the process as it aids in conveying, mixing, and discharging the molten blend through the different zones of the barrel. They determine key factors such as residence time in the equipment, facilitation of mixing, and elimination of dead no-movement zones in the molten mass. Key advantages include the continuous, scalable, and cost-effective nature of the process. In addition, the solvent-free nature increases its attractiveness from a sustainability perspective as the industry looks to reduce its environmental impact and production costs (Tambe, 2021).

1.3.2.2. *KinetiSol®*

KinetiSol® is a novel technology that uses high mechanical shear forces to prepare an amorphous solid dispersion from a blend of drug and necessary excipients. The blend is fed into a vessel containing a series of paddles and shaft with high-speed mixing blades. This process generates a tremendous amount of shear energy and frictional forces such that external heating is not necessary to render the drug amorphous. The molten mass is then discharged from the vessel

and quenched typically by pressing into a flat disk to maximize surface area and heat transfer, after which milling is performed to reduce to a target particle size. (Ellenberger et al., 2018). KinetiSol® has a number of advantages, including the ability to process thermally labile or high melting points drugs, or high molecular weight, viscous polymers. Some key considerations using this technology are the batch or semi-continuous nature, or the ability to process shear-sensitive drugs. Overall, KinetiSol® is a promising enabling technology.

1.4 Characterization Methods

1.4.1. Differential Scanning Calorimetry/Modulated Differential Scanning Calorimetry

Thermal analytical techniques such as differential scanning calorimetry (DSC) or modulated differential scanning calorimetry (mDSC) has been used to determine changes in a physical property of a material as a function of temperature and time. Important characteristics such as melting temperature, enthalpy of fusion, glass transition temperature, polymorph transitions, and physical form can be identified using DSC and mDSC. The heating rate is changed linearly with conventional DSC, and a single heat flow rate signal is acquired. With mDSC, the sample is subjected to two simultaneous heating rates: the first being a linear heating rate akin to conventional DSC and the second being a sinusoidal or modulated heating rate. The difference between DSC and mDSC can be explained with the following equation:

$$\frac{dH}{dt} = C_p \frac{dT}{dt} + f(T, t) \quad (2)$$

where dH/dt is the total heat flow, C_p is the heat capacity of the sample, dT/dt is the heating rate, and $f(T, t)$ is the kinetic heat flow. The total heat flow dH/dt has two components: the first term $C_p \cdot dT/dt$ is the ‘heat capacity component’ or ‘reversing heat flow’, and the second term $f(T, t)$ is

the ‘kinetic component’ or ‘nonreversing heat flow’ (Thomas, 2005). With conventional DSC, only the total heat flow dH/dt is measured, which shows the sum of all thermal events occurring at a specific time or temperature. With mDSC, both the total heat flow dH/dt and $C_p \cdot dT/dt$ are measured, which from which $f(T,t)$ may be calculated. The ability to resolve the reversing heat flow and the nonreversing heat flows allows the identification of complex transitions during the experiment. Information about heat capacity, melt events, or glass transition events can be obtained from the reversing heat flow signal, whereas enthalpy recovery or crystal perfection can be obtained from the nonreversing heat flow signal. Many other observations can be obtained from calorimetry experiments. For instance, phase homogeneity and miscibility have also traditionally been assessed with mDSC. The presence of a single glass transition temperature is an indication of a homogenous, single phase, whereas multiple glass transition temperatures are indications of phase separation (Baird, 2012). In addition, the deviation of the measured glass transition temperature from the predicted glass transition temperature (as calculated by models such as the Gordon-Taylor or Fox equations) are indicative of the presence of either drug-drug, polymer-polymer, or drug-polymer interactions (Schneider, 1988). Some limitations of DSC are the difficulty in resolving glass transition temperature if less than 10°C exists between distinct glass transition temperatures as well as the resolution of domains less than 30 nm in size (Sarpal, 2021).

1.4.2. Powder X-ray Diffraction

Powder X-ray diffraction (PXRD) is a non-destructive technique that provides detailed information about the crystallographic structure, chemical composition, and physical properties of a materials. A typical X-ray diffractogram pattern plots the intensity of the signal against 2θ .

The principle of using PXRD to obtain structural information is based on the Bragg equation shown below:

$$n\lambda = 2d \sin \theta \quad (3)$$

where n is an integer called the diffraction order, λ is the wavelength of the incident X-rays, d is the interplanar spacing of the crystal, and θ is the scattering angle. This equation states that when a sample with long range order is bombarded with monochromatic X-rays at a specific angle, the X-rays are diffracted by the atoms or molecules that make up the crystal lattice. This is observed as sharp, distinct peaks in the diffractogram commonly referred to as Bragg peaks, with each peak representing unique planes within the crystal lattice. This is the case for crystalline solids. For amorphous solids, the non-existence of a long-range order manifests as a broad halo pattern and absence of Bragg peaks. PXRD is a common technique that is used in identification of the crystalline and amorphous phases in ASDs, primarily due to the simplicity of operation, the non-destructive nature, and the ability to perform qualitative or quantitative assessments (Lee et al., 2014). It is important to note that some limitations exist on the resolution or detection of crystallinity in an amorphous material via PXRD; limits of detection and quantitation have previously been demonstrated to at least 0.9 and 1.8% w/w, respectively (Surana, 2000).

1.4.3. Polarized Light Microscopy

Polarized light microscopy (PLM) is a technique that provides qualitative information on the optical properties of a material. It is frequently used in the characterization of a drug's physical form in ASDs, as it leverages the difference in optical properties of crystalline and amorphous materials. Anisotropic materials are materials that exhibit different properties (such

as refractive index) depending on the direction of measurement. Conversely, isotropic materials are materials that exhibit uniform properties in all directions. The majority of crystalline solids are anisotropic, while most amorphous materials are isotropic. In a cross polarized light microscope, light is passed through two polarizers. The first polarizer restricts the light interacting with the sample to one plane of vibration. After transmission through the sample, light is split into rays along two different axes. The second polarizer then recombines the rays, and two outcomes may be observed. If the rays are out of phase due to having been transmitted through material with different refractive indices as anisotropic materials do, they exhibit as phenomena called birefringence. Birefringence in a sample is observed as bright, chromatic particles under PLM. When the light is in phase due to minimal interaction with the sample as in isotropic materials, particles appear as either transparent or dark particles under polarized light. However, it is important to note exceptions to this behavior. Some crystals such as sodium chloride are isotropic and do not exhibit birefringence. In addition, some strained amorphous materials may display some birefringence (Frandsen, 2016).

1.4.4. Thermogravimetric Analysis

Thermogravimetric analysis (TGA) is another commonly used thermal method in the analysis of ASDs. The TGA instrument is equipped with a highly sensitive balance that can be used to measure mass changes in a sample as a function of time and temperature under specified heating conditions. TGA can provide valuable information about the thermal stability, physical form changes, or volatile content of a sample. In addition, TGA has frequently been used to define acceptable processing temperatures for fusion-based methods such as HME (Moseson et al., 2020). It may also be used to determine compatibility of excipients with the drug in a formulation (Rojek, 2022).

1.4.5. Attenuated Total Reflectance-Fourier Transform Infrared Spectroscopy or Raman Spectroscopy

Infrared and Raman spectroscopy are vibrational spectroscopy techniques that have been commonly used in the analysis of ASDs. Both techniques involve the study of the interaction of radiation with molecular vibrations but differ in the manner in which photon energy is transferred to the molecule by changing its vibrational state (Larkin, 2011). In infrared spectroscopy, infrared energy over a range of frequencies is directed to a sample. When the energy of incident radiation matches that of a molecular vibration, the energy is absorbed, and the molecule is promoted to an excited state. The loss of this radiation frequency from the beam is detected and recorded. In contrast, Raman spectroscopy uses a single frequency of radiation to irradiate the sample, and it is the radiation scattered from the molecule which is detected (Smith, 2005). Although radiation is typically discussed in terms of wavelength λ , infrared and Raman spectroscopy are often expressed in terms of frequency ν or wavenumber $\bar{\nu}$ as these are easily related to energy by the following formulas:

$$\lambda = c/\nu \quad (4)$$

$$\bar{\nu} = \frac{\nu}{c} = \frac{1}{\lambda} \quad (5)$$

where λ is the wavelength of energy, c is the speed of light in vacuum 2.99792458 m/s, ν is the frequency, and $\bar{\nu}$ is the wavenumber.

Fourier Transform Infrared spectroscopy (FTIR) is a type of infrared spectroscopy instrument that uses an optical device called an interferometer. FTIR examines the interactions of materials with light in the mid-infrared region (wavenumber of 4000-400 cm^{-1} or wavelength of

2.5 to 25 μm). Attenuated total reflectance (ATR) sampling is when an IR beam is focused at a set angle onto a crystal with a high refractive index, which produces an evanescent standing wave resulting from internal reflections when energy propagates through the crystal. This wave reaches beyond the outer surface of the crystal and into the sample by a few microns (0.5 to 5 μm) (Geraldes, 2020). Raman spectroscopy is a complementary technique to FTIR, and both techniques are commonly used in the pharmaceutical industry for chemical fingerprinting or component identification. In the analysis of ASDs, both techniques are commonly used to determine the presence of intermolecular interactions between the drug and polymer. These interactions are often observed as changes in peak shape or peak position. The advantages of using ATR-FTIR or Raman spectroscopy include the speed, convenience, and accuracy, in addition to being non-destructive.

1.4.6. Ultra Performance Liquid Chromatography

Ultra performance liquid chromatography (UPLC) is a commonly used analytical technique to separate a sample into individual parts on the basis of the interactions of the sample with the mobile and stationary phases (Naushad, 2014). In pharmaceutical analysis, a detector is usually placed at the end of the chromatography column to identify and quantify a sample based on the ultraviolet spectra, mass, or size. A photodiode array (PDA) detector is a type of detector that provides spectral information on a sample. In the context of ASDs, it is a commonly used method for quantifying the drug content and for determining chemical stability issues.

1.4.7. Solid-State Nuclear Magnetic Resonance

Solid-state nuclear magnetic resonance (SS-NMR) is an atomic-level method used to determine the chemical structure, three-dimensional structure, and dynamics of solids and semi-solids (Reif et al., 2021). The fundamental principle of SS-NMR lies in the Zeeman interaction

between the magnetic moment of the nucleus and the external magnetic field. When atoms in a sample are exposed to a magnetic field, the nuclei align in a particular orientation. With the application of radiofrequency pulses at the known resonance frequency of an atom, such as hydrogen or carbon, energy transitions are initiated. The NMR transition frequencies are sensitive to the molecular environment around the nucleus and are commonly reported as chemical shifts. Because of these orientation-dependent chemical shifts, NMR spectra encode three-dimensional structural information (Reif et al., 2021). In the context of ASDs, SS-NMR has been used to probe the presence and nature of drug-polymer interactions based on changes in chemical shifts. Some limitations around use of SS-NMR are related to long experimental times and high costs.

1.5 Physical Stability of Amorphous Solid Dispersions

The drug's physicochemical properties, the compatibility of the polymer with the drug, and the processing method to prepare the ASD all need to be considered carefully in formulation and process design. The relationship between these is critical in stabilizing the drug's amorphous nature during processing and on storage. Any solubility enhancement in amorphization of the drug is lost if the drug reverts to its crystalline form. Crystallization in an ASD may generally be described in the following three phases: (1) nucleation, which is the statistical formation of crystal seeds in the ASD, (2) growth, which is the increase in size of the crystal seeds, and (3) saturation, where the crystallization process slows down as the material around the crystals is depleted of drug and ultimately comes to a halt (Kawakami, 2019). In the following section, the factors that influence the physical stability of the drug in the ASD are discussed.

1.5.1. Drug-Polymer Interactions

Numerous studies have demonstrated that formation of drug-polymer interactions such as hydrogen bonding, ionic interactions, dipole-dipole interactions, or hydrophobic interactions are a critical factor in inhibiting crystal nucleation and growth in an ASD (Konno, 2006; Mistry, 2016). These interactions significantly impact the miscibility and solubility of a drug in a polymer by facilitating molecular mixing, thereby enhancing physical stability (Bookwala, 2022). Several types of intermolecular interactions are well-known in literature, including hydrogen bonding (H-bonding), dipole-dipole interactions, and London dispersion forces. In addition, other types of intermolecular interactions such as ionic, ion-dipole, and halogen bonds remain relatively unexplored in literature. Table 2 summarizes the different types of interactions that have been shown in previous reports (Bookwala & Wildfong, 2023).

Table 2.*Different Types of Intermolecular Interactions in ASDs*

Intermolecular Interaction	Strength of Interaction	Donors	Acceptors
Ionic	Strongest -80 to -494 kJ/mol	R-C(=O)(OH)	R-NH ₂
		R-S(=O) ₂ (OH)	R-NH-R
			R-N(-R)(R)
Ion-Dipole	Stronger <-334 kJ/mol	Na ⁺ , K ⁺ , Ca ²⁺	N, O, I, Br, Cl, F
Hydrogen Bond	Strong -0.8 to -160 kJ/mol	R-H	N, O, F
		R=O>N	
Cation-π	Strong -79 to -159 kJ/mol	Na ⁺ , K ⁺ , Al ⁺ , Ca ²⁺ , NH ⁴⁺	Aromatic/electron-rich π system
Halogen Bond	Strong -5.4 to -46 kJ/mol	R-X	N, O, S, Sc, I, Br, Cl, F
		X=I>Br>Cl>F	
Dipole-Dipole	Weakest -0.06 to -21 kJ/mol	R-D	N,O, I, Br, Cl, F
		D=O>N>F>Cl>Br>I	
Hydrophobic	Weakest -2.9 to -11 kJ/mol	Aromatic/Non-aromatic rings	Aromatic/Non- aromatic rings
		C-chains	C-chains

1.5.2. Chemical Potential Reduction

Chemical potential μ is defined as the measure of the potential that a substance has for undergoing change in a system. It may also be defined as the partial molar free energy G_i (Atkins, 2009). Chemical potential is directly related to Gibbs free energy by the following equations:

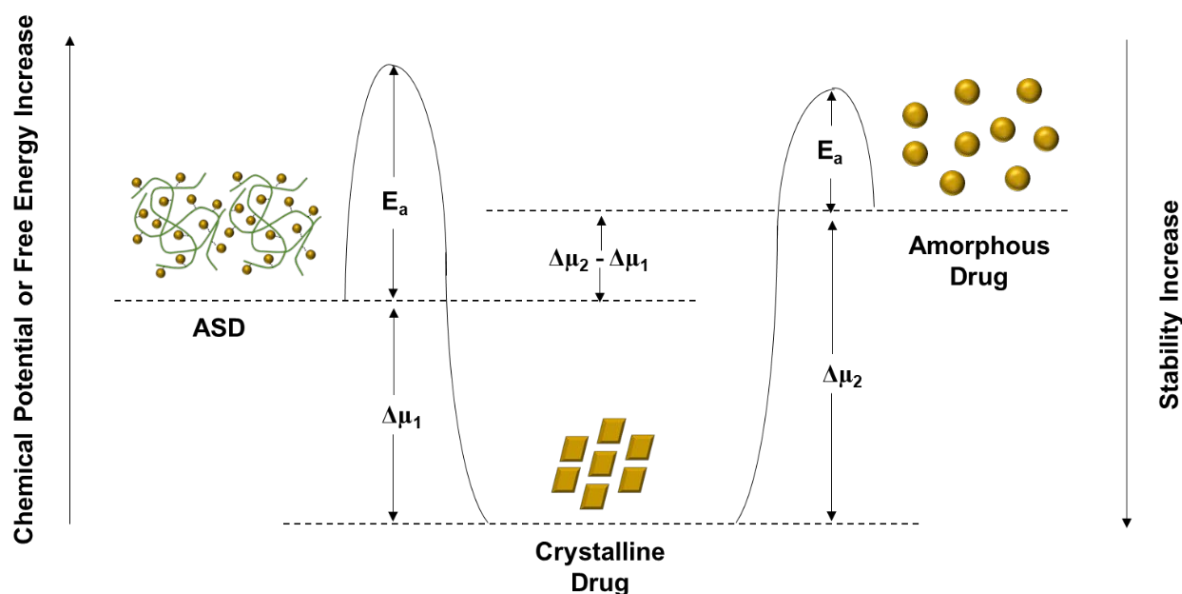
$$G = n_1 G_1 + n_2 G_2 \quad (6)$$

$$G_i = \mu_i \quad (7)$$

where G is the Gibbs free energy of the system, n_1 and n_2 and G_1 and G_2 are the number of moles and partial molar Gibbs energy of components 1 and 2, respectively, and μ_i is the chemical potential of component i . All systems tend to reduce their chemical potential to the state of the lowest potential energy (Teja et al., 2013). In the context of amorphous solid dispersions, chemical potential acts as a driving force for nucleation and crystallization since the pure amorphous drug has a higher chemical potential relative to the crystalline form of the drug. Chemical potential of the pure amorphous drug is lowered when it is combined with a polymer in an ASD, given the assumption that the drug and polymer have sufficient miscibility. The energy and chemical potential landscape for the crystalline drug, the amorphous solid dispersion, and the amorphous drug are shown in Figure 4 (Baghel et al., 2016; Teja et al., 2013).

Figure 4.

Energy Landscape of Crystalline Drug, Amorphous Solid Dispersion (ASD), and Amorphous Drug



The reduction in chemical potential (and therefore, free energy) with the addition of a polymer to the amorphous drug reduces the driving force for crystallization of the amorphous drug. This reduction in free energy is enhanced by strong intermolecular interactions between drug and polymer, where such interactions are typically observed (Newman & Zografis, 2022).

1.5.3. Molecular Mobility Reduction

Reducing the molecular mobility has been demonstrated to have a key role in physical stabilization of an ASD. In literature, the term molecular mobility may refer to global mobility or local mobility. Global mobility represents large-scale mobility and may also be referred to as structural, primary, or α -relaxations. Global mobility refers to molecular motions that are associated with the glass transition in the amorphous state (Bhattacharya & Suryanarayanan, 2009). The change in free volume in the glassy state is negligible compared to that in the

supercooled liquid during cooling; this means that neighbor molecules must ‘cooperate’ to undergo a change in relative positions and the time for molecules to diffuse through an interparticle distance increases near the glass transition temperature (Angell, 1995). On the other hand, local mobility represents small-scale mobility of drug or polymer chains, and may also be referred to as β -relaxations (Aso & Yoshioka, 2006). Local mobility typically occurs on a much faster time scale compared to global mobility, with relaxation times of $<10^{-1}$ seconds compared to 100 seconds, respectively (Bhattacharya & Suryanarayanan, 2009). These may involve motions of an entire molecule or reorientation of parts of a molecule. While distinct, molecular mobility reduction is related to drug-polymer interactions; intermolecular interactions may restrict the vibrational, rotational, and translational motions of the amorphous drug while reducing both global and local mobility (Aso & Yoshioka, 2006; Bhardwaj et al., 2014). This therefore increases the barrier to physical destabilization. For example, Mistry et al have shown that reduced molecular mobility which was attributed to stronger drug-polymer interactions between ketoconazole and polyacrylic acid ASDs could delay the crystallization onset temperature and crystallization extent (Mistry, 2016).

1.6 Determination of Drug-Polymer Interactions

Drug-polymer interactions may be probed directly using analytical techniques. They may also be probed indirectly using solubility and miscibility between drug and polymer as markers for intermolecular interactions. The following sections discuss the different techniques that have been used to determine drug-polymer interactions in literature.

1.6.1. Evaluation of Drug-Polymer Interactions

Several techniques may be used to investigate the interactions that exist between drug and polymer in an ASD. One technique that has been used to understand and characterize the

intermolecular interactions between drug and polymer in an ASD is with the use of differential scanning calorimetry (DSC) (Van den Mooter, 1999). The degree of interactions between drug and polymer have traditionally been assessed by evaluating the deviation between the experimental T_g from the predicted T_g of the drug-polymer composite (Barmapalexis, 2013; Zhang, 2014). When heteronuclear interactions (interactions between drug and polymer) are stronger than homonuclear interactions (interactions between drug and drug or polymer and polymer), there is a lower net excess of free volume upon mixing which manifests as a higher T_g than predicted. When homonuclear interactions are stronger than heteronuclear interactions, there is a higher net excess of free volume upon mixing, which manifests as a lower T_g than predicted. When there is no net excess free volume change (assumes ideal mixing), the experimental T_g is in accordance with the predicted T_g . Several models that may be used to predict the T_g are shown below; Equations 8, 9, 10, and 11 are known as the Fox Equation, Gordon-Taylor Equation, Couchman-Karaszi Equation, and Kwei Equation (Couchman, 1978; Fox, 1956; Gordon; Taylor, 1952; Kwei, 1984). These equations are based on a weighted average of the individual components' respective T_g s.

$$\frac{1}{T_{g,composite}} = \frac{W_1}{T_{g,1}} + \frac{W_2}{T_{g,2}} \quad (8)$$

$$T_{g,composite} = \frac{W_1 T_{g,1} + K_{GT} W_2 T_{g,2}}{W_1 + K_{GT} W_2} \quad (9)$$

$$T_{g,composite} = \frac{W_1 T_{g,1} + K_{CK} W_2 T_{g,2}}{W_1 + K_{CK} W_2} \quad (10)$$

$$T_{g,composite} = W_1T_{g,1} + W_2T_{g,2} + qW_1W_2 \quad (11)$$

where T_g , composite is the predicted T_g of the ASD, W_1 and W_2 , and $T_{g,1}$ and $T_{g,2}$ are the weight fractions and T_g s of components 1 and 2, respectively. K_{GT} , K_{CK} , and q are constants. K_{GT} and K_{CK} are calculated using Equations 12 and 13 below:

$$K_{GT} = \frac{\rho_1 T_{g,1}}{\rho_2 T_{g,2}} \quad (12)$$

$$K_{CK} = \frac{\Delta C_{p,1}}{\Delta C_{p,2}} \quad (13)$$

where ρ_1 and ρ_2 , and $C_{p,1}$ and $C_{p,2}$ are the densities and specific heat capacities of the components 1 and 2, respectively.

Infrared (IR) spectroscopy techniques such as Raman and Fourier Transform Infrared spectroscopy (FTIR) are routinely used to characterize drug-polymer interactions in ASDs (Kothari, 2014; Saboo et al., 2020; Sarpal, 2021). These techniques are convenient, widely available, and can be used to provide information on the molecular level. The majority of data that exist in literature leverage spectroscopy only as a qualitative measure. The representation of infrared spectra as linear vector of intensities that allows the use of mathematical algorithms for quantitative comparison and identification has been used for many years (Henschel, 2020; Tanabe, 1975); however, there have been a limited number of studies that have used these

techniques to quantitatively determine the strength and extent of intermolecular interactions in ASDs (Silva, 2016).

Solid-state NMR can be used to study drug-polymer interactions, and is a powerful tool to access structural and dynamic information (Pugliese, 2022; Sarpal, 2021). However, it can be extremely costly and not as easily accessible as other techniques.

1.6.2. Prediction of Drug-Polymer Solubility and Miscibility

Solubility is defined as the concentration of a drug that can be molecularly mixed by dissolution into an amorphous polymeric carrier such that the solid and solution phases are in equilibrium (Tao et al., 2009). The solubility of drug in a polymer can be visualized as occurring over three stages: the first stage is the disruption of the solute lattice, which in this case is the drug; the second stage involves breaking of the solvent (the polymer in this case) homonuclear interactions, creating void space for the drug to disperse into; and the third stage involves formation of drug-polymer interactions (Bellantone, 2014). Miscibility can be defined as the ability of two components to mix and generate a single homogenous phase (Baird, 2012). Miscibility of the drug and polymer can be determined from the free energy of mixing ΔG_m , which is directly related to the enthalpy of interaction between drug and polymer. Intermolecular interactions between drug and polymer directly influence solubility and miscibility; thus, solubility and miscibility may be used as indicators for drug-polymer interactions (Thakore et al., 2021).

1.6.2.1. Miscibility by Solubility Parameter Estimation (Difference in Solubility Parameters).

Thermodynamically, the free energy of mixing ΔG_{mix} in a system of components at constant temperature and pressure can be defined by the following:

$$\Delta G_{mix} = \Delta H_{mix} - T\Delta S_{mix} \quad (14)$$

where ΔH_{mix} is the enthalpy of mixing, T is the absolute temperature, and ΔS_{mix} is the entropy of mixing. The free energy of mixing is deemed to be favorable when ΔG_{mix} is negative. The entropy of mixing ΔS_{mix} is usually positive due to the increase in degree of freedom with the increased number of available configurations in the system. In ideal solutions, the ΔH_{mix} is zero, as the interactions between components are assumed to be non-existent. Deviations from ideal behavior have been proposed to be captured using the solubility parameter δ . Hildebrand defines the solubility parameter δ as the following (J. H. Hildebrand, 1950):

$$\delta = \sqrt{CED} = \sqrt{\frac{\Delta E_v}{M_v}} = \sqrt{\frac{\Delta H_v - RT}{M_v}} \quad (15)$$

where CED is the cohesive energy density derived from the heat of vaporization, ΔE_v is the free energy of vaporization, M_v is the molar volume, ΔH_v is the enthalpy of vaporization, R is the gas constant, and T is the absolute temperature. The heat of vaporization is also linked to solubility, in that the same energy needed to vaporize a component is the same amount of energy to separate the intermolecular interactions between molecules during mixing. The enthalpy of mixing is related to the solubility parameter δ through the following (J. S. Hildebrand, R., 1950):

$$\frac{\Delta H_{mix}}{M_v} = \phi_1\phi_2(\delta_1 - \delta_2)^2 \quad (16)$$

where ϕ_1 and ϕ_2 are the volume fraction for component 1 and 2, respectively. Hansen solubility parameters account for specific types of interactions with the following equation (Hansen, 1967):

$$\delta_t^2 = \delta_d^2 + \delta_p^2 + \delta_h^2 \quad (17)$$

where δ_t is the total solubility parameter, and δ_d , δ_p , and δ_h are solubility parameters due to London dispersion forces, polar forces, and hydrogen bonding forces, respectively. Several approaches to determine the total solubility parameter based on group contributions have been proposed in literature, including the methods by Hoy and Hoftyzer and Van Krevelen (Hoftyzer & Van Krevelen, 1976; Hoy, 1989). Based on the predicted solubility parameters, a theoretical approach to estimate miscibility looks at the difference between the calculated solubility parameters for the drug and the polymer in an ASD. When the difference $\Delta\delta$ between drug and polymer is $< 7.0 \text{ MPa}^{1/2}$, the two are likely to be miscible. When $\Delta\delta$ is $> 10.0 \text{ MPa}^{1/2}$, the two phases are likely to be immiscible (Greenhalgh, 1999).

1.6.2.2. Miscibility: Flory-Huggins Interaction Parameter Using Solubility Parameters.

Flory-Huggins Theory is a well-known lattice-based theory describing polymer-solvent or polymer-polymer miscibility on the basis of Gibbs free energy change before and after mixing (Flory, 1953; Zhao, 2010). It has been used to express the ΔG_{mix} of mixing the drug and polymer in terms of enthalpy and entropy as follows:

$$\Delta G_{\text{mix}} = RT(\phi_d \ln \phi_d + \frac{\phi_p}{m} \ln \phi_p + \phi_d \phi_p \chi) \quad (18)$$

where R is the gas constant, T is the absolute temperature, ϕ_d and ϕ_p are the volume fractions of drug and polymer, respectively, m is the ratio of the volume of a polymer chain to drug molecular volume, and χ is the Flory-Huggins drug-polymer interaction parameter. The first two terms represent the entropy of the system, and the last term represents the enthalpy of the system. As previously discussed, ΔG_{mix} defines the favorability of mixing. The entropy terms generally favor mixing due to the increased number of degrees of freedom when mixing components, while the enthalpy term may offset entropic gains. Flory-Huggins Theory has been used to assess the miscibility in a drug-polymer systems once χ is known. One method used to determine χ involves the use of solubility parameters δ . This method is suitable for estimating χ at room temperature.

$$\chi = \frac{v(\delta_{\text{drug}} - \delta_{\text{polymer}})^2}{RT} \quad (19)$$

where v is the volume per lattice site and δ_{drug} and δ_{polymer} are the calculated solubility parameters for the drug and polymer, respectively. As previously mentioned, group contributions methods such as Hoy or Hoftyzer and Van Krevelen have been used to estimate δ_{drug} and δ_{polymer} . Flory-Huggins interaction parameter $\chi \leq 0$ is indicative of interactions between drug and polymer, predicting miscibility, while $\chi > 0$ are indicative of stronger interactions between drug-drug or polymer-polymer, which may potentially lead to phase separation.

1.6.2.3. *Miscibility: Flory-Huggins Interaction Parameter Using Melting Point Depression*

Method

Another method that has been used to determine the Flory-Huggins interaction parameter χ was outlined by Marsac using melting point depression data obtained using DSC experiments with physical blends of drug and polymer (Marsac, 2008) :

$$\frac{1}{T_{mix}} - \frac{1}{T_{pure}} = -\frac{R}{\Delta H_m} \left[\ln \phi_d + \left(1 - \frac{1}{m}\right) \phi_p + \chi \phi_p^2 \right] \quad (20)$$

where T_{mix} and T_{pure} are the melting points of the drug in the drug-polymer blend and pure drug, respectively, ΔH_m is the heat of fusion of the pure drug. With all other values known, the terms are rearranged and linearly fitted against ϕ_p^2 , and the slope is determined to be χ at a temperature close to the drug melting point. The same criteria as discussed above can be applied here: $\chi \leq 0$ is indicative of interactions between drug and polymer, predicting miscibility, while $\chi > 0$ are indicative of stronger interactions between drug-drug or polymer-polymer, which may indicate immiscibility.

1.6.2.4. *Determination of Flory-Huggins Interaction Parameter as a Function of*

Temperature to Predict Miscibility at any Temperature.

The Flory-Huggins interaction parameter χ is expected to have a temperature and composition dependence as shown below:

$$\chi = A + \frac{B}{T} + C_1\phi + C_2\phi^2 \quad (21)$$

However, this expression has been simplified to account for temperature only, and this has been shown to be sufficient in many polymer systems. The simplified equation is shown below (Zhao, 2010).

$$\chi \cong A + \frac{B}{T} \quad (22)$$

By using χ determined by melting depression data and by solubility parameters, A and B can be calculated as a system of two equations with two unknowns. Once Equations (18) and (22) are combined, ΔG_{mix} can be determined for any temperature and composition.

1.6.2.5. Miscibility by Determination of Gibbs Free Energy of Mixing.

As previously mentioned, the Gibbs free energy change upon mixing ΔG_{mix} may be predicted as a function of temperature and composition once the temperature dependence of the Flory Huggins interaction parameter χ is determined. When $\Delta G_{\text{mix}} < 0$ and ΔG_{mix} is convex, this is indicative of a miscible system. When $\Delta G_{\text{mix}} > 0$ and concave, this is indicative of a partially miscible or immiscible system (Tian, 2013).

1.6.2.6. Kinetic Miscibility: A Single T_g .

A kinetic evaluation of miscibility can be performed based on T_g obtained by using DSC. Discussions of miscibility in previous sections have been placed in the context of thermodynamic equilibrium. However, the glassy state of an ASD is not an equilibrium state; rather, it is in a dynamic kinetic state. A single T_g has been traditionally accepted to indicate miscibility between SIM and polymer, whereas multiple T_g s denote inhomogeneity (Baird, 2012). Some limitations with this approach are related to the characteristics of the drug and

polymer. When the T_g s of each component are within 10°C of one another or are present in domains $<30\text{ nm}$, the appearance of a single T_g may be misleading (Sarpal, 2021).

1.6.2.7. Solubility using Melting Point Depression Experiments.

Melting point depressions experiments with DSC are one of the most widely used methods to determine solubility of a drug in a polymer. These methods are based on the concept that the melting point of a crystalline material may be depressed when mixed with a miscible amorphous material. Several variations of these experiments have been proposed in literature. One method proposed by Tao et al relies on the preparation of drug and polymer mixtures by milling, and subsequent measurement of the samples by DSC. By plotting the melting temperature T_m endpoint against the composition, the solubility curve of the crystalline drug in the amorphous polymer may be obtained (Tao et al., 2009). Sun et al proposed an improvement to this method by introducing a long annealing step after milling prior to melting point depression experiments (Sun et al., 2010). These methods are limited by the prediction of drug solubility at temperatures close to the glass transition temperature T_g . A comparison of these methods is outlined by Knopp (Knopp et al., 2015).

1.6.2.8. Solubility using Liquid Low Molecular Weight Polymer Analogs.

Marsac et al proposed a drug solubility in polymer method using a liquid low molecular weight analog of the polymer. In this method, the Flory-Huggins interaction parameter χ could be calculated from solubility measurements of the drug in the liquid analog of the polymer. Some limitations of this method are the assumptions that the interaction parameters for the drug/polymer and drug/monomer are the same, and that liquid analogs of the polymer exist (Marsac, 2008).

1.6.2.9. Solubility: Extrapolation using Enthalpy of Fusion ΔH_m extrapolation.

One method to determine solubility of drug in polymer is based on the enthalpy of fusion ΔH_m (Theeuwes, 1974). The enthalpy of fusion ΔH_m is defined as the heat needed to convert a material from the solid to liquid state without the temperature increasing (Atkins, 2009). When the drug concentration in a drug-polymer mixture is above the solubility, the saturated amorphous solid phase is in apparent equilibrium with the undissolved drug crystals. In a DSC experiment, the undissolved drug crystals will contribute to an endothermic melt event. The enthalpy of fusion ΔH_m for a drug may be obtained and regressed against the drug concentration in each in each mixture. The x-intercept is used to determine the theoretical solubility of drug within the polymer, with the assumption that the dissolved drug does not have any contribution to the endothermic melt event. This method has the potential to determine the solubility of a drug in a polymer system at temperatures away from the drug melting temperature T_m (Amharar et al., 2014).

2. RESEARCH AIMS

2.1 Statement of the Problem

Amorphous solid dispersions (ASDs) represent a promising strategy for improving the bioavailability of drugs with poor aqueous solubility. However, the development of ASDs continues to be a challenge due to the inherent poor physical stability of the amorphous form of a drug, which is thermodynamically driven to revert to the crystalline state. Oftentimes, formulation development of ASDs may be relegated to a trial-and-error process, which can be time-consuming and inefficient, pose a higher risk of failure, and lead to a suboptimal formulation. Elucidating the complex interplay between the drug and polymeric excipient expands the fundamental understanding of ASDs on the molecular level, which is critical to the rational design of ASDs. Ultimately, this leads to faster availability of drugs to patients and to more effective therapeutic outcomes.

2.2 Purpose

The purpose of this dissertation is to investigate the impact of drug-polymer interactions on the physical stability of simvastatin-based amorphous solid dispersions. The application of a novel mathematical algorithm to Attenuated Total Reflectance – Fourier Transform Infrared spectroscopy data is investigated as a method to quantitate the degree of interactions between simvastatin and three distinctly different polymeric excipients. The outcomes are confirmed using experimental techniques and theoretical calculations, using accessible tools such as differential scanning calorimetry and Flory-Huggins theory. Understanding drug/polymer interactions in this system using simple and accessible tools contributes to a more fundamental

comprehension of amorphous solid dispersions and aids in rational formulation and process design.

2.3 Research Aims

The specific aims of this dissertation are the following:

- Aim 1: To prepare and characterize simvastatin-based amorphous solid dispersions using hot melt extrusion at varying drug-polymer ratios with three distinctly different polymeric excipients: polyvinyl pyrrolidone vinyl acetate, hydroxypropyl methyl cellulose, and Soluplus®.
- Aim 2: To determine the degree of drug-polymer intermolecular interactions using a novel application of mathematical processing by way of Pearson correlation coefficient to infrared spectroscopy data and to confirm using a combination of experimental and theoretical techniques such as DSC and Flory-Huggins theory. To understand and characterize miscibility and solubility of simvastatin with different polymeric excipients.
- Aim 3: To determine the impact of drug-polymer interactions on the physical stability of simvastatin in an amorphous solid dispersion.

3. PREPARATION AND CHARACTERIZATION OF SIMVASTATIN-BASED AMORPHOUS SOLID DISPERSIONS USING HOT MELT EXTRUSION

3.1 Introduction

Amorphous solid dispersions (ASDs) are of great interest in the pharmaceutical industry as a strategy for designing formulations for poorly soluble compounds to improve bioavailability. There are several methods for preparing ASDs, but hot melt extrusion (HME) has gained increasing popularity in the last several decades. With its roots in the food and plastics industry in the 1930s, the first manufacturing application in the pharmaceutical industry started in the early 1970s (el-Egakey et al., 1971; Patil et al., 2016; Shah, 2013). Since then, several marketed products have been produced using HME (Simoës, 2019). Key advantages include the continuous, scalable, cost-effective, and solvent-free nature of the process. A factor that requires careful consideration when developing a drug product formulation using HME is the stability of the drug to thermal and mechanical stress. In this study, HME was used to prepare and characterize simvastatin (SIM) ASDs with three distinctly different polymers: polyvinyl pyrrolidone vinyl acetate (PVP-VA), hydroxypropyl methyl cellulose acetate succinate (HPMC-AS), and Soluplus® (SOL).

3.2 Drug Selection

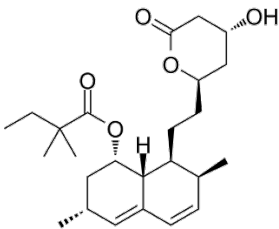
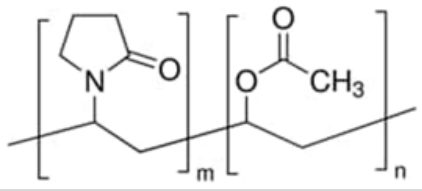
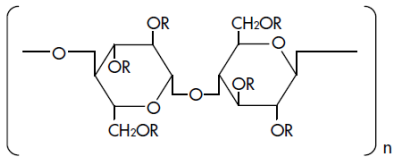
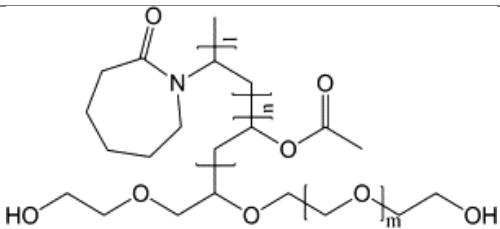
Simvastatin (SIM) was selected as a model drug for these studies. According to the Biopharmaceutics Classification System (BCS), SIM is a class II molecule, indicating poor aqueous solubility and high permeability (Murtaza, 2012). This characteristic renders SIM a particularly suitable candidate for formulation as an ASD. SIM belongs to a pharmacologically significant class of lipid-lowering agents known as statins, which are used for the reduction of cholesterol and levels and for the prevention of cardiovascular disease. Moreover, it has also

demonstrated potential efficacy in the treatment of diverse conditions such as cancer and dermatological diseases (Jowkar, 2010; Sassano, 2008). Anticipating future applications, the reformulation of SIM may be necessary for treatment in alternative therapeutic indications. Crystalline SIM has a melting point of 139°C, and amorphous SIM has a glass transition temperature $T_g \sim 30^\circ\text{C}$ (Kapourani et al., 2020). A summary of relevant properties is shown in Table 3.

3.3 Polymer Selection

The selection of polymers for ASDs is a critical aspect of formulation design. In these studies, polyvinyl pyrrolidone vinyl acetate (PVP-VA), hydroxypropyl methyl cellulose acetate succinate (HPMC-AS), and Soluplus® (SOL) were selected as the polymeric excipients due to their distinctly different characteristics. PVP-VA is a copolymer derived from the monomers N-vinylpyrrolidone and vinyl acetate. HPMC-AS is cellulose ester-based polymer containing methyl, hydroxypropyl, acetyl, and succinoyl groups. SOL is an amphiphilic graft copolymer derived from polyethylene glycol 6000 (PEG 6000), vinyl acetate, and vinyl caprolactam. Each polymer has a different propensity for formation of intermolecular bonds, including hydrogen bonds, dipole-dipole, and hydrophobic interactions, through its structure and functional groups. PVP-VA contains an ester and amide functional group that can act as H-bond acceptors, but no functional groups that can act as an H-bond donor. HPMC-AS contains functional groups that can act as both H-bond donors (alcohols and carboxylic acids) and H-bond acceptors (esters and ethers). Similar to HPMC-AS, SOL contains both H-bond donor groups (alcohols) and abundant H-bond acceptors from its amides, esters, and ethers. Table 3 summarizes each polymer's relevant physicochemical properties.

Table 3.*Physicochemical Properties of SIM, PVP-VA, HPMC-AS, and SOL*

Component	Chemical Structure	Molecular Weight (g/mol)	Melting Point (°C)	Glass Transition Temperature (°C)
SIM		418.6	139	30
PVP-VA		45,000	n/a	108
HPMC-AS	 $\left[\begin{array}{c} \text{---O---} \begin{array}{c} \text{OR} \\ \text{OR} \\ \text{CH}_2\text{OR} \end{array} \text{---O---} \begin{array}{c} \text{CH}_2\text{OR} \\ \text{OR} \end{array} \end{array} \right]_n$ <p> $R = -H$ $-CH_3$ $-CH_2CH(CH_3)OH$ $-COCH_3$ $-COCH_2CH_2COOH$ $-CH_2CH(CH_3)OCOCH_3$ $-CH_2CH(CH_3)OCOCH_2CH_2COOH$ </p>	17,800	n/a	120
SOL		118,000	n/a	70

3.4 Materials

SIM was purchased from Sigma-Aldrich (Acros Organics Geel, Belgium). HPMC-AS MP grade was a gift from Shin-Etsu (Tokyo, Japan). PVP-VA 64 (also known as Copovidone or Kollidon VA 64) and SOL were purchased from BASF (Ludwigshafen, Germany). SIM was stored at 2-8 °C whenever possible. The chemical structures of all starting materials are shown in Table 3.

3.5 Methods

3.5.1. Preparation of Physical Blends

Physical blends (PBs) of SIM and each polymer were prepared at varying weight ratios ranging from 0/100 to 100/0 %w/w SIM/polymer. SIM was thawed at room temperature prior to use. SIM and each polymer were accurately weighed on an analytical balance, combined into a mortar and pestle, and triturated for 1 minute. The resulting blend was collected and mixed by vortexing for 30 seconds prior to blending with a TURBULA T2F 3D mixer (Mettlenz, CH) for 10 minutes.

3.5.2. Preparation of Amorphous Solid Dispersions

Amorphous solid dispersions were prepared by a hot melt extrusion process using a Thermo Scientific HAAKE Minilab II Micro Compounder (Cheshire, UK) with a co-rotating twin-screw at a 5 g batch size. Physical blends of each formulation were first prepared using the procedure outlined in Section 3.5.1. Each blend was then fed into the hot-melt extruder equipped with a thin-slit die at a temperature of 140°C. The extrudate was collected and milled to a visually uniform powder using an IKA tube mill (Wilmington, NC, USA) at 15,000 RPM for approximately 1 minute until visually homogenous. A summary of the ASD formulations prepared by hot melt extrusion for this study is shown in Table 4.

Table 4.*Composition of ASD Formulations Prepared by Hot Melt Extrusion*

SIM/Polymer Ratio (% w/w)	Polymer
0/100	PVP-VA
25/75	
50/50	
75/25	
100/0	
0/100	HPMC-AS
25/75	
50/50	
75/25	
100/0	
0/100	SOL
25/75	
50/50	
75/25	
100/0	

3.5.3. Thermogravimetric Analysis

Thermogravimetric analysis (TGA) was used to analyze the samples for water content and to check chemical compatibility between SIM and each polymer. Samples were prepared at a target weight of 4 – 7 mg and loaded onto a TA Instruments TGA Q500 equipped with Universal Analysis 2000 software (New Castle, DE) and subjected to a 10°C/min ramp rate with a nitrogen purge flow of 50 mL/min. For water content analysis, samples were heated from 25°C to 150°C, and weight loss was attributed to water content. For chemical compatibility experiments, samples were heated from 25°C to 150°C. Analysis was performed using TRIOS software (New Castle, DE).

3.5.4. Modulated Differential Scanning Calorimetry

Modulated differential scanning calorimetry (mDSC) was used to determine thermal characteristics such as the melting point T_m , enthalpy of fusion ΔH_m , glass transition temperature T_g of the starting materials, physical blends, and ASDs. A TA Instruments DSC 2500 equipped with TRIOS software (New Castle, DE) was used, and samples weighing 4 – 7 mg were analyzed in a sealed Tzero aluminum pan at a nitrogen purge flow of 50 mL/min. For characterization of starting materials and ASDs, a 3°C/min ramp rate with a modulation cycle of $\pm 1^\circ\text{C}$ every 60 seconds was used. Duplicate measurements were performed, and the average values are reported. Analysis was performed using TRIOS software (New Castle, DE).

3.5.5. Powder X-ray Diffraction

Samples were analyzed for physical form using a Malvern Panalytical Empyrean (Westborough, MA). Each sample was mounted on a background-free silicon sample holder. Samples were scanned in reflection mode over a $2.0000 - 39.9990^\circ 2\theta$ range with a Cu $K\alpha 1$

radiation source and a detector at 45 kV and 40 mA. The step size was 0.0131 °2 θ and the scan rate was 0.08 sec/step.

3.5.6. Polarized Light Microscopy

Samples were analyzed using an Olympus BX53F light microscope (Tokyo, Japan) with two polarizing filters. A drop of silicone oil with viscosity 1000 cP was placed on a glass slide, and a small amount of sample was deposited into the oil phase prior to covering with a glass coverslip. Glass slide is loaded onto the sample stage prior to analysis with Linkam software (Salfords, United Kingdom).

3.5.7. Ultra Performance Liquid Chromatography

Chemical purity was evaluated using a Waters ACQUITY Premier Ultra Performance Liquid Chromatography (UPLC) system equipped with an ACQUITY UPLC BEH C8 2.1 x 100 mm column (Milford, MA). A method using water with 0.1% trifluoroacetic acid (TFA) and acetonitrile with 0.1% TFA was employed for separation. The flow rate was 0.5 mL/min, with an injection volume of 2 μ L. Injections are performed in triplicate. Detection was performed with a photodiode array detector, and analysis was performed at a wavelength of 236 nm.

3.6 Results and Discussion

3.6.1. Characterization of Starting Materials

SIM starting material was confirmed to exist as a solid crystalline form. This is demonstrated by the presence of distinct Bragg peaks by PXRD as shown in Figure 5 and by the pronounced birefringence observed under polarized light in Figure 6, both of which are indicative of long-range molecular order. In addition, a single T_m onset of 139°C was measured by DSC and thermal degradation onset as indicated by weight loss began at

approximately 200°C, as shown in Figure 3. These data are consistent with what has been reported in literature (Aceves-Hernandez, 2011; Modhave, 2020).

PVP-VA, HPMC-AS, and SOL starting materials were confirmed to exist as amorphous solid forms by the broad, featureless scattering pattern observed by PXRD as well as by absence of birefringence under polarized light, as shown in Figure 5 and Figure 6. T_g for PVP-VA, HPMC-AS, and SOL were measured as 108°C, 120°C, and 67°C, respectively, as shown in Figure 7. Thermal degradation onset as indicated by weight loss began at 244°C, 205°C, and 248°C, respectively, as shown in Figure 7. These align well with previous reports (Diogo, 2022; Moseson, 2018; Sarabu, 2020).

Figure 5.

Physical Form of SIM, PVP-VA, HPMC-AS, SOL Starting Materials by PXRD

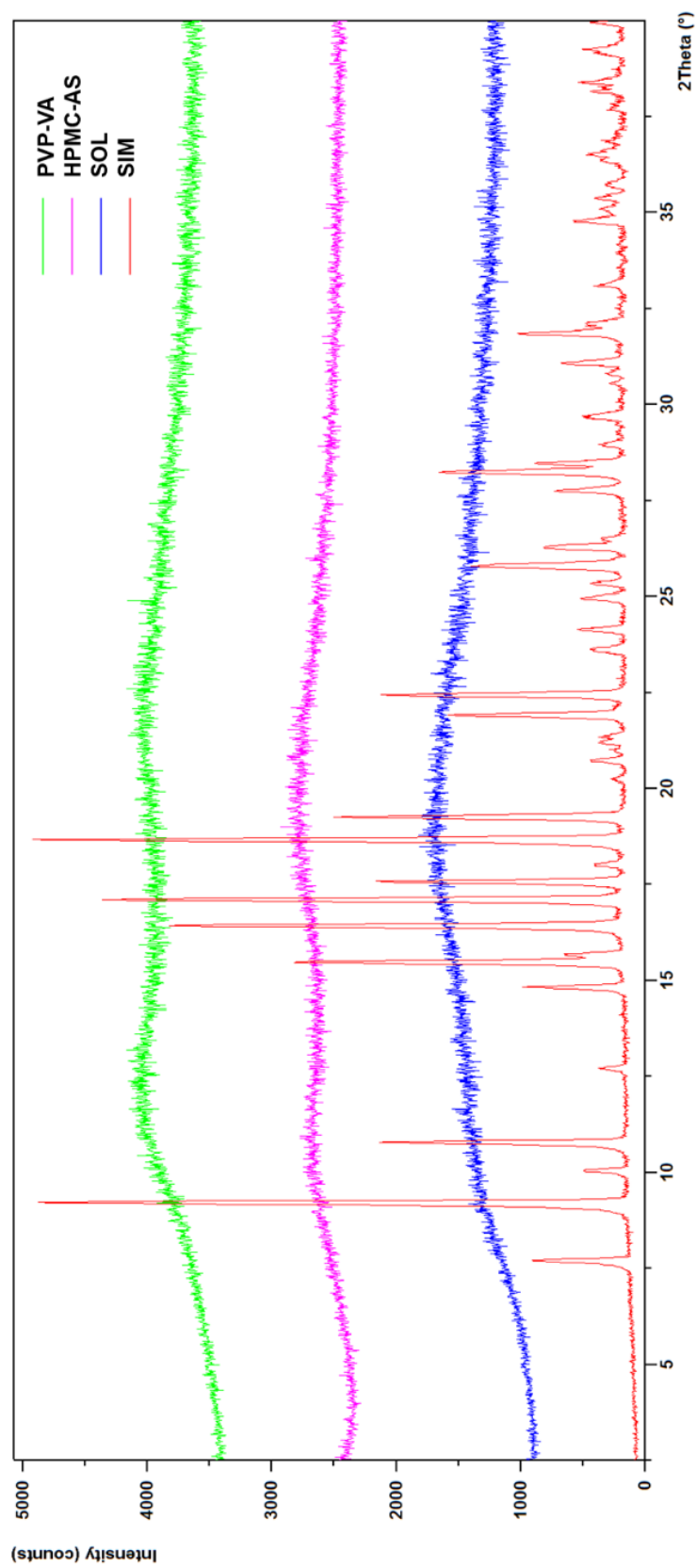


Figure 6.

PLM Images of SIM, PVP-VA, HPMC-AS, SOL Starting Materials

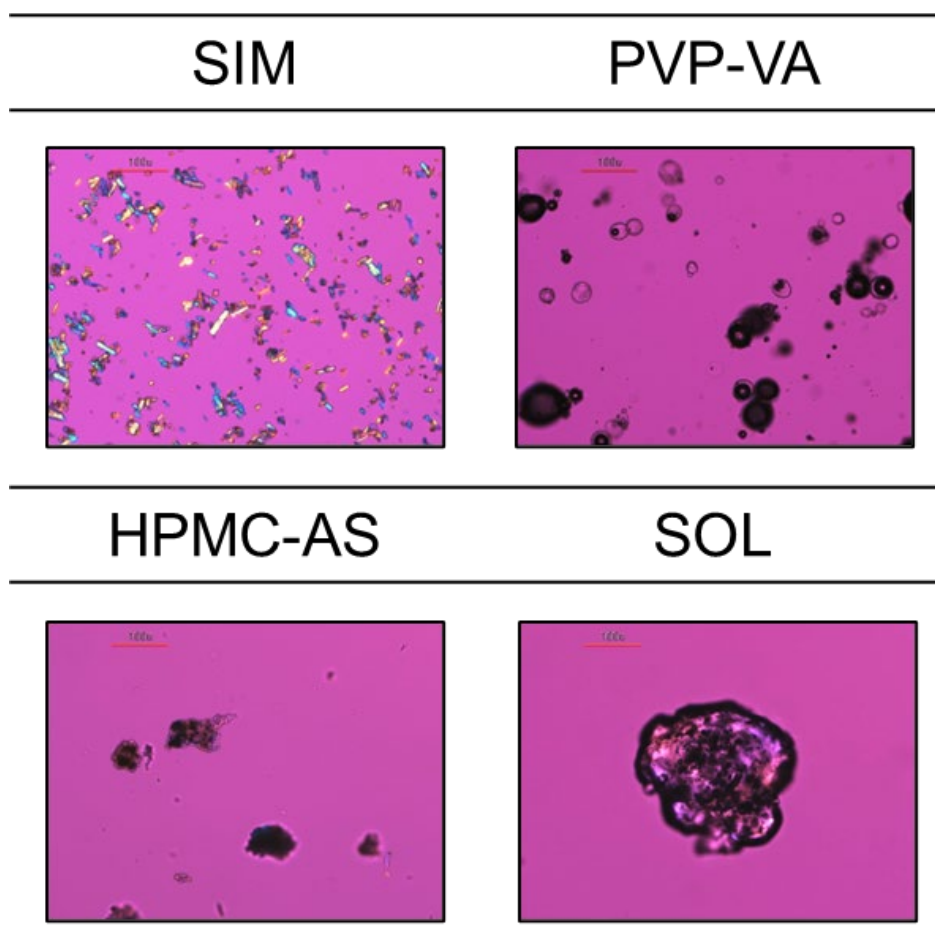
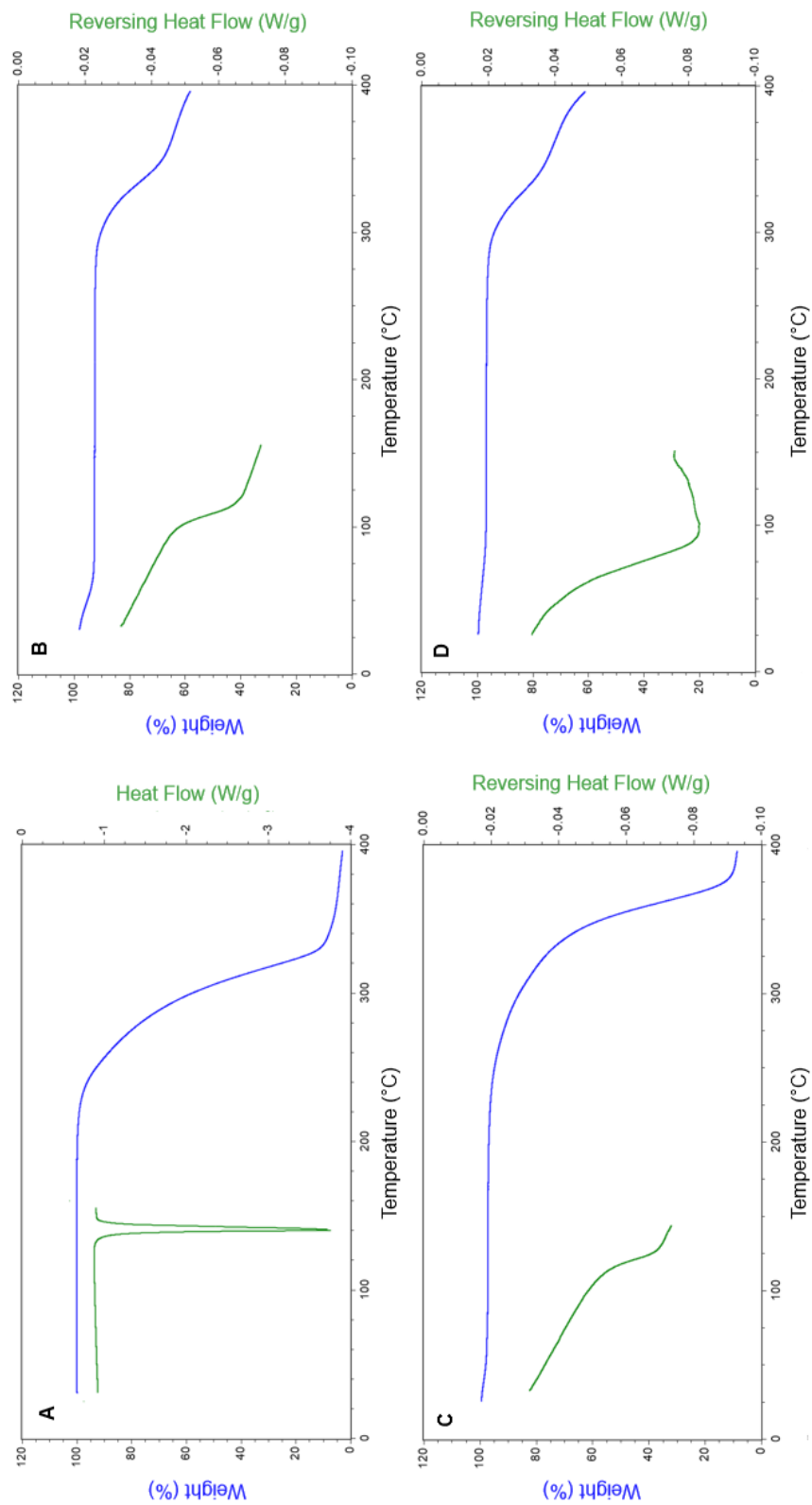


Figure 7.

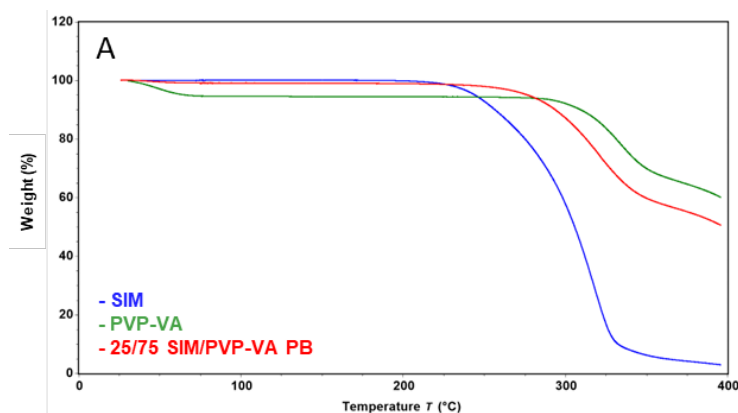
TGA (blue curve) and mDSC (green) Thermograms of (A) SIM, (B) PVP-VA, (C) HPMC-AS, (D) SOL Starting Materials



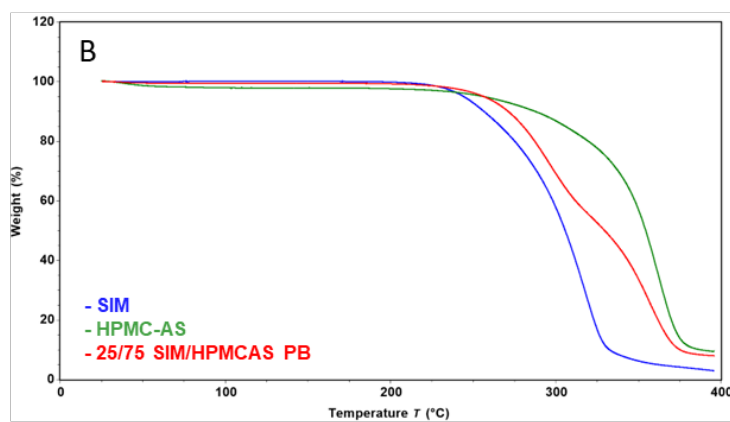
The chemical compatibility between SIM and each polymer was evaluated using TGA. A physical blend of SIM and each polymer was heated and compared to the thermogravimetric analysis of the neat starting materials. Data is shown in Figure 8. Blue, green, and red curves represent the thermograms for neat SIM, neat polymer, and physical blend, respectively. The degradation onset temperatures for SIM/PVP-VA, SIM/HPMC-AS, and SIM/SOL are higher than that of neat SIM, indicating that there are no expected chemical stability issues when heated up to approximately 200°C. Based on this, no thermal stability or chemical compatibility issues are expected at the selected HME processing temperature of 140°C.

Figure 8.

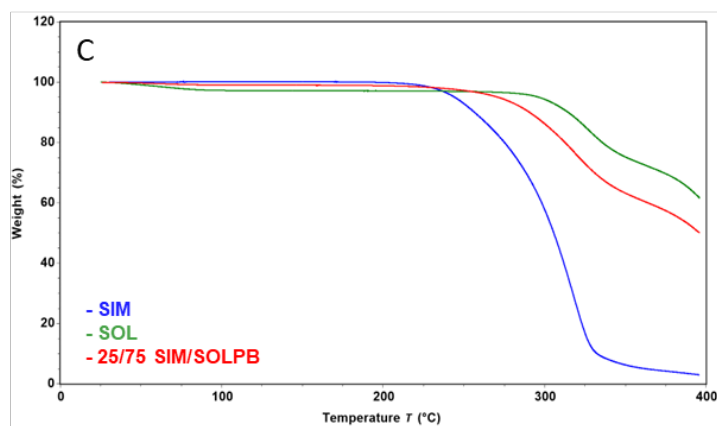
Chemical Compatibility by Thermogravimetric Analysis for (A) SIM and PVP-VA, (B) SIM and HPMC-AS, (C) SIM and SOL



SIM/PVP-VA



SIM/HPMC-AS



SIM/SOL











3.6.2. Hot Melt Extrusion Observations










Extrusion and milling for SIM/PVP-VA and SIM/SOL formulations were straightforward. At a SIM drug load of 75% and 100%, extrudates were noticeably less viscous compared to lower SIM drug load formulations. All extrudates were clear, colorless to pale yellow in appearance and visually homogenous. Images of HME ribbons are shown in Figure 9. Residence time was approximately 5 minutes for each formulation.

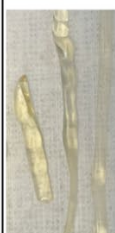








Extrusion and milling for SIM/HPMC-AS formulations presented more challenges relative to SIM/PVP-VA and SIM/SOL ASDs. At SIM drug load of ranging from 0% to 50%, extrudates were noticeably of high viscosity, and necessitated the maximization of the motor force setting to the operational capacity of the extruder. Residence time for these formulations exceeded 10 minutes. Extrudates were clear, pale yellow to yellow in appearance and visually homogenous. At SIM drug load of 75%, a discernible level of inhomogeneity was observed as some solids appeared to be embedded within the ribbon. Extrudates were passed twice through the extruder, after which the extrudate appeared to be visually homogenous. Images of HME ribbons and powders post milling are shown in Figure 9.

Figure 9.

Appearance of HME Ribbons and Post Milling Powder Appearance for SIM/PVP-VA, SIM/HPMC-AS, and SIM/SOL ASDs

	0/100 SIM/PVP-VA	25/75 SIM/PVP-VA	50/50 SIM/PVP-VA	75/25 SIM/PVP-VA	100/0 SIM/PVP-VA
HME Ribbon Appearance					
Post Mill Powder Appearance					

	0/100 SIM/HPMCAS	25/75 SIM/HPMCAS	50/50 SIM/HPMCAS	75/25 SIM/HPMCAS	100/0 SIM/HPMCAS
HME Ribbon Appearance					
Post Mill Powder Appearance					

	0/100 SIM/SOL	25/75 SIM/SOL	50/50 SIM/SOL	75/25 SIM/SOL	100/0 SIM/SOL
HME Ribbon Appearance					
Post Mill Powder Appearance					

3.6.3. Characterization of Amorphous Solid Dispersions Prepared by Hot Melt Extrusion

All ASDs were characterized after extrusion and milling. The physical form of SIM was determined using PXRD, PLM, and DSC. Water content was determined using TGA. Chemical purity was determined using UPLC.

In all formulations, SIM was confirmed to be in the amorphous form by the absence of Bragg peaks in the PXRD diffractograms as shown in Figure 10. PLM was used as an orthogonal method for confirming SIM physical form, as shown in Figure 11. No birefringence was observed in SIM/PVP-VA and SIM/SOL ASDs, confirming SIM to be in the amorphous form in these formulations. For SIM/HPMC-AS ASDs, some birefringence was observed in drug loads of 0% to 50%. Notably, even 100% HPMC-AS when extruded displays some birefringence. However, mDSC also confirmed the amorphous nature of SIM as there was no fusion endotherm observed in the thermograms as shown in Figure 12. Furthermore, the homogeneity and kinetic miscibility of all ASDs were confirmed by the observance of a single T_g for all ASDs. Measurement of multiple T_g s may indicate immiscibility or phase separation between components.

Figure 10.

PXRD Diffractograms for (A) SIM/PVP-VA ASDs, (B) SIM/HPMC-AS ASDs, (C) SIM/SOL ASDs with Crystalline SIM

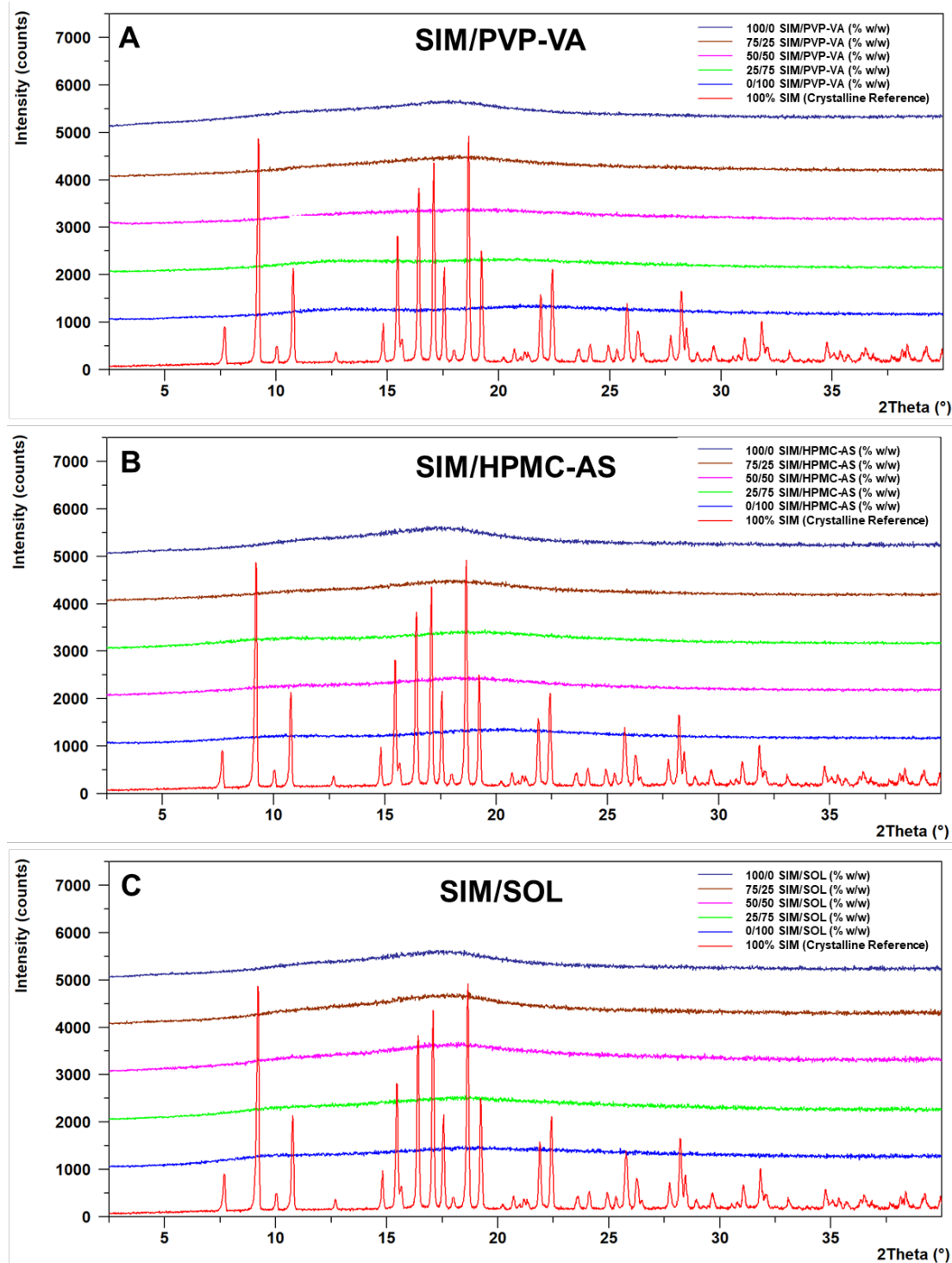


Figure 11.

PLM Images for SIM/PVP-VA, SIM/HPMC-AS, SIM/SOL ASDs


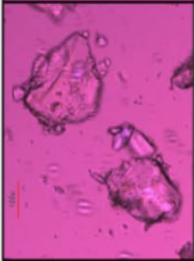

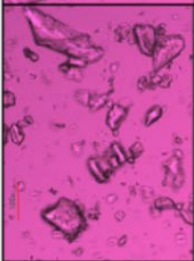
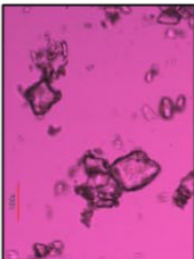
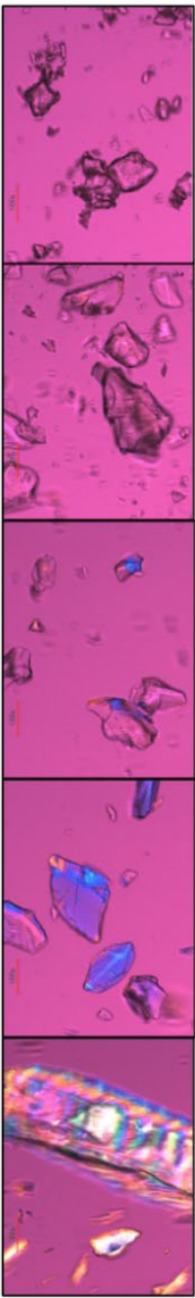
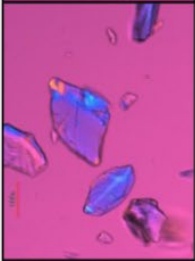
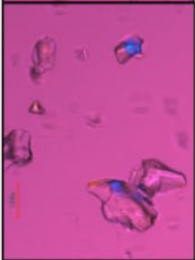
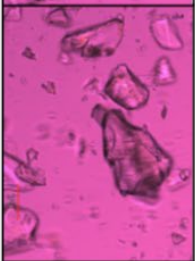
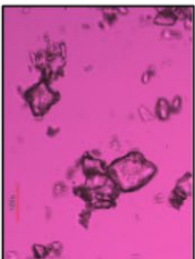
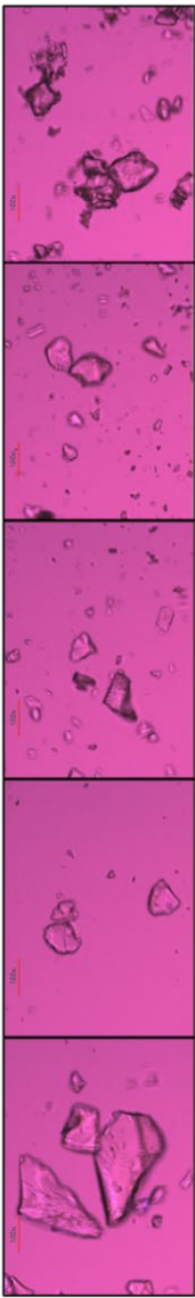

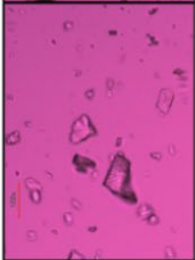
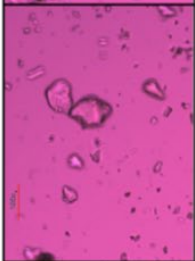
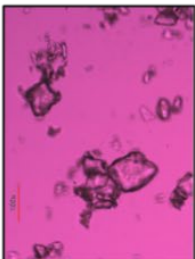
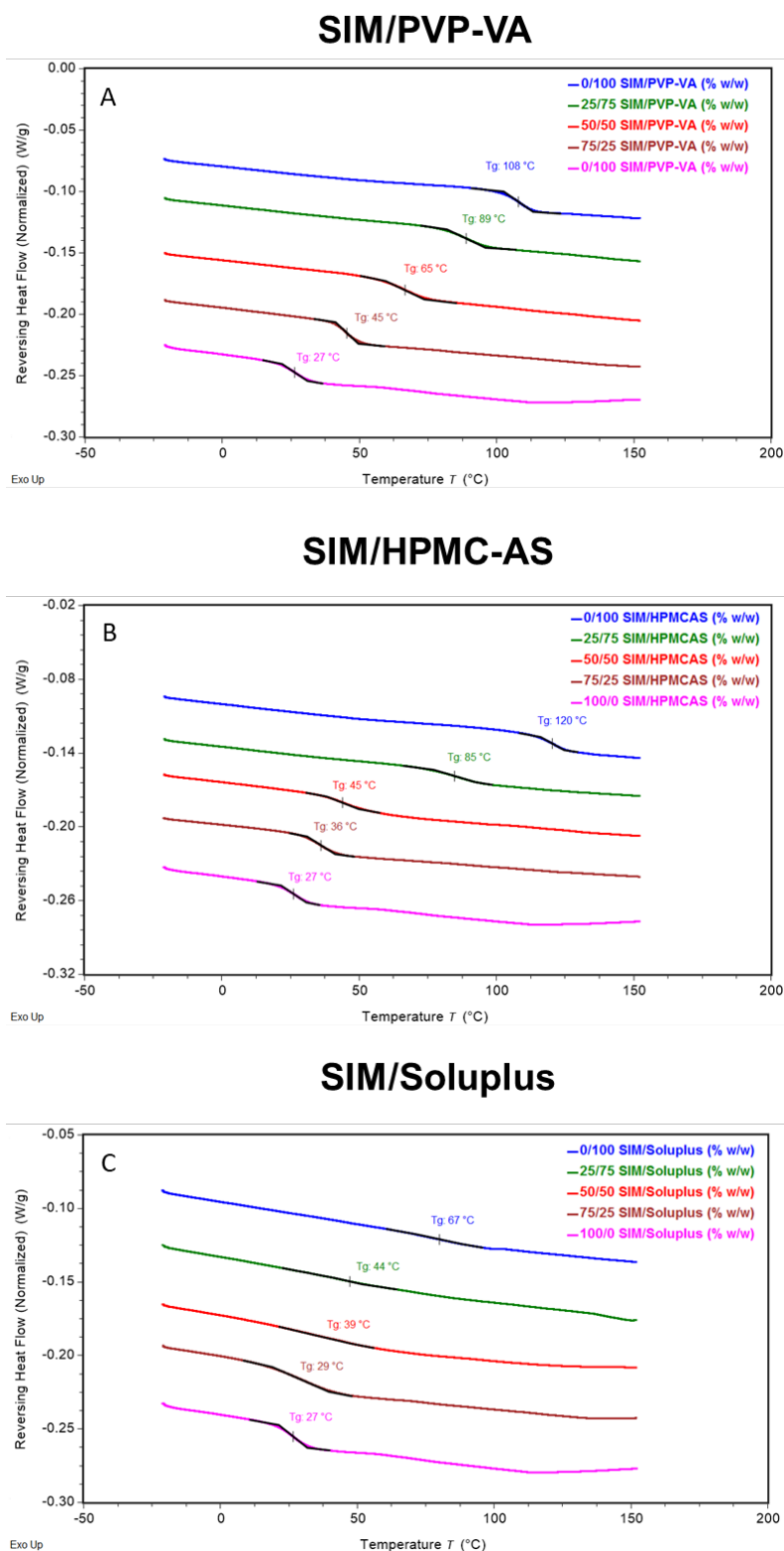
SIM/Polymer ASD	Composition (% w/w)				
	0/100	25/75	50/50	75/25	100/0
SIM/ PVP-VA					
SIM/ HPMC-AS					
SIM/ Soluplus					

Figure 12.

mDSC Thermograms for (A) SIM/PVP-VP ASDs, (B) SIM/HPMC-AS ASDs, (C) SIM/SOL ASDs



Water content for all extruded formulations were determined by TGA. Minimal water content was observed, particularly at high SIM drug load of 75% and 100%. Results are shown in Table 5.

Table 5.

Water Content of SIM/Polymer ASDs

Polymer	SIM/Polymer Ratio (% w/w)	Water Content by TGA (%)
PVP-VA	0/100	1.7
	25/75	1.4
	50/50	0.6
	75/25	0.4
	100/0	0.3
HPMC-AS	0/100	1.0
	25/75	0.8
	50/50	0.7
	75/25	0.6
	100/0	0.3
SOL	0/100	1.6
	25/75	1.2
	50/50	0.7
	75/25	0.3
	100/0	0.3

Chemical purity ranged from 98% to 100% for all formulations, except for the 25/75 % SIM/HPMC-AS ASD, where extrusion proved to be challenging. For this formulation, the residence time was over 10 mins, which may have contributed to the slightly lower chemical purity by UPLC. Chemical purity of all ASDs is shown in Table 6.

Table 6.

Chemical Purity of SIM/Polymer ASDs

Polymer	SIM/Polymer Ratio (% w/w)	SIM Purity (%)
PVP-VA	0/100	-
	25/75	98.29 ± 0.02
	50/50	100.00 ± 0.00
	75/25	100.00 ± 0.00
	100/0	100.00 ± 0.00
HPMC-AS	0/100	-
	25/75	95.17 ± 0.02
	50/50	100.00 ± 0.00
	75/25	100.00 ± 0.00
	100/0	100.00 ± 0.00
SOL	0/100	-
	25/75	97.98 ± 0.01
	50/50	98.38 ± 0.01
	75/25	100.00 ± 0.00
	100/0	100.00 ± 0.00

Characterization of amorphous solid dispersions can be complex and often requires multiple orthogonal techniques to overcome limitations with each method. This study used PXRD, mDSC, and PLM to elucidate the physical form of SIM in the ASD. It is known that PXRD and mDSC may have limitations in resolution due to sample size. PXRD diffractograms may exhibit broadening of Bragg peaks, which could suggest decrease in particle size in addition to generation of amorphous content. Furthermore, mDSC may fail to detect crystalline domains <30 nm (Sarpal, 2021). PLM, likewise, may have limitations wherein the absence of birefringence may be attributed to the material's isotropic nature rather than its amorphous nature. Conversely, the presence of birefringence may arise from factors such as mechanical strain or changes in optical properties unrelated to its crystalline form. Interpretation requires some nuance informed by prior knowledge of the system. In this study, reliance on PLM alone could erroneously lead to the conclusion that HPMC-AS is crystalline upon hot melt extrusion; however, the complementary use of PXRD and mDSC corroborates the amorphous nature of the extruded polymer. The birefringence observed from HPMC-AS by PLM could be attributed to higher order structure in the polymer or the mechanical stress on the glass (Chen, 2009). Overall, SIM/polymers ASDs were successfully prepared by HME and SIM was confirmed to be amorphous in the ASDs.

4. DETERMINATION OF INTERMOLECULAR INTERACTIONS

4.1 Determination of Intermolecular Interactions

Several mechanisms contribute to the stabilization of an amorphous drug in an amorphous solid dispersion (ASD) – the nature of intermolecular interactions between the drug and the stabilizing polymer, the thermodynamic factor of chemical potential reduction, and the kinetic factor of molecular mobility restriction. These mechanisms are distinct but related. Strong and/or extensive intermolecular interactions facilitate the miscibility and solubility of a drug and a polymer, which leads to a reduction in the system's chemical potential. This helps achieve molecular mixing and promotes physical stabilization (Bookwala & Wildfong, 2023). Molecular mobility is also strongly influenced by drug-polymer intermolecular interactions, which restrict the overall degrees of freedom. Interactions limit the motions of the amorphous drug in the ASD, thereby increasing the barrier to physical destabilization. The selection of the polymeric excipients to use with a drug is a key factor in rational design of ASDs.

Numerous studies have demonstrated that drug-polymer interactions are a critical factor in the stabilization of ASDs by facilitating molecular mixing, which enhances physical stability (Bookwala, 2022; Konno, 2006; Mistry, 2016). Solid-state NMR may perhaps be the gold standard in determining structural and dynamic information in ASDs; however, it can be extremely costly and not as easily accessible as other techniques. DSC and infrared spectroscopy such as Raman or FTIR are routinely used to characterize drug-polymer interactions in ASDs as these techniques are convenient, widely available, and can be used to provide information on the molecular level. However, most studies leverage these techniques as a qualitative measure of drug-polymer interactions. In this study, we propose the novel application of mathematical

processing and statistical analysis by way of the Pearson moment correlation coefficient (Pearson coefficient) to ATR-FTIR data as a relative quantitation of the degree of intermolecular interactions between simvastatin and three selected polymers (polyvinyl pyrrolidone vinyl acetate, hydroxypropyl methyl cellulose acetate succinate, and Soluplus®) in ASDs prepared by hot melt extrusion (HME). Results are verified using experimental and theoretical approaches such as mDSC and Flory-Huggins theory.

4.2 Materials

Simvastatin (SIM) was purchased from Sigma-Aldrich (Acros Organics Geel, Belgium). Hydroxypropyl methyl cellulose acetate succinate MP (HPMC-AS MP) was a gift from Shin-Etsu (Tokyo, Japan). Polyvinyl pyrrolidone vinyl acetate 64 (PVP-VA 64, Copovidone, or Kollidon VA 64) and Soluplus® (SOL) were purchased from BASF (Ludwigshafen, Germany). Physical blends (PBs) of SIM and each polymer at varying weight ratios were prepared as outlined in Section 3.5.1. A hot melt extrusion (HME) process was used to prepare SIM-based ASDs with each polymeric excipient at varying weight ratios as outlined in Section 3.5.2.

4.3 Methods

4.3.1. Attenuated Total Reflectance-Fourier Transform Infrared Spectroscopy (ATR-FTIR)

The spectra of starting materials, physical blends, and ASDs were obtained using a Thermo Fisher Scientific Nicolet iS50 FTIR spectrometer (Madison, WI). Samples were scanned at room temperature on the iS50 ATR sample compartment with a diamond window, at a range of 400 – 4000 cm^{-1} at 32 scans with a resolution of 0.482 cm^{-1} for each sample.

4.3.2. Pearson Moment Correlation Coefficient

Spectra analysis and determination of the Pearson coefficient was performed using OriginPro software (Northampton, MA, USA). The Pearson coefficient for each physical blend and ASD was determined using the following algorithm. First, a reference library containing FTIR spectra of all native starting materials and processed hot melt extrudates was constructed. All spectra were baseline corrected and normalized such that all intensities are between 0 and 1 to allow for further mathematical processing. Next, the native polymer reference or the processed hot melt polymer extrudate reference was subtracted from the physical blend or ASD. The residual spectrum after polymer subtraction is assigned to be the spectral contribution of SIM in the physical blend or ASD. The residual spectrum is quantitatively examined for degree of similarity to the native SIM reference spectra in the case of a physical blend or the processed hot melt SIM extrudate in the case of an ASD by using the Pearson coefficient. Divergence of the SIM residual spectra from the reference SIM spectra are attributed to the formation of intermolecular bonds between SIM and the polymer. Pearson coefficients between 0.8 and 1.0 are considered high correlation, between 0.5 and 0.8 are considered moderate correlation, and below 0.5 are considered low correlation.

4.3.3. Prediction of Intermolecular Interactions using mDSC

A comparison of predicted T_g vs measured T_g was used to assess interactions in the SIM-based ASDs. The Gordon-Taylor equations shown in Equation 9 and Equation 12 (Gordon; Taylor, 1952) were used to calculate the predicted composite T_g . The measured T_g was obtained using an mDSC method outlined in Section 3.5.4. The deviation between the predicted T_g and measured T_g has traditionally been used to determine the absence or presence of intermolecular interactions between the drug and polymer.

4.3.4. Kinetic Miscibility using mDSC

A kinetic evaluation of miscibility was performed based on T_g obtained by an mDSC method described in Section 3.5.4. A single T_g indicates miscibility between SIM and polymer, whereas multiple T_g s denote inhomogeneity (Baird, 2012).

4.3.5. Prediction of Miscibility using Solubility Parameters

A theoretical approach to estimating miscibility examines the difference between solubility parameters of each component, as outlined in Section 1.6.2. Solubility parameters for each component were obtained, and the difference was calculated between SIM and each polymer. When the difference $\Delta\delta$ between drug and polymer is $< 7.0 \text{ MPa}^{1/2}$, the two are likely to be miscible. When $\Delta\delta$ is $> 10.0 \text{ MPa}^{1/2}$, the two phases are likely to be immiscible (Greenhalgh, 1999).

4.3.6. Prediction of Miscibility using Flory-Huggins Interaction Parameter

Another method for estimating miscibility involves the use of the Flory-Huggins interaction parameter χ , as outlined previously in Section 1.6.2. To calculate χ at room temperature, the difference between SIM and each polymer's solubility parameters was taken and Equation 19 was used.

To determine χ at temperatures close to the melting point of SIM, the melting point depressions experiments using DSC as proposed by Marsac et al was used. First, SIM/polymer physical blends were prepared using a method outlined in Section 3.5.1. A TA Instruments DSC 2500 equipped with TRIOS software (New Castle, DE, USA) was used, and physical blend samples weighing 4 – 7 mg were analyzed in a sealed Tzero aluminum pan at a nitrogen purge flow of 50 mL/min. A 10°C/min ramp rate with no modulation was used. Data analysis was performed using TRIOS software (New Castle, DE, USA). The onset temperature of the heat of

fusion ΔH_m was used for determining the melting point of the pure drug T_m and the melting point of the physical blend T_{mix} . Duplicate measurements were performed, and the average values were used for all calculations. Obtained values were placed into Equation 20; terms were rearranged and linearly fitted against ϕ_p^2 , and the slope was determined to be χ at a temperature close to SIM's melting point.

The interaction parameter χ is known to have a strong temperature dependence, as seen in Equation 22. Using χ determined by solubility parameters and by melting depression data outlined above, A and B in Equation 22 was calculated as a system of two equations with two unknowns. Flory-Huggins interaction parameter $\chi \leq 0$ is indicative of interactions between drug and polymer, predicting miscibility, while $\chi > 0$ are indicative of stronger interactions between drug-drug or polymer-polymer, which may potentially lead to phase separation.

4.3.7. Miscibility by Gibbs Free Energy of Mixing

The Gibbs free energy of mixing ΔG_{mix} as a function of composition was determined using Equation 18 once the temperature-dependent interaction parameter χ was obtained. As proposed by Tian et al, miscibility is predicted when $\Delta G_{mix} < 0$ and ΔG_{mix} is convex. When $\Delta G_{mix} > 0$ and concave, this is indicative of a partially miscible or immiscible system.

4.3.8. Solubility using Heat of Fusion ΔH_m

Melting point depression experiments were conducted for blends ranging from 10/90 to 90/10 %w/w SIM/polymer, and the enthalpy of fusion ΔH_m for SIM in each blend was obtained using DSC method outlined in Section 4.3.6. As described by Theeuwes and outlined in Section 1.6.2, ΔH_m was regressed against the amount of SIM in each blend, and the x-intercept can be used to determine the theoretical solubility of SIM within the polymer.

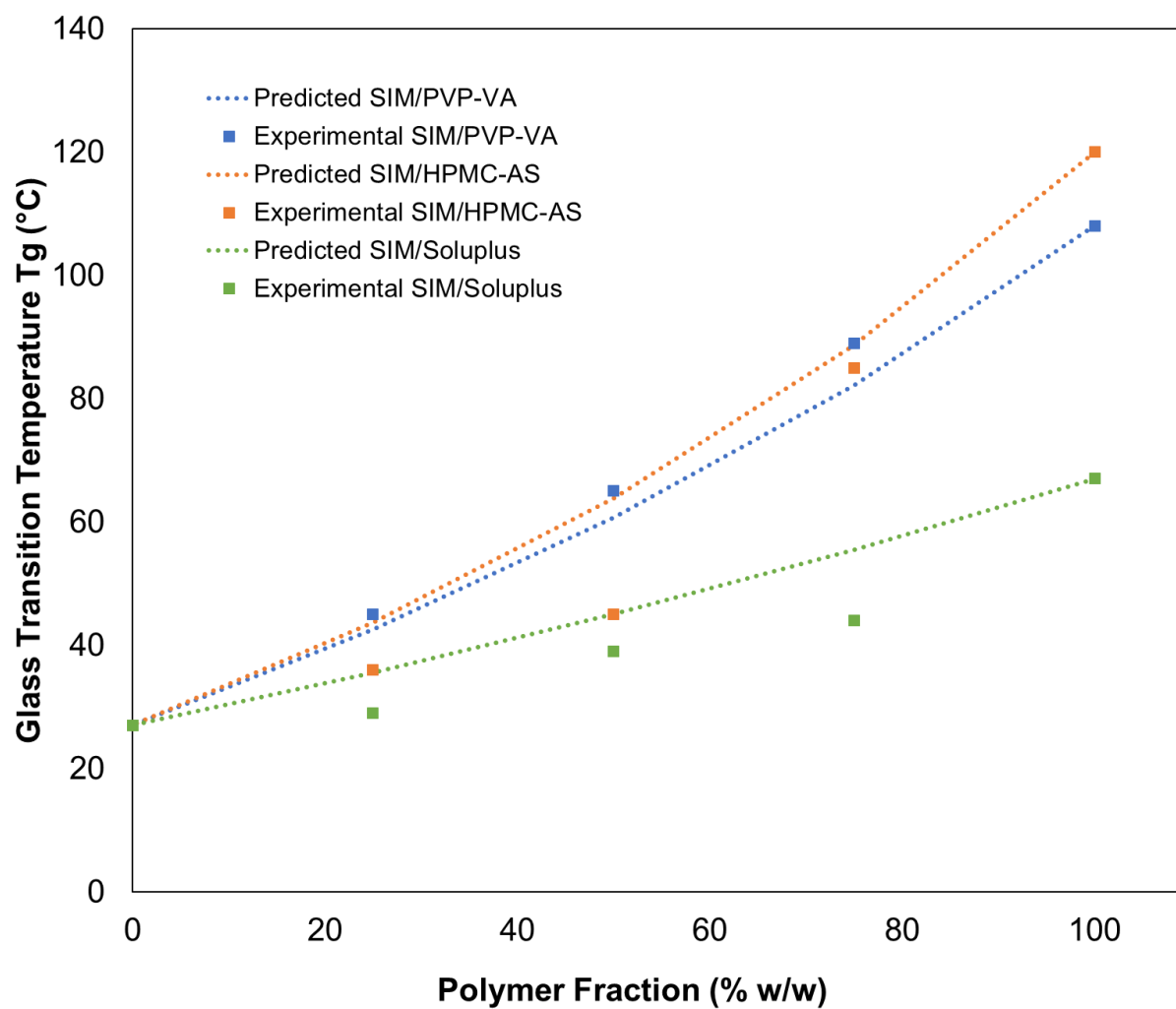
4.4 Results and Discussions

4.4.1. Prediction of Intermolecular Interactions using mDSC

Figure 13 below shows the difference between the predicted T_g as obtained by the Gordon-Taylor equation compared to the actual measured T_g of the ASDs prepared by HME.

Figure 13.

Predicted vs. Measured T_g of SIM/Polymer ASDs



Traditionally, an analysis of T_g may be used to predict the degree of interactions between drug and polymer based on the deviation of experimental T_g from the predicted T_g (Barmapalexis, 2013; Zhang, 2014). Positive deviations from predicted T_g are indicative of favorable drug-polymer interactions in an ASD. This is due to change in free volume of drug and polymer. Negative deviations from the predicted T_g could be indicative of several different phenomena, including more favorable interactions between drug-drug or polymer-polymer, or T_g depression due to residual water content. Comparing the predicted T_g from the Gordon-Taylor equation and measured T_g from mDSC, SIM is expected to form the most bonds with PVP-VA, then SOL, then HPMC-AS (PVP-VA > SOL > HPMC-AS arranged in decreasing order of favorable interactions). Positive deviations, where the experimental T_g is higher than the predicted T_g , as observed with SIM and PVP-VA are attributed to heteronuclear interactions between SIM and PVP-VA. Minor negative deviations are observed with SOL, and slightly larger negative deviations are observed with HPMC-AS. Negative deviations may be attributed to more favorable interactions between drug-drug or polymer-polymer, or T_g depression due to residual water content. Slightly positive deviation from predicted T_g with SIM/PVP-VA systems and slight negative deviations from predicted T_g with SIM/SOL systems are also consistent with previous reports (Myslinska, 2023; Zhang, 2014).

4.4.2. Kinetic Miscibility by mDSC

Figure 12 shows mDSC thermograms for the SIM ASDs prepared by HME. A single T_g is observed for all compositions, indicating kinetic miscibility between SIM and each polymer. Based on this method, rank-ordering of which system has the highest degree of interactions was not possible. While that being the case, this method demonstrates that a level of homogeneity is demonstrated by the ASDs. It is important to note however that this method has limitations. In a

study by Qian et al, ASDs of BMX-A with PVP-VA were prepared by HME at two different processing conditions. A single T_g was observed after preparing both ASDs, but demonstrated different levels of physical stability against crystallization over time. It was therefore shown that a single T_g may not always be a reliable indicator of homogeneity and optimal stability, and other supplemental techniques may need to be leveraged to capture a full picture (Qian et al., 2010).

4.4.3. ATR-FTIR and Pearson Coefficient

ATR-FTIR spectra for all physical blends and ASDs were obtained and are shown in Figure 14. To understand the strength and extent of intermolecular bonds between SIM and each polymeric excipient, the Pearson coefficient was employed in the analysis of ATR-FTIR data. The calculated Pearson coefficient for each physical blend and ASD is listed below in Figure 15.

Figure 14.

ATR-FTIR Spectra of (A) SIM/PVP-VA PBs, (B) SIM/PVP-VA ASDs, (C) SIM/HPMC-AS PBs, (D) SIM/HPMC-AS ASDs, (E) SIM/SOL PBs, (F) SIM/SOL ASDs

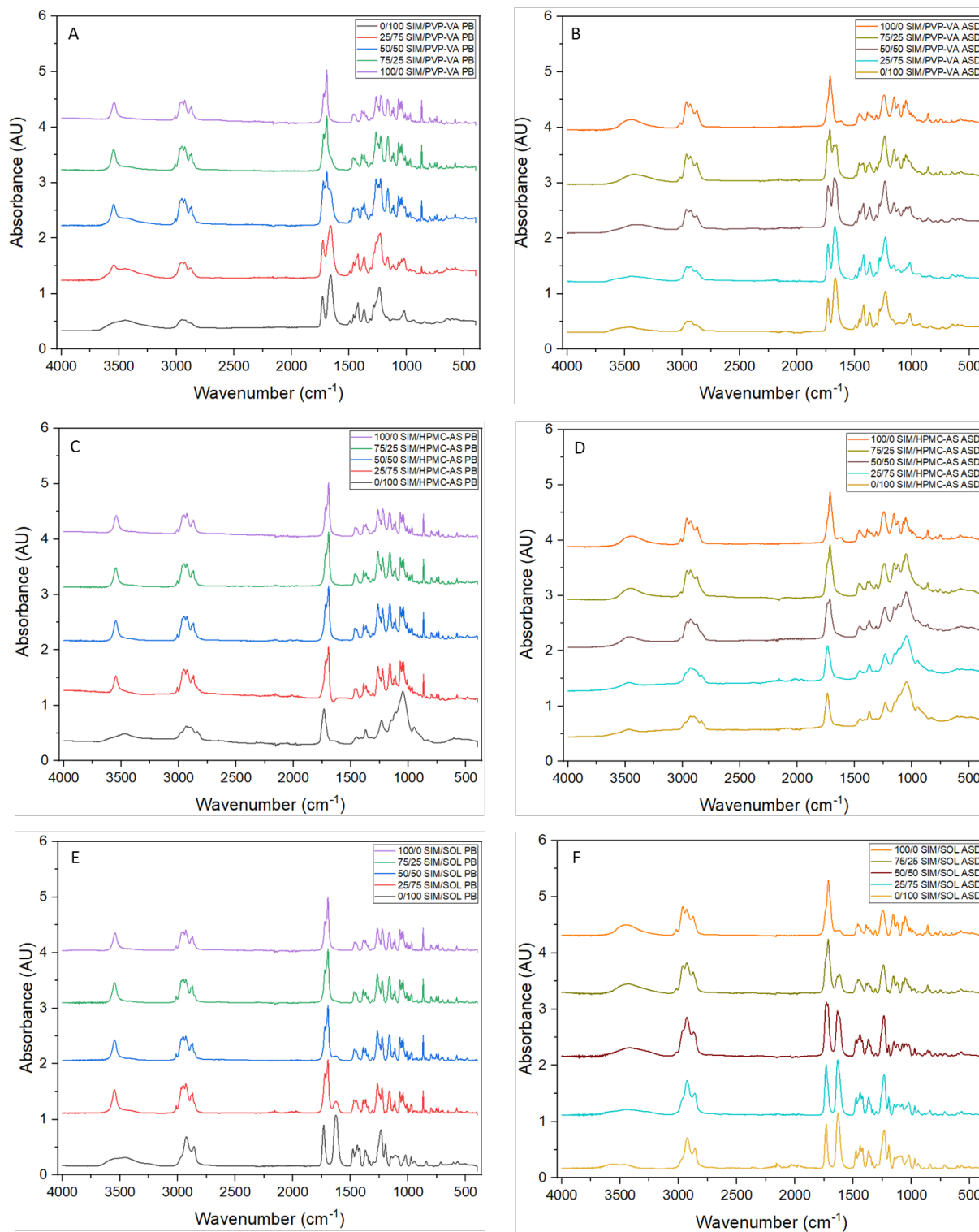
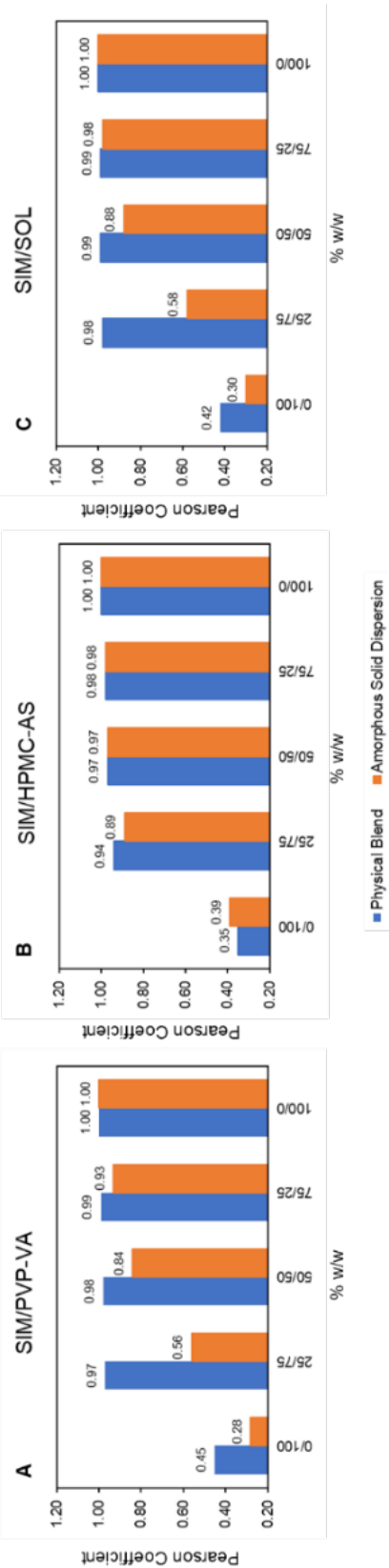


Figure 15.
Pearson Coefficient as a Measure of Degree of Intermolecular Bonds Between (A) SIM/PVP-VA, (B) SIM/HPMC-AS, (C) SIM/SOL in Physical Blends (Blue) and ASDs (Orange)



Conventional evaluation of drug-polymer interactions using spectroscopic data rely on qualitative observations such as peak shifting or peak broadening. However, this type of approach may provide a limited analysis due to overlapping signals. The use of mathematical analysis of ATR-FTIR data to evaluate drug-polymer interactions remains scarce. While some studies use advanced techniques such as Two-Dimensional Correlation Spectroscopy (2D COS) or Principal Component Analysis (PCA) (Bookwala, 2022), the adoption limited due to complexity or inaccessibility. Pearson coefficient analysis is an attractive option due to the simplicity in analysis and interpretation of drug-polymer interactions.

High Pearson coefficients (between 0.8 and 1.0), suggest the absence of intermolecular bonds in the ASDs. Moderate coefficients (between 0.5 and 0.8), indicate the formation of intermolecular bonds. Coefficients below 0.5 may suggest chemical degradation or the presence of other compounds. In the physical blends, Pearson coefficients between the native reference SIM and the residual SIM are consistently high, ranging from 0.94 to 0.99. This confirms the absence of drug-polymer interactions, as expected in a physical mixture. Pearson coefficient between native reference SIM and polymer only are low, which indicates no relationship between the spectra as expected. Pearson coefficient between native reference SIM and SIM only are 1.00, as expected since the spectra for these are the same.

In the ASDs, Pearson coefficients between 100% extruded SIM and the residual SIM show varying degrees of intermolecular bonding between SIM and polymer. For 25/75 SIM/PVP-VA and 25/75 SIM/SOL, Pearson coefficients clearly indicate the presence of intermolecular bonds, as values were 0.56 and 0.58, respectively. For 50/50 SIM/PVP-VA, 50/50 SIM/SOL, and 25/75 SIM/HPMC-AS, Pearson coefficients are considered high, with values at 0.84, 0.89, and 0.88, respectively. While these are considered high, these may indicate some

degree of interaction. For 75/25 SIM/PVP-VA, 50/50 and 75/25 SIM/HPMC-AS, and 75/25 SIM/SOL, Pearson coefficient is high with all values >0.93 . This suggests that there is an excess of SIM relative to polymer that is no longer able to form intermolecular interactions. Overall, Pearson coefficients for 25/75 and 50/50 SIM/polymer ASDs provide the same rank order of degree of intermolecular interactions as by evaluation of the difference in predicted T_g vs observed T_g . This suggests that using the Pearson coefficient analysis with ATR-FTIR spectra may be used as a useful tool to evaluate drug-polymer interactions.

4.4.4. Miscibility using Solubility Parameters

The difference between solubility parameter of the drug and polymer can be used to predict the miscibility of the two phases. The solubility parameters for SIM, PVP-VA, HPMC-AS, and SOL have been calculated and were obtained from literature (Jha, 2021; Kolter, 2012; Shakeel, 2021). The differences between SIM and each polymer are tabulated in Table 7.

Table 7.

Solubility Parameters for SIM, PVP-VA, HPMC-AS, and SOL

Component	Solubility Parameter, δ (MPa ^{1/2})	$\Delta\delta$ (MPa ^{1/2})
SIM	18.70	-
PVP-VA	19.70	0.99
HPMC-AS	26.15	7.45
SOL	19.40	0.71

When the difference $\Delta\delta$ between drug and polymer is $< 7.0 \text{ MPa}^{1/2}$, the two components are likely to be miscible. When $\Delta\delta$ is $> 10.0 \text{ MPa}^{1/2}$, the two phases are likely to be immiscible (Greenhalgh, 1999). Based on the solubility parameters differences between SIM and each polymer in Table 7, SIM is likely to be miscible with SOL and PVP-VA, and less likely to be miscible with HPMC-AS. Since an increase in miscibility is expected with an increase of drug-polymer interactions, this also consistent with the rank order of SIM-polymer interactions as seen by mDSC and ATR-FTIR.

4.4.5. Miscibility by Flory Huggins Interaction Parameters

Using the solubility parameters in Table 7 and Equation 19, the interaction parameter χ between SIM and each polymer was estimated at room temperature. The results are tabulated in Table 8.

Using melting point depression data, Equation 3 was rearranged and plotted, and the data are shown in Figure 16. The slope of each line is determined to be interaction parameter χ between SIM and each polymer at temperatures close to $T_{m,SIM}$ of 139°C . All other values used in this calculation are tabulated in Appendix A.

Figure 16.

Melting Point Depression Data for Determination of Interaction Parameters at 139°C

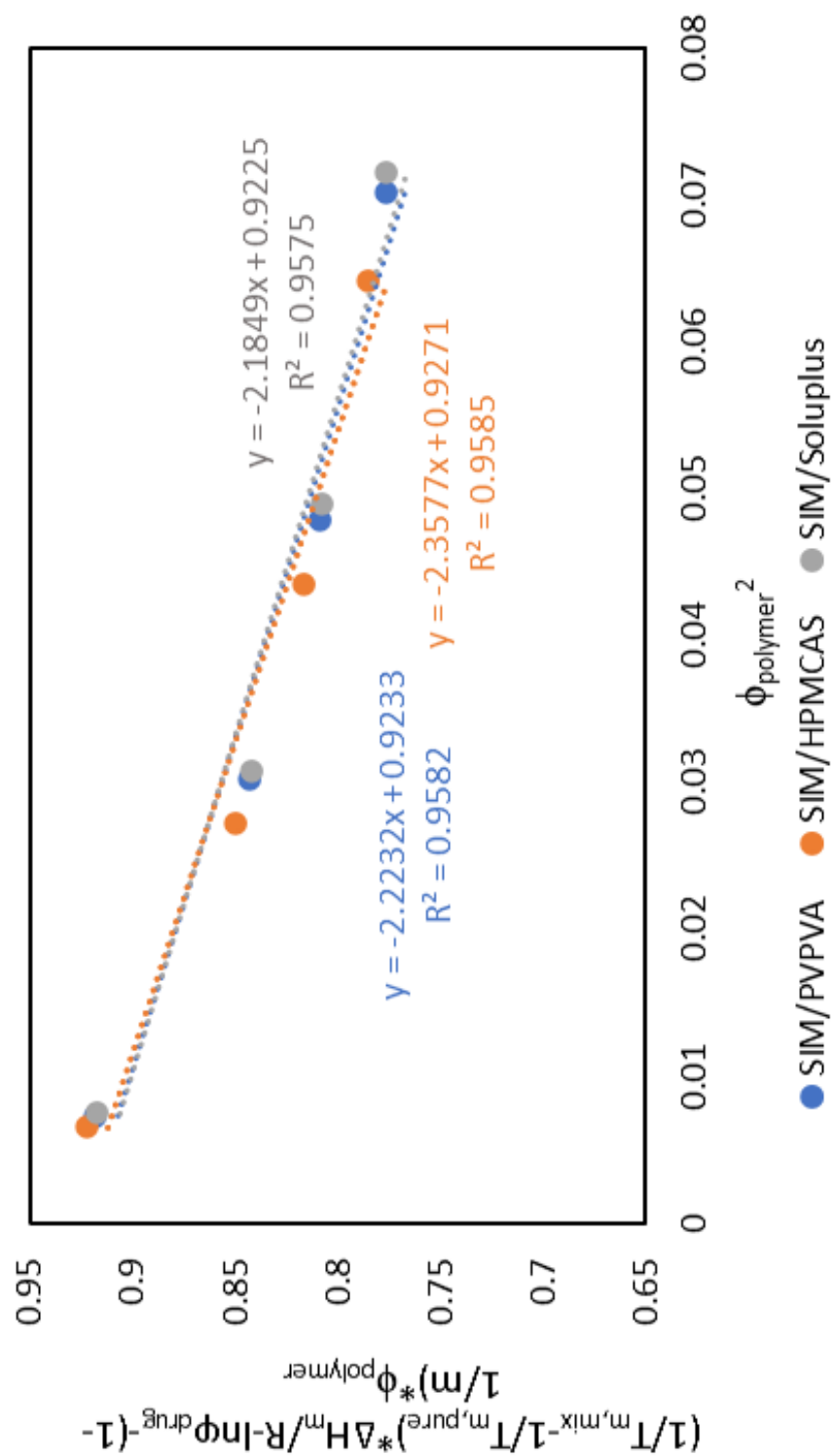


Table 8.*Calculated Interaction Parameters at 25°C and 139°C*

System	χ at 25°C	χ at 139°C	A	B
SIM/PVP-VA	0.1502	-2.2232	-8.4274	2556
SIM/HPMC-AS	8.5250	-2.3577	-30.8055	11720
SIM/SOL	0.0778	-2.1849	-8.0997	2437

Each component's solubility parameters may also be used to calculate the Flory Huggins interaction parameter χ at room temperature using Equation 4. In addition, χ may also be calculated from melting point depression experiments, which allows determination of χ close to SIM's T_m . Table 8 summarizes the χ at both temperatures. When $\chi < 0$, mixing is exothermic and favorable. When $\chi > 0$, mixing is endothermic and unfavorable. When $\chi = 0$, mixing is athermal and neither favorable or unfavorable. At room temperature, χ is close to zero for PVP-VA and SOL, while χ is positive for HPMC-AS. This indicates unfavorable mixing between SIM and HPMC-AS, and neither favorable/unfavorable mixing between SIM and PVP-VA and SOL. This provides a rank-order of PVP-VA \sim SOL $>$ HPMC-AS. At temperatures close to SIM's T_m , χ was determined to be negative for all polymers, indicating favorable mixing. Since an increase in miscibility is expected with an increase of drug-polymer interactions, miscibility predictions (particularly at room temperature) provide a similar rank order of SIM-polymer interactions as seen by mDSC and ATR-FTIR.

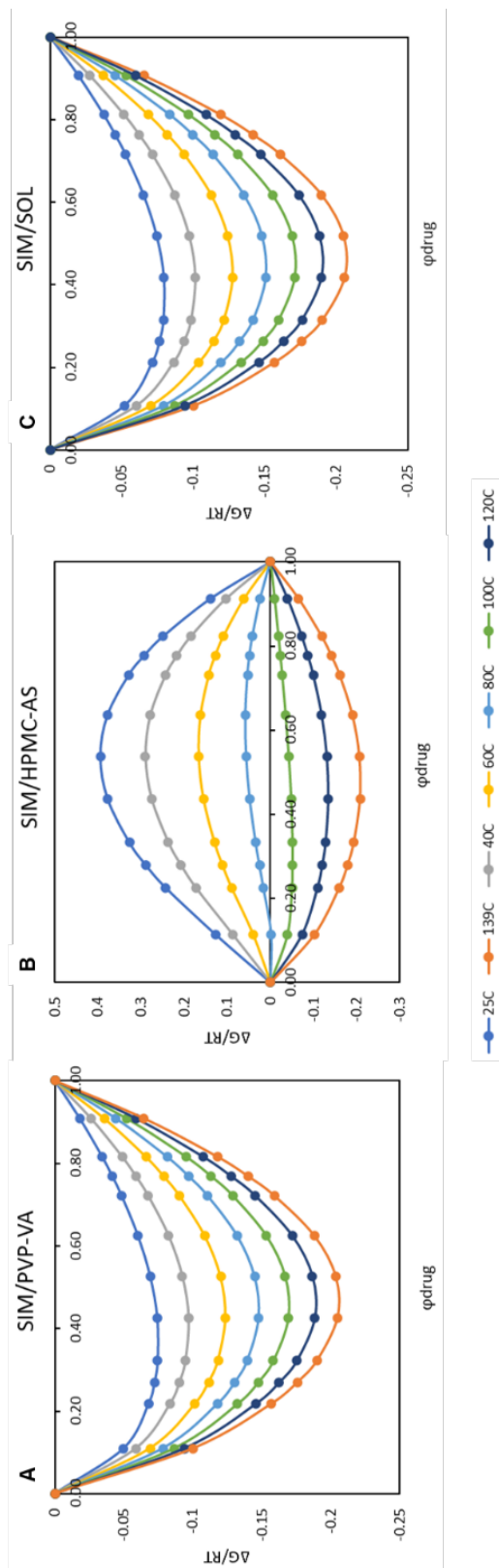
4.4.6. Miscibility by Gibbs Free Energy of Mixing

Combining Equation 2 and Equation 5 allows the construction of Gibb's Free Energy diagram as a function of temperature and composition, as shown in Figure 17. When $\Delta G_{\text{mix}} < 0$,

this is indicative of a miscible system, whereas when $\Delta G_{\text{mix}} > 0$, this is indicative of a partially miscible or immiscible system (Tian, 2013). From Figure 17, both SIM/PVP-VA and SIM/SOL suggesting completely miscible systems at all temperatures, compared to SIM/HPMC-AS where miscibility is only suggested at temperature $> 100^{\circ}\text{C}$.

Figure 17.

Gibbs Free Energy as a Function of Drug Volume Fraction ϕ_d for (A) SIM/PVP-VA, (B) SIM/HPMC-AS, (C) SIM/SOL

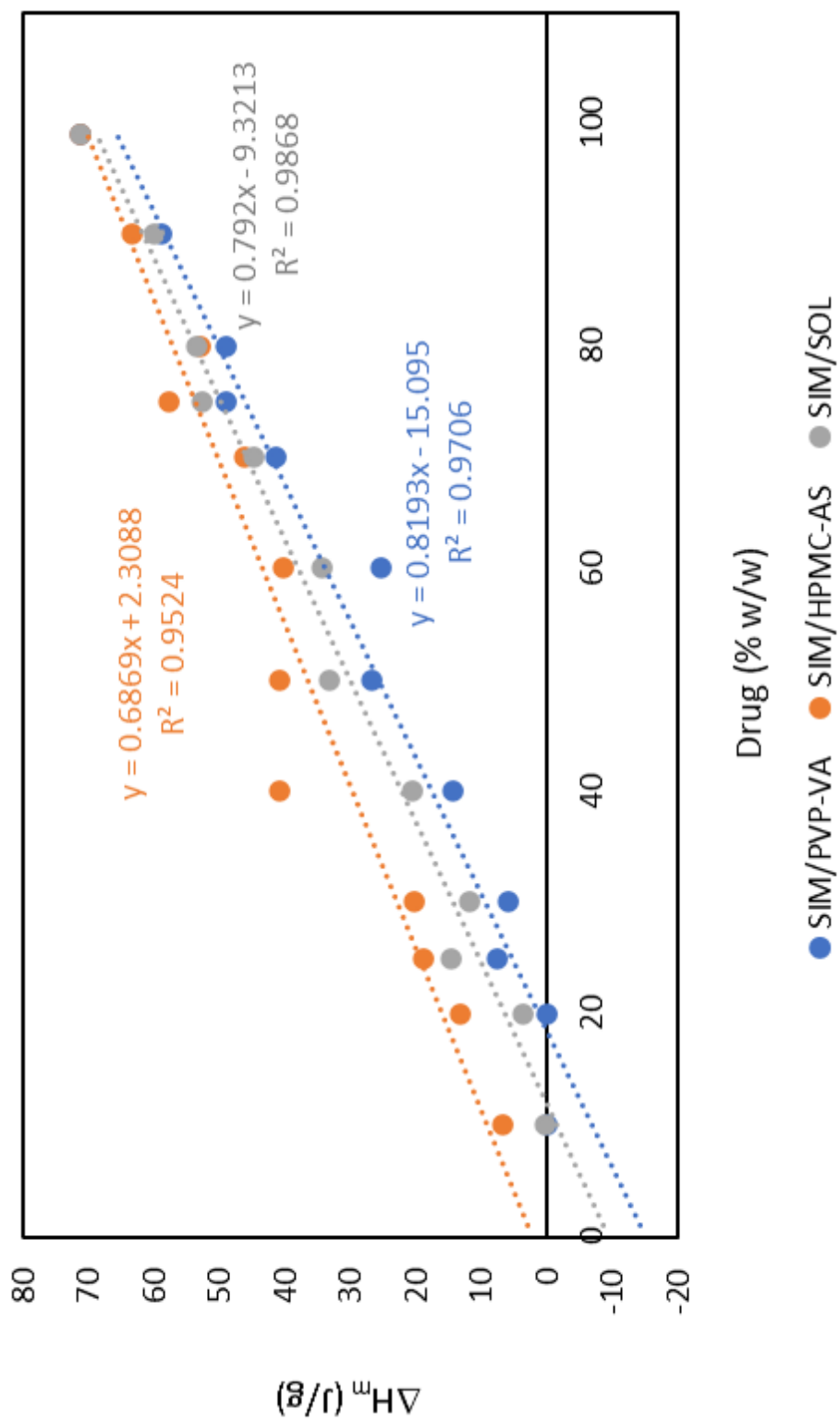


4.4.7. SIM Theoretical Solubility in Polymers

The theoretical solubility of a drug within a polymer can be predicted by plotting the enthalpy of fusion ΔH_m as a function of drug load, with the assumption that the dissolved drug has zero contributions to the endothermic melt event. This approach has been used in previous reports (Lu, 2016; Theeuwes, 1974). The enthalpy of fusion for SIM/polymer blends from 10/90 to 90/10 % w/w SIM/polymer was regressed against the fraction of SIM, with the x-intercept as the theoretical solubility of SIM in the polymer. The regression is shown in Figure 18. It can be concluded that SIM's theoretical solubility is 15% and 9% in PVP-VA and SOL, respectively. SIM is theoretically insoluble in HPMC-AS based on the negative intercept. Theoretical solubility of SIM can be rank-ordered as PVP-VA > SOL > HPMC-AS, which is in line with the previous miscibility evaluations. This is also consistent with the rank order of drug-polymer interactions as predicted by application of Pearson coefficient to ATR-FTIR data.

Figure 18.

SIM Theoretical Solubility in PVP-VA, HPMC-AS, and SOL



5. PHYSICAL STABILITY OF AMORPHOUS SOLID DISPERSIONS

5.1 Introduction

Amorphous solid dispersions (ASDs) are an effective means of improving the solubility and bioavailability of poorly soluble drugs. However, one of the major challenges with ASDs is the physical instability of the amorphous drug form. ASDs are a thermodynamically unstable system and have a propensity to crystallize on storage. In this study, the physical stability of amorphous solid dispersions containing simvastatin (SIM) were monitored using powder X-ray diffraction (XRPD), polarized light microscopy (PLM), and modulated differential scanning calorimetry (mDSC).

5.2 Materials

Simvastatin (SIM) was purchased from Sigma-Aldrich (Acros Organics Geel, Belgium). Hydroxypropyl methyl cellulose acetate succinate MP (HPMC-AS MP) was a gift from Shin-Etsu (Tokyo, Japan). Polyvinyl pyrrolidone vinyl acetate 64 (PVP-VA 64, Copovidone, or Kollidon VA 64) and Soluplus® (SOL) were purchased from BASF (Ludwigshafen, Germany). A hot melt extrusion (HME) process was used to prepare SIM-based ASDs with each polymeric excipient at varying weight ratios as outlined in Section 3.5.2. Potassium sulfate was purchased from Sigma Aldrich (Saint Louis, MO, USA).

5.3 Methods

5.3.1. Stability

Formulations were stored at 50°C/96% relative humidity (RH) and monitored for changes in physical stability over 2 weeks. Aliquots with a target of 100 mg of each powder formulation were weighed into a glass vial and placed uncapped in a humidity chamber containing a

saturated salt slurry of potassium sulfate. The humidity chamber containing the samples was stored inside a 50°C oven with a temperature-humidity probe and monitored periodically. At each time point, a glass vial containing each formulation was removed from the humidity chamber, capped, and allowed to come to room temperature prior to testing.

5.3.2. Powder X-ray Diffraction

Samples were analyzed for physical form using powder X-ray diffraction (pXRD). A Malvern Panalytical Empyrean (Westborough, MA) was used for this study. Each sample was mounted on a background-free silicon sample holder. Samples were scanned in reflection mode over a 2.0000 – 39.9990 °2 θ range with a Cu K α 1 radiation source and a detector at 45 kV and 40 mA. The step size was 0.0131 °2 θ and the scan rate was 0.08 sec/step.

5.3.3. Modulated Differential Scanning Calorimetry

Modulated differential scanning calorimetry (mDSC) was used to determine thermal events such as glass transition temperature T_g of the ASDs on stability. A TA Instruments DSC 2500 equipped with TRIOS software (New Castle, DE) was used, and samples weighing 4 – 7 mg were analyzed in a sealed Tzero aluminum pan at a nitrogen purge flow of 50 mL/min. A ramp rate of 3°C/min with a modulation cycle of $\pm 1^\circ\text{C}$ every 60 seconds was used. Analysis was performed using TRIOS software (New Castle, DE). Samples were prepared in duplicate, and the average values are reported in this paper.

5.3.4. Polarized Light Microscopy

Polarized light microscopy (PLM) was used as an orthogonal method for determining the physical form of SIM in the ASDs. Stability samples were analyzed using an Olympus BX53F light microscope (Tokyo, Japan) with two polarizing filters. A drop of silicone oil with viscosity 1000 cP was placed on a glass slide, and a small amount of sample was deposited into the oil

phase prior to covering with a glass coverslip. The glass slide is loaded onto the sample stage prior to analysis with Linkam software (Salfords, United Kingdom).

5.4 Results and Discussions

Each ASD was dispensed into individual glass vials, stored at 50°C/96% RH, and monitored for changes in physical form primarily using PXRD. Evidence of crystallization was observed as early as one day on stability for ASD containing 100/0 SIM/Polymer. In the case of SIM/PVP-VA ASDs, a reversion to the crystalline form of SIM was observed after 3 days on stability. Conversely, SIM maintained the amorphous form in all formulations of SIM/HPMC-AS, excluding the 75/25 SIM/HPMC-AS formulation. In the case of SIM/SOL ASDs, SIM maintained the amorphous form for all formulations. Figure 19 shows the PXRD diffractograms after 3 days of storage at 50°C/96% RH.

To corroborate the PXRD findings, PLM and DSC were employed as orthogonal techniques to confirm the physical form of SIM in the ASDs. Figure 20 shows the PLM images. Examination of PLM images after 3 days of storage at 50°C/96%RH reveals birefringence for all SIM-containing PVP-VA ASDs, aligning with PXRD observations. Conversely, no birefringence was noted in PLM images of SIM-containing SOL ASDs, validating the PXRD results. It is important to note the nuanced application of PLM in confirming SIM's physical form in HPMC-AS ASDs, particularly considering the inherent birefringence exhibited by ASDs containing 50% to 100% HPMC-AS even immediately after extrusion. Nonetheless, comparative analysis at the 3-day time point indicated a lack of observable changes in birefringence, with the exception of the 75/25 SIM/HPMC-AS formulation, where birefringence emerged, signifying a shift in SIM's physical form. Figure 21 summarizes the DSC thermograms after three days of storage at 50°C/96% RH. Endotherms are observed in the ASDs that were also confirmed to contain

crystalline SIM, thereby corroborating the data obtained from PXRD. Results from all three analytical techniques were consistent.

Figure 19.

PXRD Diffractograms of ASDs on Stability at 3 days, 50°C/96% RH (A) SIM/PVP-VA, (B) SIM/HPMC-AS, (C) SIM/SOL

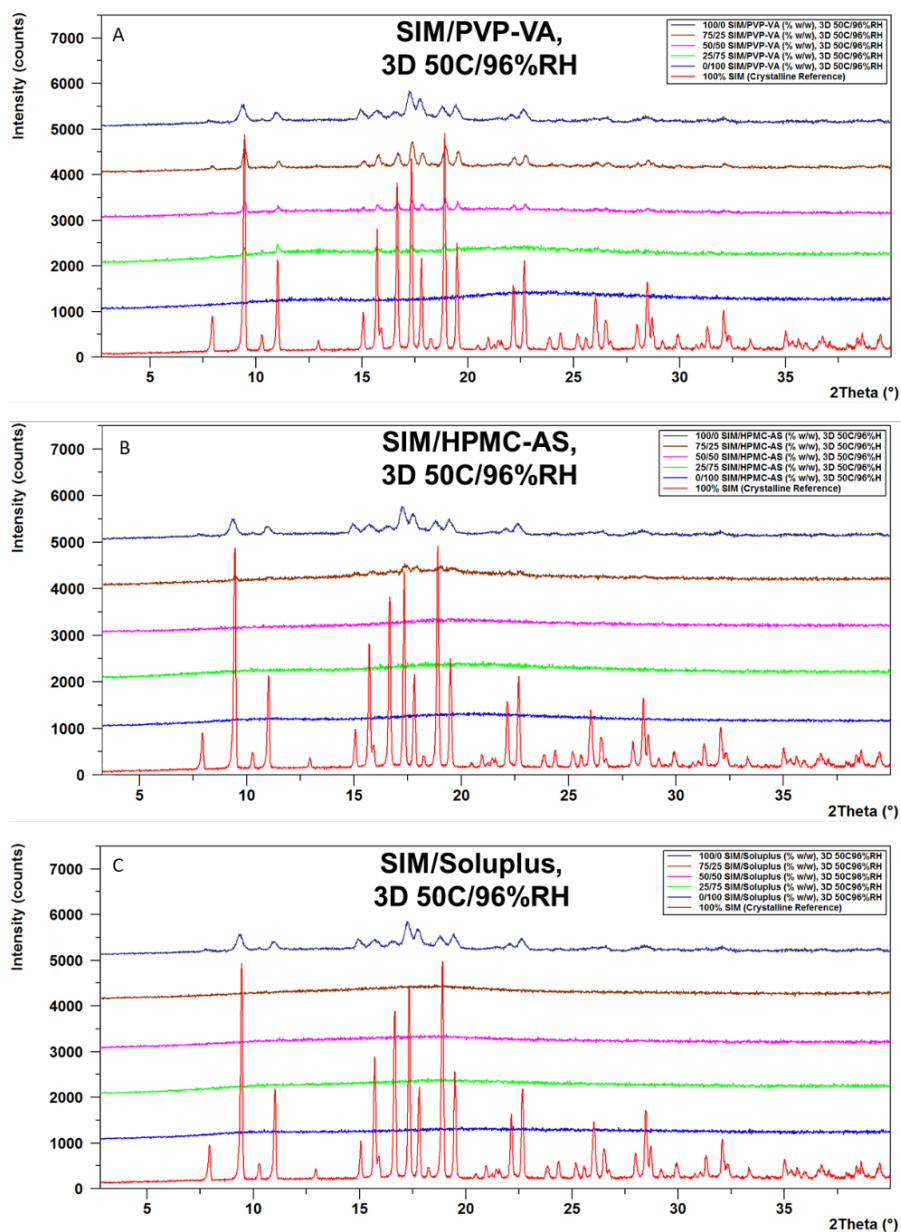


Figure 20.

PLM Images for SIM/PVP-VA, SIM/HPMC-AS, SIM/SOL ASDs After 3 Days at 50°C/96% RH

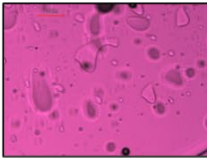
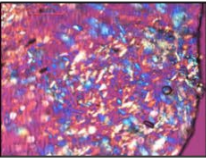
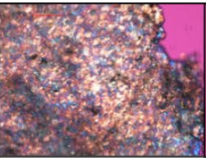
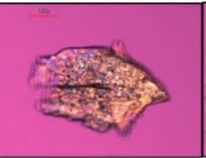
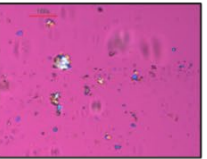
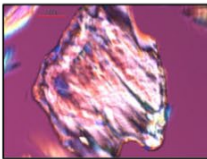
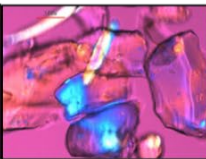
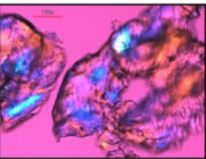
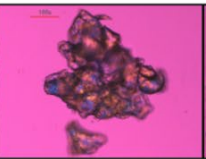
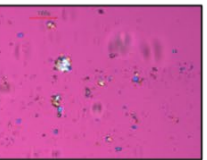
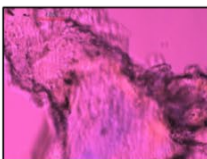
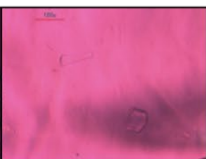
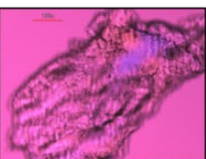
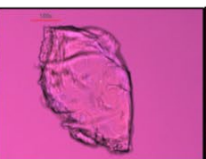
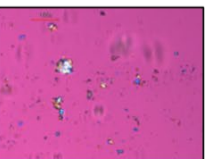
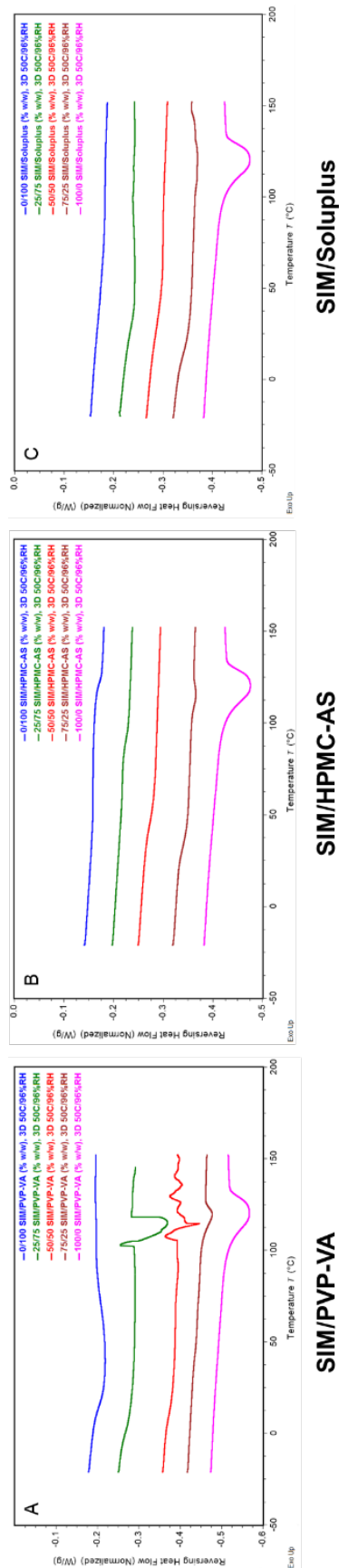
SIM/Polymer ASD	Composition (% w/w)				
	0/100	25/75	50/50	75/25	100/0
SIM/ PVP-VA					
SIM/ HPMC-AS					
SIM/ Soluplus					

Figure 21.

DSC Thermograms of ASDs on Stability at 3 days, 50C/96% RH (A) SIM/PVP-VA, (B) SIM/HPMC-AS, (C) SIM/SOL



ASDs were subjected to aggressive storage conditions of 50°C/96% RH. This condition was selected to exert significant stress to the system and use it as an effective screening tool to determine stability. ASDs were followed on stability up to 2 weeks, but crystallization of SIM was observed as early as 1 day when not stabilized by any polymeric excipients. For SIM/PVP-VA ASDs, SIM was found to crystallize 3 days on stability at all ratios. For SIM/HPMC-AS ASDs, SIM was found to be crystalline at 3 days only for 75/25 % SIM/HPMC-AS. For SIM-SOL ASDs, SIM remained stable throughout the duration of the study. Interestingly, although SIM and PVP-VA appeared to form the most extensive intermolecular interactions through theoretical and experimental assessments, PVP-VA was found to be the least effect at stabilizing the SIM amorphous form in the ASD. HPMC-AS appeared to be effective at SIM stabilization up to a certain SIM drug load, while SOL appeared to be effective at all SIM drug loads. This could be attributed to the hygroscopicity and propensity of PVP-VA to interact with water as it is exposed on stability. It has been demonstrated that PVP-VA is more hygroscopic than SOL and HPMC-AS (Obara, 2013; Patel, 2022). Although PVP-VA could interact extensively with SIM through H-bonds, H-bonds are also susceptible to get disrupted in the presence of moisture.

Notably, a high T_g alone is an inadequate predictor of physical stability. Despite the lower T_g exhibited by SOL-based ASDs relative to HPMC-AS and PVP-VA-based ASDs, SOL was observed to stabilize SIM more effectively in the amorphous state than HPMC-AS and PVP-VA. This phenomenon has been observed in previous reports (Kapourani et al., 2019). This underscores the pivotal combined role of factors such as drug-polymer interactions, restricted diffusion/anti-plasticization, and decrease of chemical potential in development of physically stable ASDs.

6. SUMMARY AND CONCLUSIONS

In this work, the impact of drug-polymer intermolecular interactions on the physical stability of amorphous solid dispersions (ASDs) containing simvastatin (SIM) was investigated. Hot melt extrusion was used to prepared SIM-based ASDs with three distinctly different polymers: polyvinyl pyrrolidone vinyl acetate (PVP-VA), hydroxypropyl methyl cellulose acetate succinate (HPMC-AS) and Soluplus® (SOL), and a novel application of mathematical processing and Pearson moment correlation coefficient (Pearson coefficient) was investigated as a method to quantitate the degree of intermolecular interactions between SIM and each polymer. The outcomes were confirmed with theoretical calculations and experimental techniques, using miscibility and solubility of drug in polymer as an indicator of intermolecular interactions. Theoretical calculations were performed by evaluating drug-polymer miscibility using solubility parameters. mDSC and melting point depressions experiments were used to gauge the degree of intermolecular interactions between SIM and PVP-VA, HPMC-AS, and SOL in the ASD. Methods consistently showed that SIM formed drug-polymer interactions in the following decreasing order of strength and extent: PVP-VA ~ SOL > HPMC-AS. This investigation underscores the utility of readily accessible tools such as mDSC and ATR-FTIR to assess intermolecular interactions between SIM and each polymer. In particular, the use of Pearson coefficient in the analysis of ATR-FTIR data can be a useful tool to quantitatively assess drug-polymer interactions. Future investigations may further extend the application of this methodology to diverse drug-polymer combinations for a comprehensive evaluation of the utility. In addition, other methods to confirm the degree of intermolecular interactions such as solid state nuclear magnetic resonance (SS-NMR) spectroscopy or molecular modeling may be

useful to confirm the rank order provided by Pearson coefficient analysis of ATR-FTIR spectra. Formulations were stored at accelerated conditions of 50°C/96%RH and physical stability of amorphous SIM in the ASD was evaluated. It was found that SIM was most physically stable in SOL-based systems, followed by HPMC-AS, and lastly with PVP-VA. This underscores that while drug-polymer interactions are critical in helping to stabilize the amorphous form of a drug, other mechanisms of physical stabilization must also be considered in the rational design of ASDs.

References

- Aceves-Hernandez, J. (2011). Solubility of simvastatin: A theoretical and experimental study. *Journal of Molecular Structure*, 995, 41-50.
- Alqahtani, M. S., Kazi, M., Alsenaidy, M. A., & Ahmad, M. Z. (2021). Advances in Oral Drug Delivery. *Front Pharmacol*, 12, 618411. <https://doi.org/10.3389/fphar.2021.618411>
- Amharar, Y., Curtin, V., Gallagher, K. H., & Healy, A. M. (2014). Solubility of crystalline organic compounds in high and low molecular weight amorphous matrices above and below the glass transition by zero enthalpy extrapolation. *Int J Pharm*, 472(1-2), 241-247. <https://doi.org/10.1016/j.ijpharm.2014.06.038>
- Amidon, G. L., Lennernas, H., Shah, V. P., & Crison, J. R. (1995). A theoretical basis for a biopharmaceutic drug classification: the correlation of in vitro drug product dissolution and in vivo bioavailability. *Pharm Res*, 12(3), 413-420. <https://doi.org/10.1023/a:1016212804288>
- Angell, C. A. (1995). Formation of glasses from liquids and biopolymers. *Science*, 267(5206), 1924-1935. <https://doi.org/10.1126/science.267.5206.1924>
- Aso, Y., & Yoshioka, S. (2006). Molecular mobility of nifedipine-PVP and phenobarbital-PVP solid dispersions as measured by ¹³C-NMR spin-lattice relaxation time. *J Pharm Sci*, 95(2), 318-325. <https://doi.org/10.1002/jps.20545>
- Atkins, P. D. P., J. (2009). *Physical Chemistry* (8 ed.). Oxford University Press.
- Baghel, S., Cathcart, H., & O'Reilly, N. J. (2016). Polymeric Amorphous Solid Dispersions: A Review of Amorphization, Crystallization, Stabilization, Solid-State Characterization, and Aqueous Solubilization of Biopharmaceutical Classification System Class II Drugs. *J Pharm Sci*, 105(9), 2527-2544. <https://doi.org/10.1016/j.xphs.2015.10.008>

- Baird, J. A. T., L.S. (2012). Evaluation of amorphous solid dispersion properties using thermal analysis techniques. *Advanced Drug Delivery Reviews*, 64, 396.
- Barmapalexis, P. (2013). Development of PVP/PEG mixtures as appropriate carriers for the preparation of drug solid dispersions by melt mixing technique and optimization of dissolution using artificial neural networks. *European Journal of Pharm Biopharm* 85, 1219–1231.
- Bellantone, R. A. (2014). *Fundamentals of Amorphous Systems: Thermodynamic Aspects*. Springer.
- Bhardwaj, S. P., Arora, K. K., Kwong, E., Templeton, A., Clas, S. D., & Suryanarayanan, R. (2014). Mechanism of amorphous itraconazole stabilization in polymer solid dispersions: role of molecular mobility. *Mol Pharm*, 11(11), 4228-4237.
<https://doi.org/10.1021/mp5004515>
- Bhattacharya, S., & Suryanarayanan, R. (2009). Local mobility in amorphous pharmaceuticals--characterization and implications on stability. *J Pharm Sci*, 98(9), 2935-2953.
<https://doi.org/10.1002/jps.21728>
- Bhujbal, S. V. M. B. J., U.; Gong, Y.; Agrawal. A.; Karki, S.; Taylor, L.S.; Kumar, S.; Zhou, Q. (2021). Pharmaceutical amorphous solid dispersion: A review of manufacturing strategies. *Acta Pharmaceutica Sinica B*, 11(8), 2505-2536.
- Bookwala, M. (2022). Implications of Coexistent Halogen and Hydrogen Bonds in Amorphous Solid Dispersions on Drug Solubility, Miscibility, and Mobility. *Molecular Pharmaceutics*, 19, 3959-3972.

- Bookwala, M., & Wildfong, P. L. D. (2023). The Implications of Drug-Polymer Interactions on the Physical Stability of Amorphous Solid Dispersions. *Pharm Res*, 40(12), 2963-2981. <https://doi.org/10.1007/s11095-023-03547-4>
- Chen, R. (2009). Characterization of Hypromellose Acetate Succinate by Size Exclusion Chromatography (SEC) Using Viscotek Triple Detector. *International Journal of Polymer Analytical Characterization*, 14, 617-630.
- Chiou, W. L., & Riegelman, S. (1971). Pharmaceutical applications of solid dispersion systems. *J Pharm Sci*, 60(9), 1281-1302. <https://doi.org/10.1002/jps.2600600902>
- Couchman, P. R. K., F.E. (1978). A Classical Thermodynamic Discussion of the Effect of Composition on Glass-Transition Temperatures. *Macromolecules*, 11(1), 117-119.
- Diogo, H. (2022). Molecular mobility in Soluplus, a polymer with extremely low dynamic fragility; A study by thermally stimulated depolarization currents *Journal of Non-Crystalline Solids*, 591, 121738.
- el-Egakey, M. A., Soliva, M., & Speiser, P. (1971). Hot extruded dosage forms. I. Technology and dissolution kinetics of polymeric matrices. *Pharm Acta Helv*, 46(1), 31-52. <https://www.ncbi.nlm.nih.gov/pubmed/5542801>
- Ellenberger, D. J., Miller, D. A., & Williams, R. O., 3rd. (2018). Expanding the Application and Formulation Space of Amorphous Solid Dispersions with KinetiSol(R): a Review. *AAPS PharmSciTech*, 19(5), 1933-1956. <https://doi.org/10.1208/s12249-018-1007-2>
- Flory, P. J. (1953). *Principles of Polymer Chemistry*. Cornell University Press. <https://books.google.com/books?id=CQ0EbEkT5R0C>

- Food and Drug Administration, C. f. D. E. a. R. C., Center for Biologics Evaluation and Research (CBER). (2021). Guidance for Industry: M9 Biopharmaceutics Classification SystemBased Biowaivers. In.
- Fox, G. T. (1956). Influence of Diluent and of Copolymer Composition on the Glass Temperature of a Polymer System. *Bulletin of the American Physical Society*, 1, 123.
- Frandsen, A. (2016). Polarized Light Microscopy. In: NASA Technical Reports Server (NTRS).
- Geraldes, C. (2020). Introduction to Infrared and Raman-Based Biomedical Molecular Imaging and Comparison with Other Modalities. *Molecules*, 25(23).
<https://doi.org/10.3390/molecules25235547>
- Gordon; Taylor, J. S. (1952). Ideal co-polymers and the second order transitions of synthetic rubbers. *Journal of Applied Chemistry*, 2, 493-500.
- Greenhalgh, D. J. W., A.C.; Timmins, P.; York, P. (1999). Solubility parameters as predictors of miscibility in solid dispersions. *Journal of Pharmaceutical Sciences*, 88, 1182–1190.
- Hancock, B. C., Shamblin, S. L., & Zografi, G. (1995). Molecular mobility of amorphous pharmaceutical solids below their glass transition temperatures. *Pharm Res*, 12(6), 799-806. <https://doi.org/10.1023/a:1016292416526>
- Hansen, C. M. (1967). The Three Dimensional Solubility Parameter and Solvent Diffusion Coefficient. In. Danish Technical Press.
- Henschel, H. (2020). Theoretical Infrared Spectra: Quantitative Similarity and Force Fields. *Journal of Chemical Theory and Computation*, 16, 3307-3315.
- Hildebrand, J. H. (1950). Factors Determining Solubility among Non-Electrolytes. *Proc Natl Acad Sci U S A*, 36(1), 7-15. <https://doi.org/10.1073/pnas.36.1.7>
- Hildebrand, J. S., R. (1950). *Solubility on non-electrolytes* (3 ed.). Reinhold.

- Hofsteyn, P., & Van Krevelen, D. (1976). Properties of polymers. *Elsevier Science Publishers*, 2, 152-155.
- Hoy, K. L. (1989). Solubility Parameter as a Design Parameter for Water Borne Polymers and Coatings. *Journal of Coated Fabrics*, 19(1), 53-67.
<https://doi.org/10.1177/152808378901900106>
- Iyer, R., Petrovska Jovanovska, V., Berginc, K., Jaklic, M., Fabiani, F., Harlacher, C., Huzjak, T., & Sanchez-Felix, M. V. (2021). Amorphous Solid Dispersions (ASDs): The Influence of Material Properties, Manufacturing Processes and Analytical Technologies in Drug Product Development. *Pharmaceutics*, 13(10).
<https://doi.org/10.3390/pharmaceutics13101682>
- Jha, D. S., D.; Amin, P. (2021). Effect of Hypromellose Acetate Succinate Substituents on Miscibility Behavior of Spray-dried Amorphous Solid Dispersions: Flory-Huggins Parameter Prediction and Validation. *Carbohydrate Polymer Technologies and Applications*, 2, 100317.
- Jowkar, F. (2010). Statins in dermatology. *International Journal of Dermatology*, 49, 1235–1243.
- Kapourani, A., Chatziteodoridou, M., Kontogiannopoulous, K., & Barmpalexis, P. (2020). Experimental, Thermodynamic, and Molecular Modeling Evaluation of Amorphous Simvastatin-Poly(vinylpyrrolidone) Solid Dispersions. *Molecular Pharmaceutics*, 17, 2703-2720.
- Kapourani, A., Vardaka, E., Katopodis, K., Kachrimanis, K., & Barmpalexis, P. (2019). Rivaroxaban polymeric amorphous solid dispersions: Moisture-induced thermodynamic

- phase behavior and intermolecular interactions. *Eur J Pharm Biopharm*, 145, 98-112.
<https://doi.org/10.1016/j.ejpb.2019.10.010>
- Kawabata, Y., Wada, K., Nakatani, M., Yamada, S., & Onoue, S. (2011). Formulation design for poorly water-soluble drugs based on biopharmaceutics classification system: basic approaches and practical applications. *Int J Pharm*, 420(1), 1-10.
<https://doi.org/10.1016/j.ijpharm.2011.08.032>
- Kawakami, K. (2019). Nucleation and crystallization of celecoxib glass: Impact of experience of low temperature on physical stability. *Thermochimica Acta*, 671.
- Knopp, M. M., Tajber, L., Tian, Y., Olesen, N. E., Jones, D. S., Kozyra, A., Lobmann, K., Paluch, K., Brennan, C. M., Holm, R., Healy, A. M., Andrews, G. P., & Rades, T. (2015). Comparative Study of Different Methods for the Prediction of Drug-Polymer Solubility. *Mol Pharm*, 12(9), 3408-3419. <https://doi.org/10.1021/acs.molpharmaceut.5b00423>
- Kolter, K. K., M.; Gryczke, A. (2012). Hot-Melt Extrusion with BASF Pharma Polymers. In.
- Konno, H. (2006). Influence of different polymers on the crystallization tendency of molecularly dispersed amorphous felodipine. *Journal of Pharmaceutical Sciences*, 95(12), 2692-2705.
- Kothari, K. (2014). The Role of Drug–Polymer Hydrogen Bonding Interactions on the Molecular Mobility and Physical Stability of Nifedipine Solid Dispersions. *Molecular Pharmaceutics*, 12, 162-170.
- Kwei, T. K. (1984). The effect of hydrogen bonding on the glass transition temperature of polymer mixtures. *Journal of Polymer Science*, 22(6), 307-313.
- Larkin, P. (2011). *Introduction: Infrared and Raman Spectroscopy*. Elsevier.
<https://doi.org/https://doi.org/10.1016/B978-0-12-386984-5.10001-1>.

- Lee, T. W., Boersen, N. A., Hui, H. W., Chow, S. F., Wan, K. Y., & Chow, A. H. (2014).
Delivery of poorly soluble compounds by amorphous solid dispersions. *Curr Pharm Des*,
20(3), 303-324. <https://doi.org/10.2174/13816128113199990396>
- Lu, J. C., K.; Hammer, N.I.; Jo, H.; Gryczke, A.; Kolter, K.; Langley, N.; Repka, M.A. (2016).
Solid-state Characterization of Felodipine-Soluplus Amorphous Solid Dispersions. *Drug
Development and Industrial Pharmacy*, 42(3), 485-496.
- Marsac, P. J. (2008). Estimation of Drug–Polymer Miscibility and Solubility in Amorphous
Solid Dispersions Using Experimentally Determined Interaction Parameters.
Pharmaceutical Research, 26(1), 139-151.
- Mendonsa, N., Almutairy, B., Kallakunta, V. R., Sarabu, S., Thipsay, P., Bandari, S., & Repka,
M. A. (2020). Manufacturing strategies to develop amorphous solid dispersions: An
overview. *J Drug Deliv Sci Technol*, 55. <https://doi.org/10.1016/j.jddst.2019.101459>
- Mistry, P. (2016). Strength of Drug-Polymer Interactions: Implications for Crystallization in
Dispersions. *Crystal Growth & Design*, 16(9), 5141-5149.
- Modhave, D. (2020). Understanding Concomitant Physical and Chemical Transformations of
Simvastatin During Dry Ball Milling. *AAPS PharmSciTech*, 21(5), 152.
- Moseson, D. E. (2018). The application of temperature-composition phase diagrams for hot melt
extrusion processing of amorphous solid dispersions to prevent residual crystallinity.
International Journal of Pharmaceutics, 553, 454-466.
- Moseson, D. E., Jordan, M. A., Shah, D. D., Corum, I. D., Alvarenga, B. R., Jr., & Taylor, L. S.
(2020). Application and limitations of thermogravimetric analysis to delineate the hot
melt extrusion chemical stability processing window. *Int J Pharm*, 590, 119916.
<https://doi.org/10.1016/j.ijpharm.2020.119916>

- Murtaza, G. (2012). Solubility Enhancement of Simvastatin: A Review. *Acta Poloniae Pharmaceutica*, 69, 581-590.
- Myslinska, M. (2023). A Comparison of Spray-Drying and Co-Precipitation for the Generation of Amorphous Solid Dispersions (ASDs) of Hydrochlorothiazide and Simvastatin. *Journal of Pharmaceutical Sciences*, 112(8), 2097-2114.
- Narayan, P., Porter III, W. W., Brackhagen, M., & Tucker, C. (2015). Polymers and Surfactants. In *Pharmaceutical Sciences Encyclopedia* (pp. 1-43).
[https://doi.org/https://doi.org/10.1002/9780470571224.pse523](https://doi.org/10.1002/9780470571224.pse523)
- Naushad, M. K., M.R. (2014). *Ultra Performance Liquid Chromatography Mass Spectrometry: Evaluation and Applications in Food Analysis*. CRC Press.
- Newman, A. (2016). *Rational design for amorphous solid dispersion*. Academic Press.
- Newman, A., & Zografi, G. (2022). What Are the Important Factors That Influence API Crystallization in Miscible Amorphous API-Excipient Mixtures during Long-Term Storage in the Glassy State? *Mol Pharm*, 19(2), 378-391.
<https://doi.org/10.1021/acs.molpharmaceut.1c00519>
- Nikolakakis, I., & Partheniadis, I. (2017). Self-Emulsifying Granules and Pellets: Composition and Formation Mechanisms for Instant or Controlled Release. *Pharmaceutics*, 9(4).
<https://doi.org/10.3390/pharmaceutics9040050>
- Noyes, A. A. W., W.R. . (1897). The rate of solution of solid substances in their own solutions. *Journal of the American Chemical Society*, 54, 930–934.
- Obara, S. T., F.K.; Sarode, A. (2013). *Properties and Applications of Hypromellose Acetate Succinate (HPMCAS) for Solubility Enhancement Using Melt Extrusion*. Springer.

- Pasquali, I., Bettini, R., & Giordano, F. (2008). Supercritical fluid technologies: an innovative approach for manipulating the solid-state of pharmaceuticals. *Adv Drug Deliv Rev*, 60(3), 399-410. <https://doi.org/10.1016/j.addr.2007.08.030>
- Patel, N. G. S., A.T.M. (2022). Moisture sorption by polymeric excipients commonly used in amorphous solid dispersion and its effect on glass transition temperature: I. Polyvinylpyrrolidone and related copolymers. *International Journal of Pharmaceutics*, 616, 121532.
- Patil, H., Tiwari, R. V., & Repka, M. A. (2016). Hot-Melt Extrusion: from Theory to Application in Pharmaceutical Formulation. *AAPS PharmSciTech*, 17(1), 20-42. <https://doi.org/10.1208/s12249-015-0360-7>
- Percy, S. R. (1872). *Improvement in drying and concentrating liquid substances by atomizing* (US Patent No.
- Pugliese, A. T., M.; Hawarden, L.E.; Abraham, A.; Blanc, F. (2022). New Development in Understanding Drug–Polymer Interactions in Pharmaceutical Amorphous Solid Dispersions from Solid-State Nuclear Magnetic Resonance. *Molecular Pharmaceutics*, 19, 3685-3699.
- Qian, F., Huang, J., Zhu, Q., Haddadin, R., Gawel, J., Garmise, R., & Hussain, M. (2010). Is a distinctive single Tg a reliable indicator for the homogeneity of amorphous solid dispersion? *Int J Pharm*, 395(1-2), 232-235. <https://doi.org/10.1016/j.ijpharm.2010.05.033>
- Reif, B., Ashbrook, S. E., Emsley, L., & Hong, M. (2021). Solid-state NMR spectroscopy. *Nat Rev Methods Primers*, 1. <https://doi.org/10.1038/s43586-020-00002-1>

- Repka, M. A., Bandari, S., Kallakunta, V. R., Vo, A. Q., McFall, H., Pimparade, M. B., & Bhagurkar, A. M. (2018). Melt extrusion with poorly soluble drugs - An integrated review. *Int J Pharm*, 535(1-2), 68-85. <https://doi.org/10.1016/j.ijpharm.2017.10.056>
- Rojek, B. W., M. (2022). A combined differential scanning calorimetry and thermogravimetry approach for the effective assessment of drug substance-excipient compatibility. *Journal of Thermal Analysis and Calorimetry*, 148, 845-858.
- Saboo, S., Kestur, U. S., Flaherty, D. P., & Taylor, L. S. (2020). Congruent Release of Drug and Polymer from Amorphous Solid Dispersions: Insights into the Role of Drug-Polymer Hydrogen Bonding, Surface Crystallization, and Glass Transition. *Mol Pharm*, 17(4), 1261-1275. <https://doi.org/10.1021/acs.molpharmaceut.9b01272>
- Samineni, R., Chimakurthy, J., & Konidala, S. (2022). Emerging Role of Biopharmaceutical Classification and Biopharmaceutical Drug Disposition System in Dosage form Development: A Systematic Review. *Turk J Pharm Sci*, 19(6), 706-713. <https://doi.org/10.4274/tjps.galenos.2021.73554>
- Sarabu, S. (2020). Hypromellose Acetate Succinate based Amorphous Solid Dispersions via Hot Melt Extrusion: Effect of Drug Physicochemical Properties. *Carbohydrate Polymers*, 233, 115828.
- Sarpal, K. (2021). Amorphous Solid Dispersions of Felodipine and Nifedipine with Soluplus: Drug-Polymer Miscibility and Intermolecular Interactions. *Journal of Pharmaceutical Sciences*, 110, 1457-1469.
- Sassano, A. (2008). Statins in tumor suppression. *Cancer Letters*, 260, 11-19.
- Schneider, H. A. (1988). The Gordon-Taylor equation. Additivity and interaction in compatible polymer blends. *Macromolecular Chemistry and Physics*, 189(8), 1739-1963.

- Schonfeld, B. V., Westedt, U., & Wagner, K. G. (2022). Compression Modulus and Apparent Density of Polymeric Excipients during Compression-Impact on Tabletability. *Pharmaceutics*, 14(5). <https://doi.org/10.3390/pharmaceutics14050913>
- Shah, S. R., M.A. (2013). Melt Extrusion in Drug Delivery: Three Decades of Progress. In M. A. L. Repka, N.; DiNunzio, J. (Ed.), *Melt Extrusion: Materials, Technology and Drug Product Design*.
- Shakeel, F. (2021). Solubilization and thermodynamic properties of simvastatin in various micellar solutions of different non-ionic surfactants: Computational modeling and solubilization capacity. *PLOS ONE*.
- Silva, E. P. d. (2016). Compatibility study between atorvastatin and excipients using DSC and FTIR. *Journal of Thermal Analysis and Calorimetry*, 123, 933-939.
- Simoes, M. F. (2019). Hot-melt extrusion in the pharmaceutical industry: toward filing a new drug application. *Drug Discovery Today*, 24, 1749-1768.
- Singh, A., & Van den Mooter, G. (2016). Spray drying formulation of amorphous solid dispersions. *Adv Drug Deliv Rev*, 100, 27-50. <https://doi.org/10.1016/j.addr.2015.12.010>
- Smith, E. D., G. (2005). *Modern Raman Spectroscopy – A Practical Approach*. John Wiley & Sons, Ltd.
- Srinarong, P., de Waard, H., Frijlink, H. W., & Hinrichs, W. L. (2011). Improved dissolution behavior of lipophilic drugs by solid dispersions: the production process as starting point for formulation considerations. *Expert Opin Drug Deliv*, 8(9), 1121-1140. <https://doi.org/10.1517/17425247.2011.598147>
- Sun, Y., Tao, J., Zhang, G. G., & Yu, L. (2010). Solubilities of crystalline drugs in polymers: an improved analytical method and comparison of solubilities of indomethacin and

- nifedipine in PVP, PVP/VA, and PVAc. *J Pharm Sci*, 99(9), 4023-4031.
<https://doi.org/10.1002/jps.22251>
- Surana, R. S., R. (2000). Quantitation of crystallinity in substantially amorphous pharmaceuticals and study of crystallization kinetics by X-ray powder diffractometry. *Powder Diffraction*, 15(1), 2-6. <https://doi.org/10.1017/S0885715600010757>
- Tambe, S. (2021). Hot-melt extrusion: Highlighting recent advances in pharmaceutical applications *Journal of Drug Delivery Science and Technology*, 63, 102452.
- Tanabe, K. (1975). Computer Retrieval of Infrared Spectra by a Correlation Coefficient Method. *Analytical Chemistry*, 47(1), 118-122.
- Tao, J., Sun, Y., Zhang, G. G., & Yu, L. (2009). Solubility of small-molecule crystals in polymers: D-mannitol in PVP, indomethacin in PVP/VA, and nifedipine in PVP/VA. *Pharm Res*, 26(4), 855-864. <https://doi.org/10.1007/s11095-008-9784-z>
- Teja, S. B., Patil, S. P., Shete, G., Patel, S., & Bansal, A. K. (2013). Drug-excipient behavior in polymeric amorphous solid dispersions. *Journal of Excipients and Food Chemicals*, 4, 70-94.
- Thakore, S. D., Akhtar, J., Jain, R., Paudel, A., & Bansal, A. K. (2021). Analytical and Computational Methods for the Determination of Drug-Polymer Solubility and Miscibility. *Mol Pharm*, 18(8), 2835-2866.
<https://doi.org/10.1021/acs.molpharmaceut.1c00141>
- Theeuwes, F. H., A.; Higuchi, T. (1974). Quantitative analytical method for determination of drugs dispersed in polymers using differential scanning calorimetry. *Journal of Pharmaceutical Sciences*, 63(3), 427-429.
- Thomas, L. C. (2005). Why Modulated DSC? An Overview and Summary

of Advantages and Disadvantages Relative to Traditional DSC In. New Castle, DE.

Tian, Y. B., J.; Meehan, E.; Jones, D.S.; Li, S.; Andrews, G.P. (2013). Construction of drug-polymer thermodynamic phase diagrams using Flory-Huggins Interaction Theory: identifying the relevance of temperature and drug weight fraction to phase separations within solid dispersions. *Molecular Pharmaceutics*, 10(236).

Van den Mooter, G. V. d. B., J. (1999). Glass forming properties of benzodiazepines and co-evaporate systems with poly(hydroxyethyl methacrylate). *Journal of Thermal Analysis and Calorimetry*, 57, 493-507.

Vasconcelos, T., Sarmiento, B., & Costa, P. (2007). Solid dispersions as strategy to improve oral bioavailability of poor water soluble drugs. *Drug Discov Today*, 12(23-24), 1068-1075.
<https://doi.org/10.1016/j.drudis.2007.09.005>

Vasconcelos, T. M., S.; Neves, J.D.; Sarmiento, B. (2016). Amorphous solid dispersions: Rational selection of a manufacturing process. *Advanced Drug Delivery Reviews*, 100, 85-101.

Zhang, Y. (2014). Extruded Soluplus/SIM as an oral delivery system: characterization, interactions, in vitro and in vivo evaluations. *Drug Delivery*, 23(6), 1902-1911.

Zhao, Y. (2010). Prediction of the Thermal Phase Diagram of Amorphous Solid Dispersions by Flory-Huggins Theory. *Journal of Pharmaceutical Sciences*, 100(8), 3196-3207.

Zografi, G., & Newman, A. (2015). *Pharmaceutical Amorphous Solid Dispersions*. Wiley.

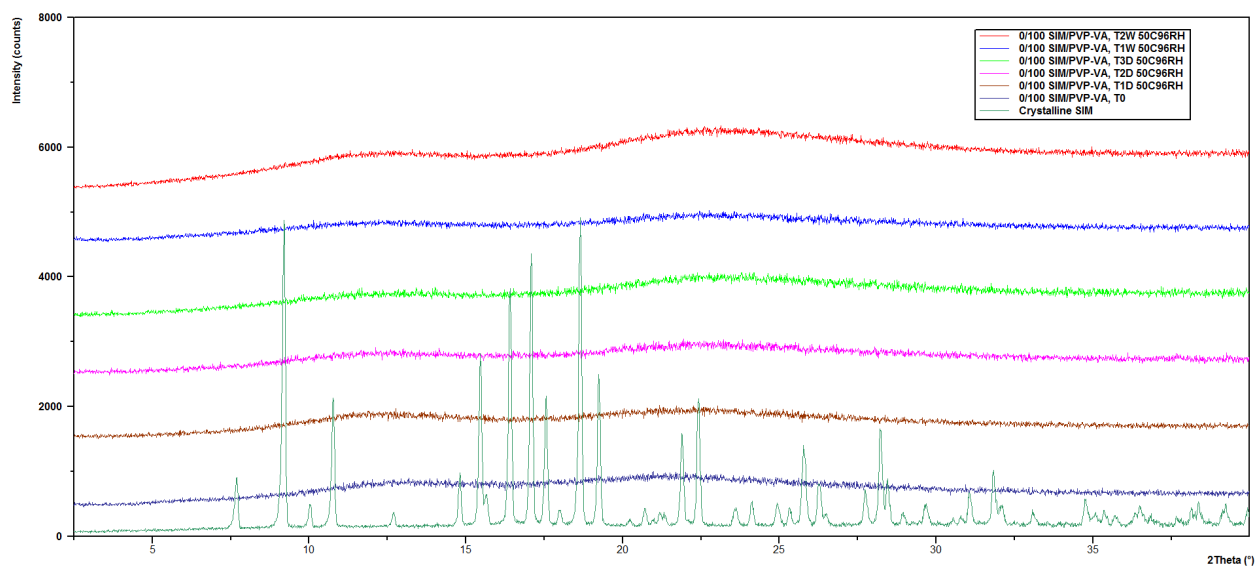
Appendix A: Values used for Melting Point Depression Experiments

SIM	Molar mass (g/mol)	418.6
	True density (g/mL)	1.1
	Molar volume (mL/mol)	380.6
PVP-VA	Molar mass (g/mol)	58000
	True density (g/mL)	1.308
	Molar volume (mL/mol)	44342.5
HPMC-AS	Molar mass (g/mol)	17800
	True density (g/mL)	1.390
	Molar volume (mL/mol)	12805.8
SOL	Molar mass (g/mol)	118000
	True density (g/mL)	1.291
	Molar volume (mL/mol)	91402.0

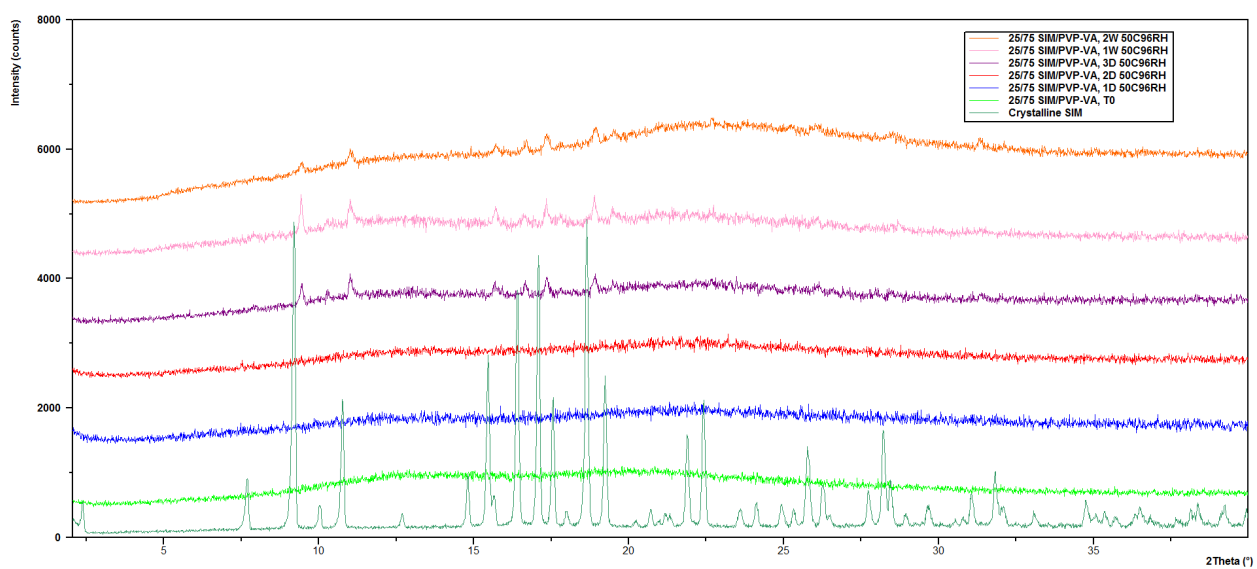
True density values adapted (Schonfeld et al., 2022)

Appendix B: PXRD Diffractograms

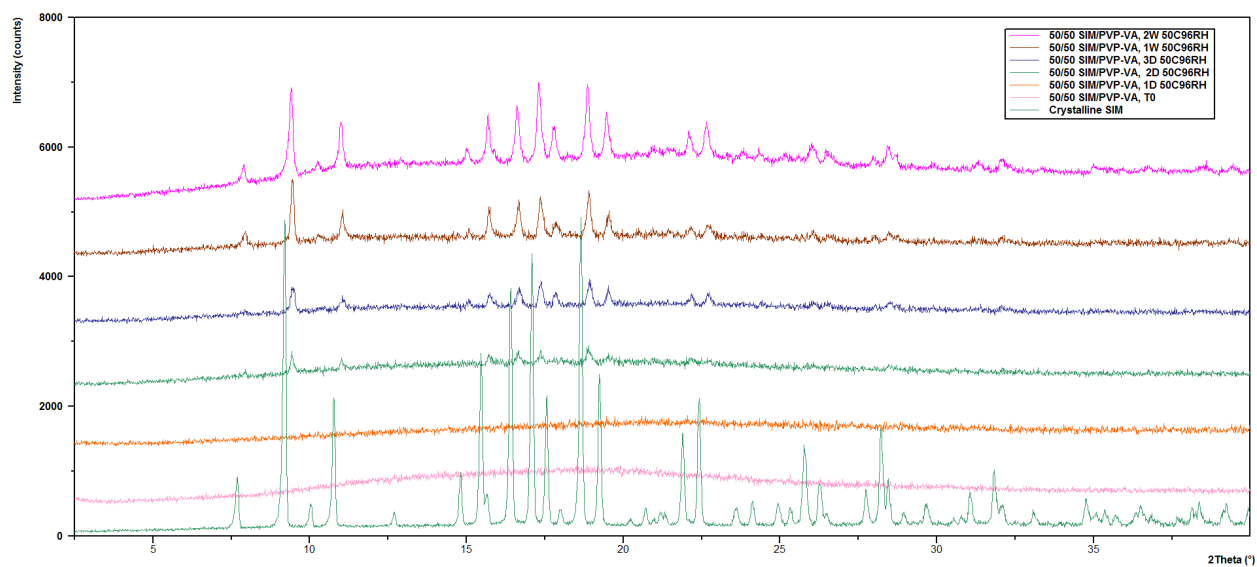
0/100 SIM/PVP-VA on Stability at 50°C, 96%RH:



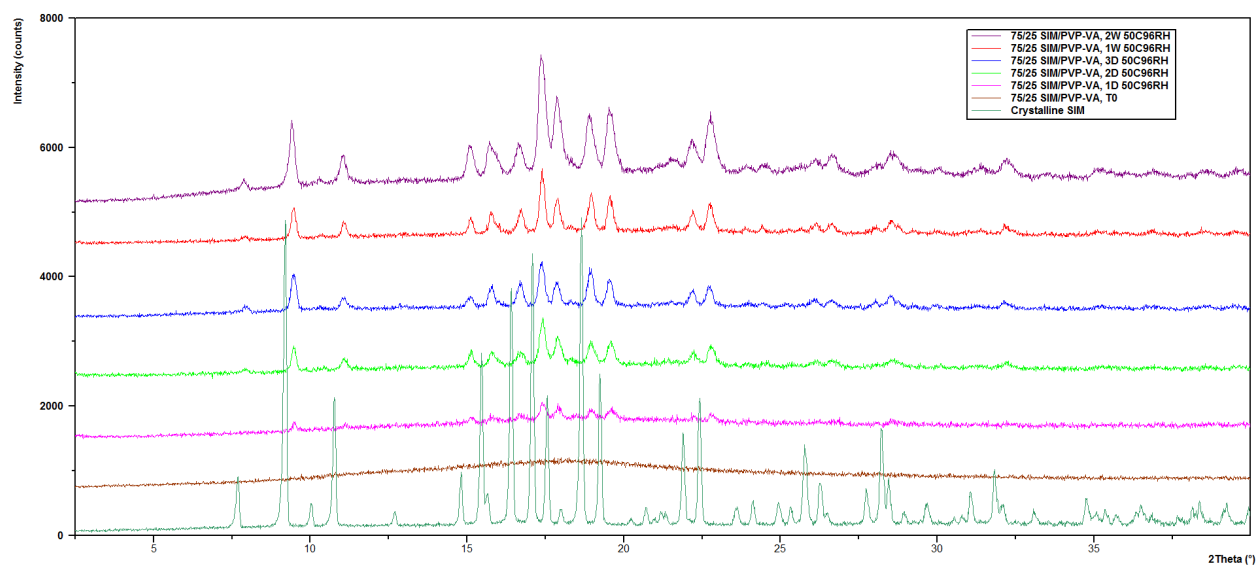
25/75 SIM/PVP-VA on Stability at 50°C, 96%RH:



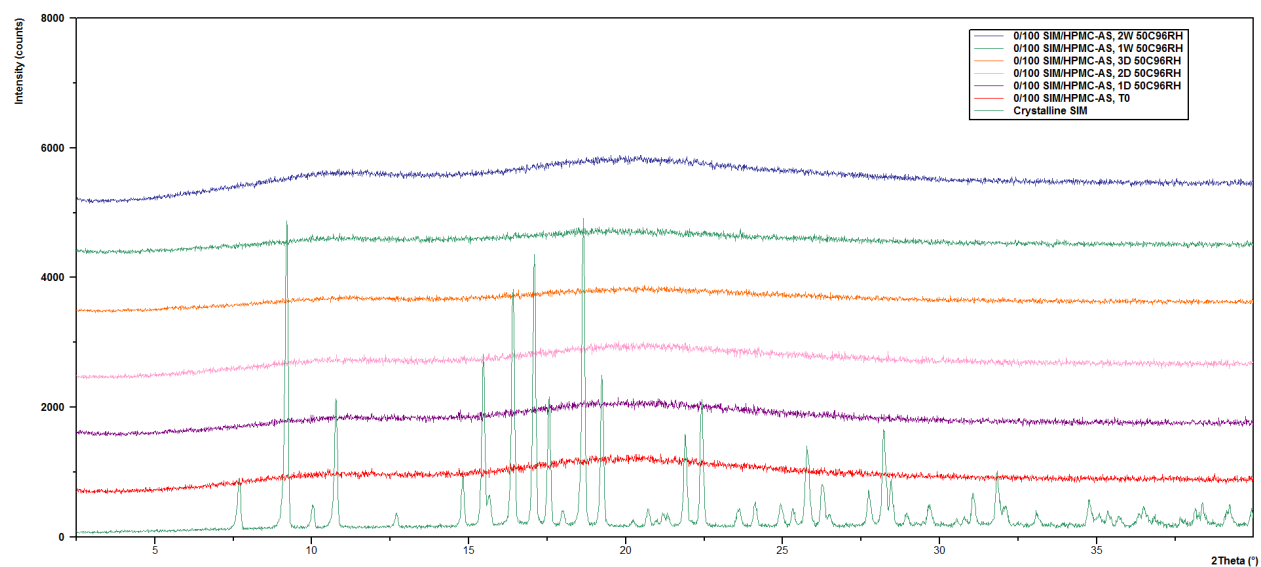
50/50 SIM/PVP-VA on Stability at 50°C, 96%RH:



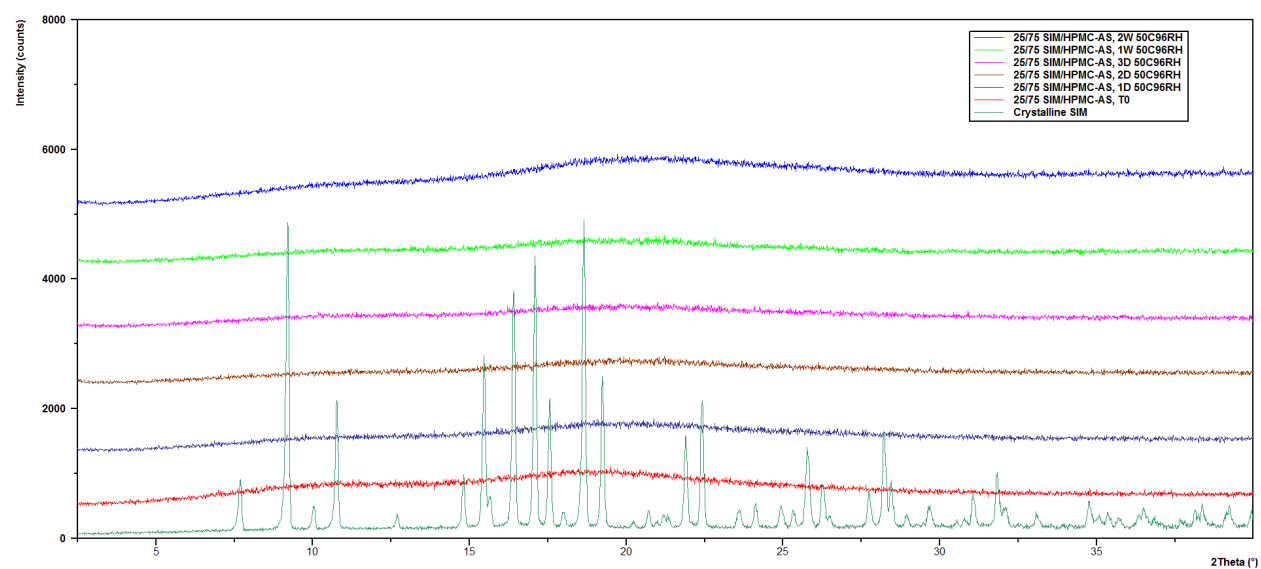
75/25 SIM/PVP-VA on Stability at 50°C, 96%RH:



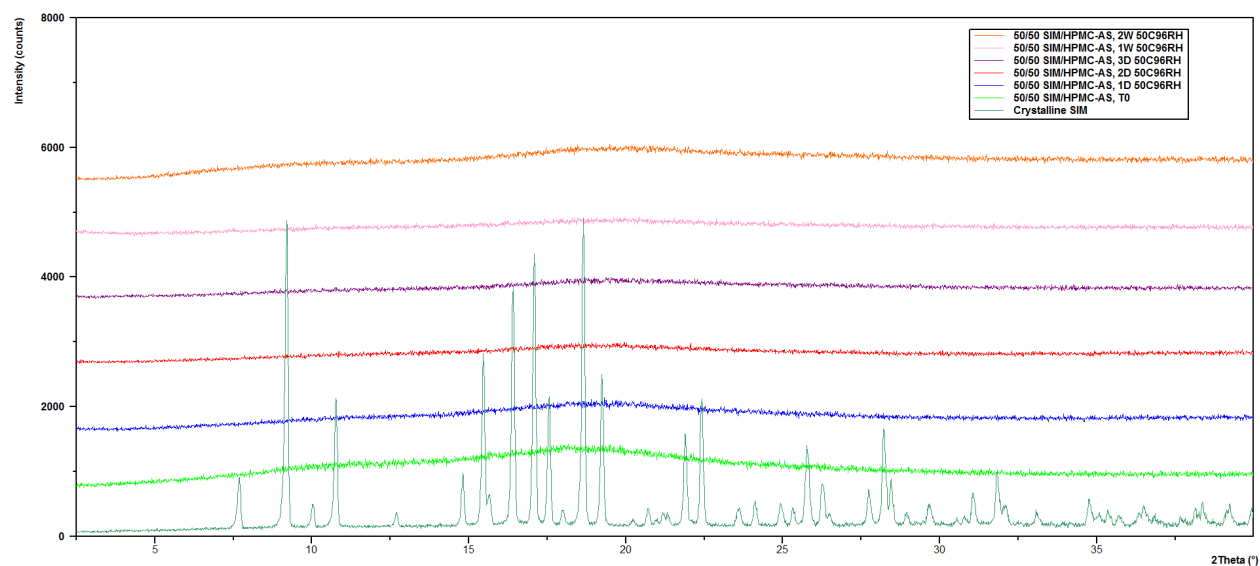
0/100 SIM/HPMC-AS on Stability at 50°C, 96%RH:



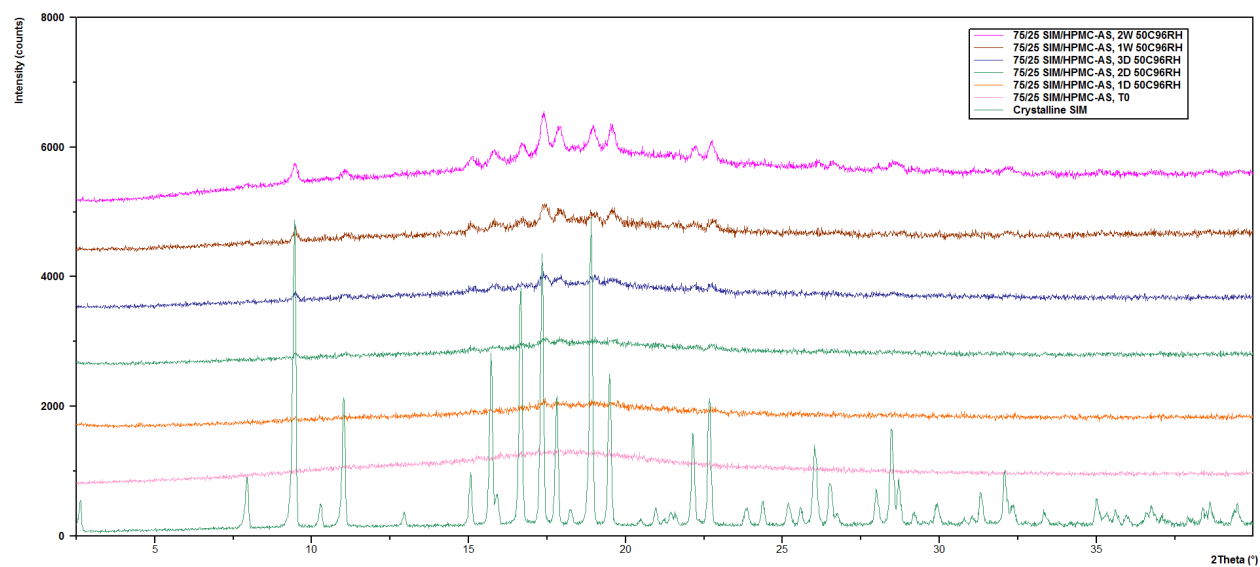
25/75 SIM/HPMC-AS on Stability at 50°C, 96%RH:



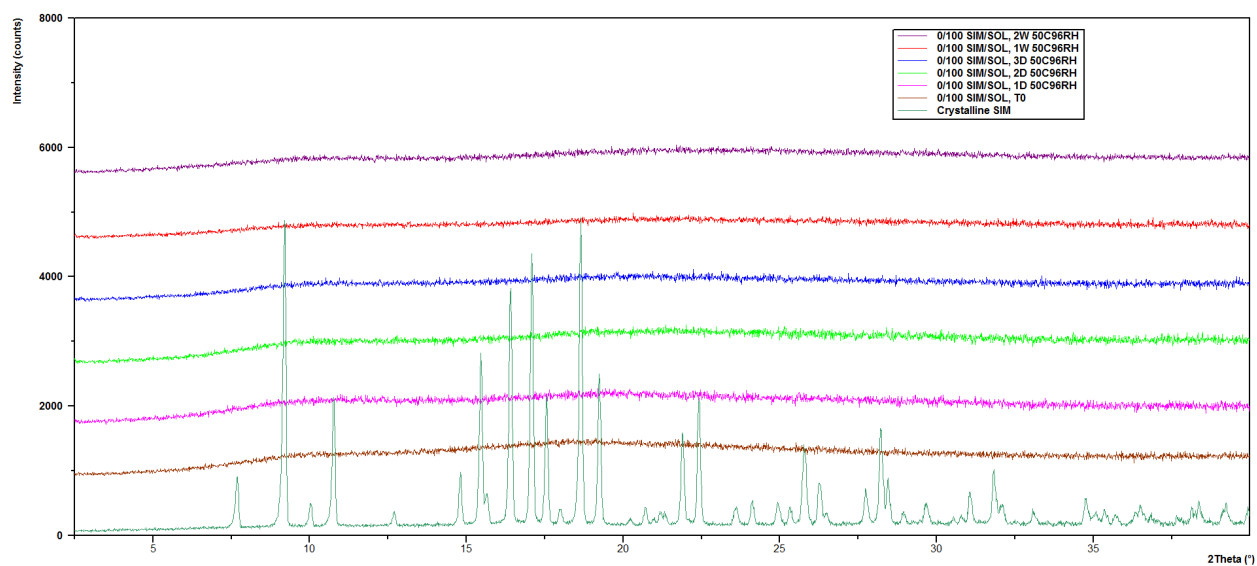
50/50 SIM/HPMC-AS on Stability at 50°C, 96%RH:



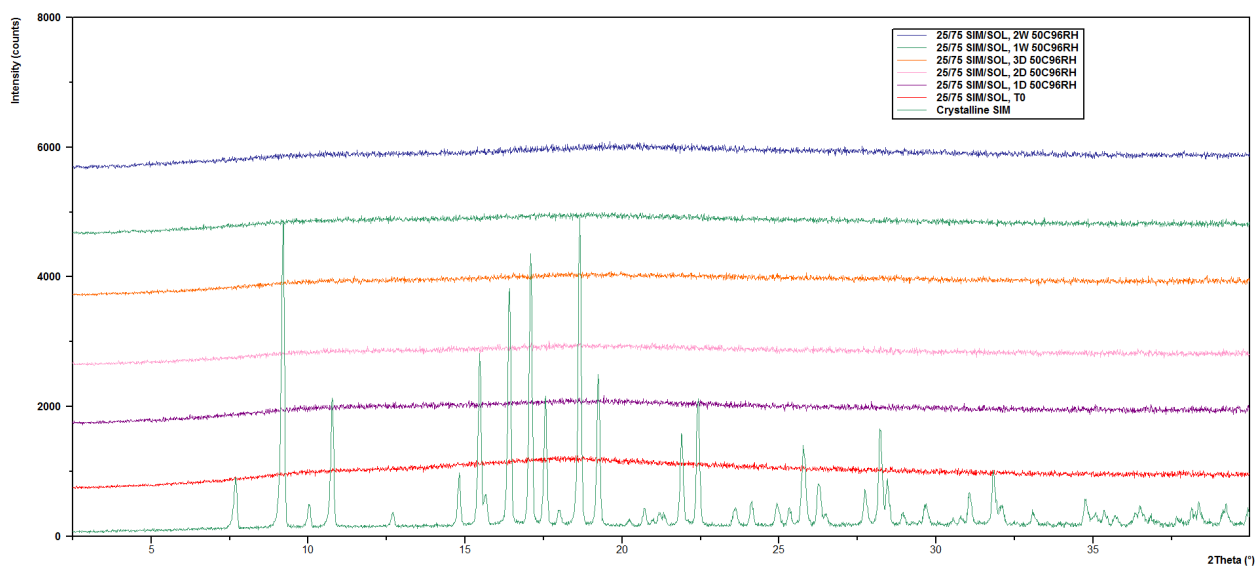
75/25 SIM/HPMC-AS on Stability at 50°C, 96%RH:



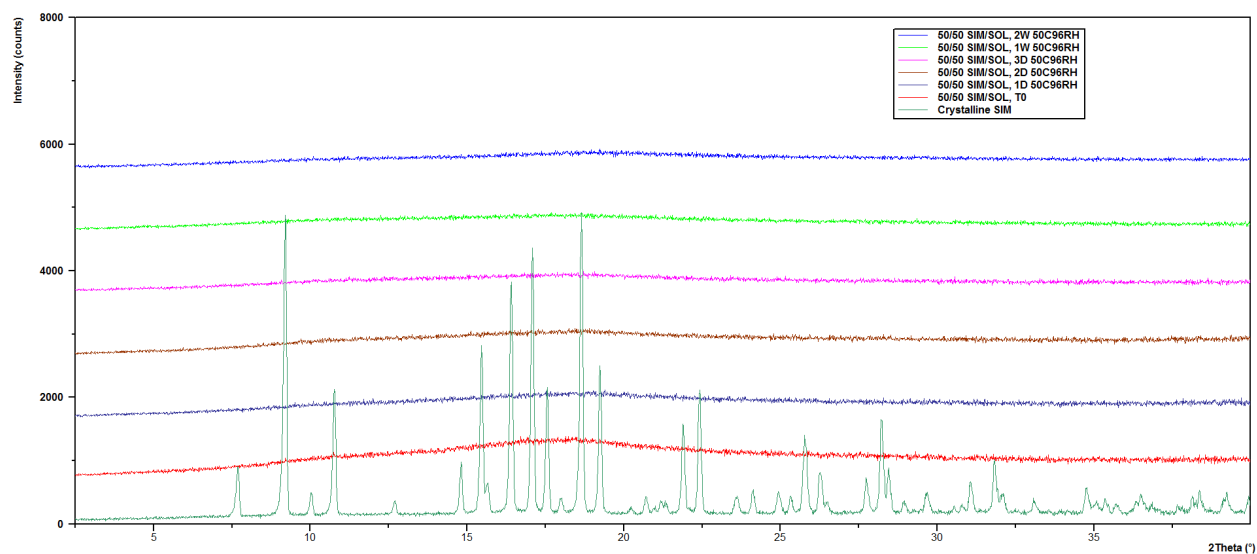
0/100 SIM/SOL on Stability at 50°C, 96%RH:



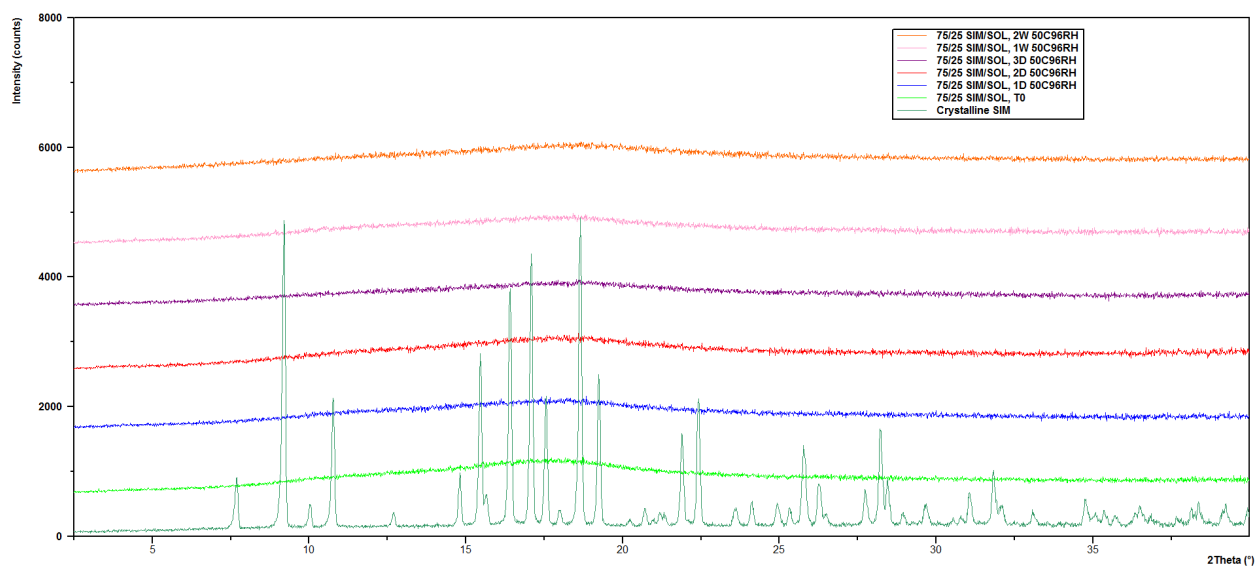
25/75 SIM/SOL on Stability at 50°C, 96%RH:



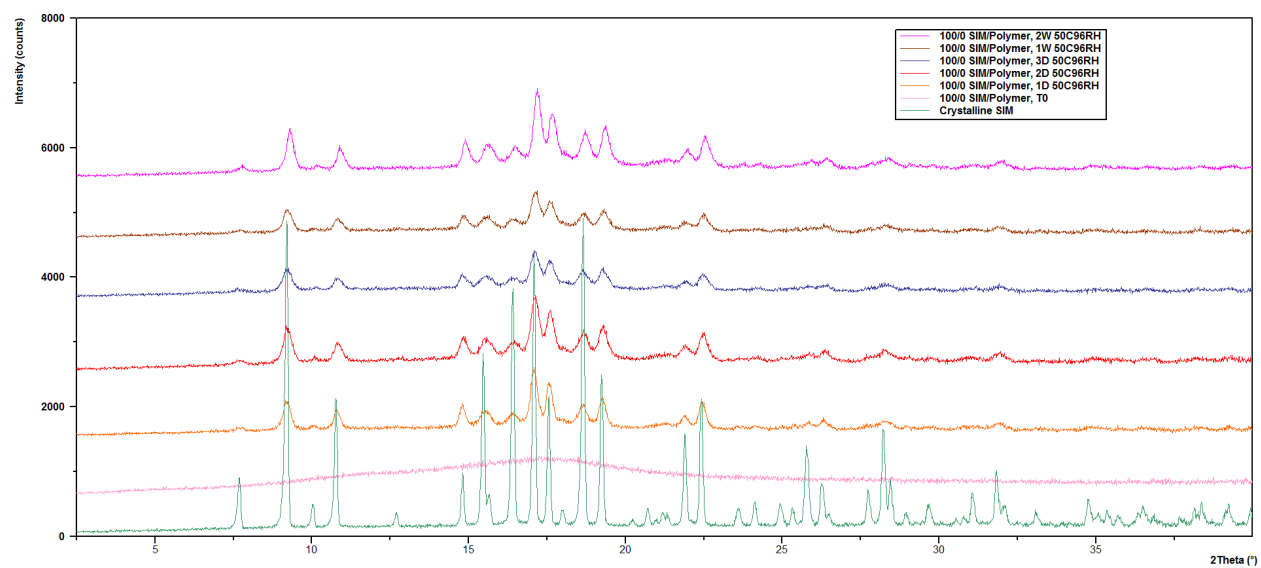
50/50 SIM/SOL on Stability at 50°C, 96%RH:



75/25 SIM/SOL on Stability at 50°C, 96%RH:


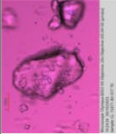


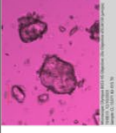

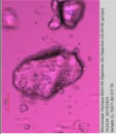


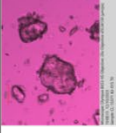

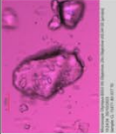


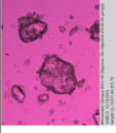

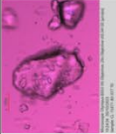


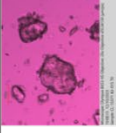

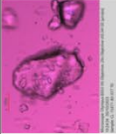


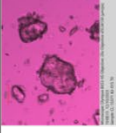

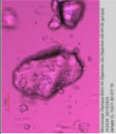


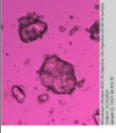


100/0 SIM/Polymer on Stability at 50°C, 96%RH

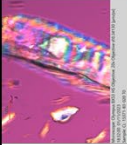
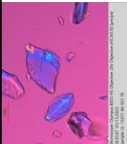
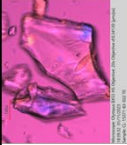
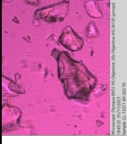
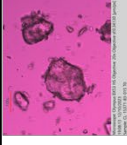
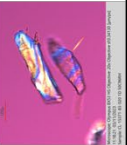
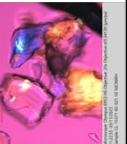

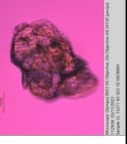
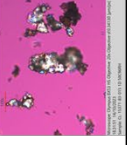

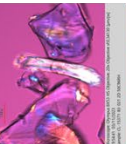

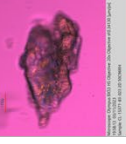
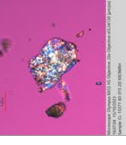
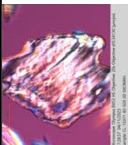
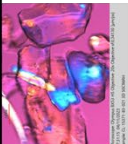
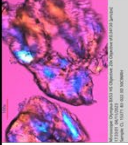
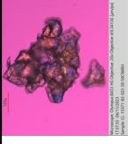
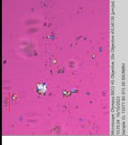


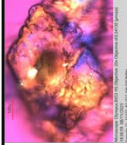
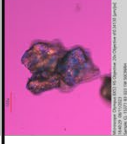
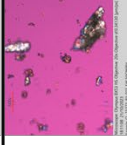
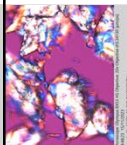

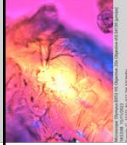
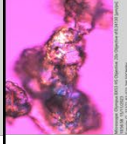
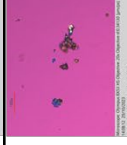


Appendix C: PLM Images



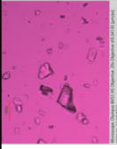

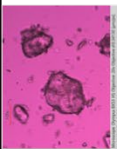

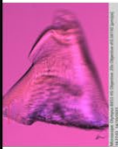
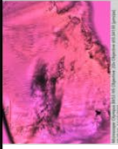
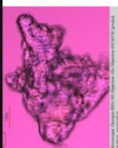


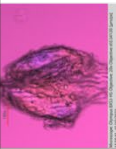



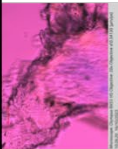

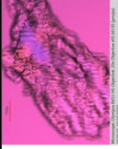

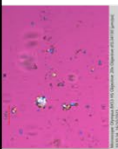

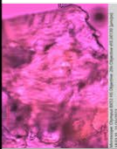
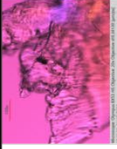

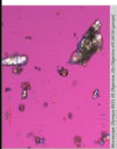
SIM/PVP-VA Systems on Stability at 50°C, 96%RH

	0/100 SIM/PVP-VA	25/75 SIM/PVP-VA	50/50 SIM/PVP-VA	75/25 SIM/PVP-VA	100/0 SIM/PVP-VA
Initial					
1 day, 50°C, 96% RH					
2 days, 50°C, 96% RH					
3 days, 50°C, 96% RH					
1 week, 50°C, 96% RH					
2 weeks, 50°C, 96% RH					

SIM/HPMC-AS Systems on Stability at 50°C, 96%RH

	0/100 SIM/HPMC-AS	25/75 SIM/HPMC-AS	50/50 SIM/HPMC-AS	75/25 SIM/HPMC-AS	100/0 SIM/HPMC-AS
Initial					
1 day, 50°C, 96% RH					
2 days, 50°C, 96% RH					
3 days, 50°C, 96% RH					
1 week, 50°C, 96% RH					
2 weeks, 50°C, 96% RH					

SIM/SOL Systems on Stability at 50°C, 96%RH

	0/100 SIM/SOL	25/75 SIM/SOL	50/50 SIM/SOL	75/25 SIM/SOL	100/0 SIM/SOL
Initial					
1 day, 50°C, 96% RH					
2 days, 50°C, 96% RH					
3 days, 50°C, 96% RH					
1 week, 50°C, 96% RH					
2 weeks, 50°C, 96% RH	